

Review

Not peer-reviewed version

Revolutionizing Gas Turbine Aerodynamics: Advanced Numerical Methods for High-Fidelity Simulations, Turbulence Modeling, and Aerothermodynamic Analysis

[Mohammad Yaghoub Abdollahzadeh Jamalabadi](#)*

Posted Date: 19 June 2025

doi: 10.20944/preprints202506.1588.v1

Keywords: Gas turbine aerodynamics; computational fluid dynamics; high-fidelity simulations; turbulence modeling; aerothermodynamic analysis; numerical methods; heat transfer; performance optimization



Preprints.org is a free multidisciplinary platform providing preprint service that is dedicated to making early versions of research outputs permanently available and citable. Preprints posted at Preprints.org appear in Web of Science, Crossref, Google Scholar, Scilit, Europe PMC.

Copyright: This open access article is published under a Creative Commons CC BY 4.0 license, which permit the free download, distribution, and reuse, provided that the author and preprint are cited in any reuse.

Disclaimer/Publisher's Note: The statements, opinions, and data contained in all publications are solely those of the individual author(s) and contributor(s) and not of MDPI and/or the editor(s). MDPI and/or the editor(s) disclaim responsibility for any injury to people or property resulting from any ideas, methods, instructions, or products referred to in the content.

Review

Revolutionizing Gas Turbine Aerodynamics: Advanced Numerical Methods for High-Fidelity Simulations, Turbulence Modeling, and Aerothermodynamic Analysis

Mohammad Yaghoub Abdollahzadeh Jamalabadi

Department of Mechanical Engineering Chabahar Maritime University, Chabahar 99717, Iran;
my.abdollahzadeh@cmu.ac.i

Abstract: Gas turbine engines represent one of the most complex and sophisticated engineering systems in modern technology, with applications spanning power generation, aviation, and marine propulsion. The aerodynamic performance of these systems directly impacts their efficiency, reliability, and environmental footprint. This comprehensive review examines the revolutionary advancements in numerical methods that have transformed our understanding and analysis of gas turbine aerodynamics. The paper explores the evolution from traditional computational approaches to cutting-edge high-fidelity simulation techniques, including Direct Numerical Simulation (DNS), Large Eddy Simulation (LES), and hybrid RANS-LES methods. We provide an in-depth analysis of advanced turbulence modeling approaches, highlighting their theoretical foundations, implementation strategies, and practical applications in gas turbine environments. The review further investigates state-of-the-art aerothermodynamic analyses, focusing on conjugate heat transfer, film cooling optimization, and multi-physics coupling. Through detailed case studies and critical evaluation of current methodologies, this paper demonstrates how revolutionary numerical methods have redefined our understanding of flow physics, heat transfer mechanisms, and overall performance prediction in gas turbine systems. Finally, we discuss emerging technologies and future research directions, including exascale computing, digital twin implementation, and machine learning integration, that promise to further advance the field of gas turbine aerodynamics.

Keywords: gas turbine aerodynamics; computational fluid dynamics; high-fidelity simulations; turbulence modeling; aerothermodynamic analysis; numerical methods; heat transfer; performance optimization

1. Introduction

1.1. Background and Significance

Gas turbines represent one of the most significant technological achievements in modern engineering, serving as the cornerstone of power generation, aviation propulsion, and marine applications worldwide. These sophisticated thermal machines convert the chemical energy of fuel into mechanical work through a series of aerodynamic and thermodynamic processes that involve complex fluid flow phenomena [1]. The aerodynamic performance of gas turbines directly influences their efficiency, power output, fuel consumption, emissions, and overall reliability—parameters that have profound economic, environmental, and societal implications in our energy-intensive global economy [2].

The significance of gas turbine aerodynamics extends beyond the immediate performance metrics. As the world transitions toward more sustainable energy systems, the role of high-efficiency gas turbines becomes increasingly critical. Modern combined-cycle power plants utilizing advanced gas turbines can achieve thermal efficiencies exceeding 60%, substantially reducing carbon emissions

per unit of electricity generated compared to conventional power generation technologies [3]. In aviation, improvements in gas turbine aerodynamics have enabled significant reductions in fuel consumption and emissions, contributing to the industry's sustainability goals [4].

The economic impact of even marginal improvements in gas turbine aerodynamic performance cannot be overstated. For power generation applications, a mere 1% increase in efficiency can translate to millions of dollars in annual fuel savings for a typical utility-scale plant and thousands of tons of avoided carbon emissions [5]. In aerospace applications, aerodynamic optimizations that reduce specific fuel consumption directly impact operating costs, range capabilities, and payload capacity of commercial and military aircraft [6].

Given these far-reaching implications, the scientific community and industry have invested substantial resources in advancing our understanding of gas turbine aerodynamics. The complexity of the flow phenomena involved—including compressibility effects, turbulence, secondary flows, shock waves, boundary layer development, separation, and their interactions with heat transfer and combustion processes—presents formidable challenges that have driven continuous innovation in analytical, experimental, and computational methods [7].

1.2. Historical Development of Gas Turbine Aerodynamics

The evolution of gas turbine aerodynamics as a scientific discipline parallels the development of the machines themselves. The conceptual foundations of gas turbines date back to the early 20th century, with the first practical gas turbine for power generation developed by Brown Boveri Company in 1939 and the first jet engine successfully tested by Frank Whittle in Great Britain and Hans von Ohain in Germany in the late 1930s [8]. During this pioneering era, aerodynamic design relied primarily on empirical methods, simplified analytical models, and extensive experimental testing.

The post-World War II period witnessed rapid advancements in gas turbine technology, driven by military and commercial aviation requirements. The 1950s and 1960s saw the development of more sophisticated analytical methods for aerodynamic analysis, including two-dimensional cascade theory, streamline curvature methods, and simplified boundary layer calculations [9]. These approaches, while limited in their ability to capture the full complexity of three-dimensional flows, provided valuable insights that guided early design iterations.

The 1970s marked a significant transition with the emergence of computational methods for fluid dynamics. Early numerical approaches, based on potential flow theory and inviscid Euler equations, offered new capabilities for analyzing complex geometries but still lacked the ability to accurately model viscous effects and turbulence [10]. The introduction of the first Reynolds-Averaged Navier-Stokes (RANS) solvers in the late 1970s and early 1980s represented a watershed moment, enabling more comprehensive analysis of turbulent flows in turbomachinery components [11].

The subsequent decades saw continuous refinement of computational fluid dynamics (CFD) methods for gas turbine applications. The 1990s brought significant improvements in turbulence modeling, mesh generation techniques, and numerical algorithms, making three-dimensional viscous flow simulations increasingly practical for industrial design applications [12]. Concurrently, experimental techniques evolved with the introduction of advanced laser-based diagnostics, providing detailed flow field measurements for validation of computational models [13].

The early 2000s witnessed the emergence of high-performance computing capabilities that enabled more sophisticated simulation approaches. Large Eddy Simulation (LES) and hybrid RANS-LES methods began to be applied to specific gas turbine components, offering unprecedented insights into unsteady flow phenomena and turbulence structures [14]. This period also saw increased emphasis on multi-disciplinary approaches that coupled aerodynamics with heat transfer, combustion, and structural mechanics to provide more holistic analysis of gas turbine systems [15].

In recent years, the field has experienced another revolutionary transformation with the advent of exascale computing, advanced numerical methods, and data-driven approaches. These developments have made previously impractical simulation techniques, such as Direct Numerical

Simulation (DNS) for turbulent flows at realistic Reynolds numbers, increasingly feasible for specific applications [16]. The integration of artificial intelligence and machine learning with traditional CFD has opened new frontiers in aerodynamic optimization, reduced-order modeling, and uncertainty quantification [17].

1.3. Current Challenges and Opportunities

Despite remarkable progress, the field of gas turbine aerodynamics continues to face significant challenges that limit our ability to fully predict and optimize performance. These challenges stem from both the inherent complexity of the physical phenomena involved and the practical constraints of computational resources and methodologies.

One of the most persistent challenges remains the accurate prediction of turbulent flows across the wide range of conditions encountered in gas turbines. Traditional RANS approaches, while computationally efficient, rely on empirical turbulence models that introduce significant uncertainties, particularly for flows involving strong pressure gradients, curvature, rotation, and transition [18]. Scale-resolving simulations such as LES offer improved accuracy but at computational costs that remain prohibitive for routine design applications, especially at the high Reynolds numbers characteristic of gas turbines [19].

The multi-physics nature of gas turbine flows presents additional complexities. The strong coupling between aerodynamics, heat transfer, combustion, and structural mechanics requires integrated simulation approaches that can accurately capture these interactions without imposing excessive computational burdens [20]. Particularly challenging are phenomena such as film cooling, where the interaction between coolant jets and the hot gas path involves complex mixing processes that impact both aerodynamic performance and component durability [21].

Geometric complexity and scale disparities further complicate numerical simulations. Modern gas turbine designs incorporate intricate features such as film cooling holes, squealer tips, and non-axisymmetric endwall contouring that span multiple length scales, from millimeters to meters [22]. Adequately resolving these features while maintaining computational efficiency requires advanced meshing strategies and numerical methods that can handle highly anisotropic grids and complex boundaries [23].

The unsteady nature of many flow phenomena in gas turbines—including rotor-stator interactions, vortex shedding, and combustion instabilities—necessitates time-accurate simulations that can be computationally intensive [24]. Capturing these transient effects accurately while maintaining practical simulation times remains a significant challenge, particularly for whole-engine simulations that must account for multiple components and their interactions [25].

Alongside these challenges, however, lie unprecedented opportunities for advancing the field. The continued growth in computing power, particularly with the emergence of exascale systems and specialized hardware accelerators, is expanding the feasibility of high-fidelity simulations for increasingly complex configurations [26]. Novel numerical methods, including high-order schemes, adaptive mesh refinement, and improved wall modeling approaches, offer pathways to enhance both accuracy and efficiency [27].

Data-driven approaches represent another frontier with immense potential. Machine learning techniques are being increasingly integrated with traditional physics-based models to improve turbulence modeling, develop reduced-order models, and enable more efficient design optimization [28]. The concept of digital twins—high-fidelity virtual replicas of physical systems that can be updated in real-time with operational data—promises to revolutionize how gas turbines are designed, operated, and maintained [29].

Advanced experimental techniques, including high-speed particle image velocimetry, pressure-sensitive paints, and additive manufacturing of instrumented components, are providing unprecedented validation data for computational models [30]. The synergistic combination of these experimental capabilities with advanced simulation methods offers new opportunities for understanding complex flow phenomena and developing more accurate predictive tools.

1.4. Scope and Objectives of the Review

This comprehensive review aims to synthesize and critically evaluate the revolutionary advancements in numerical methods that have transformed our understanding and analysis of gas turbine aerodynamics. The paper adopts a holistic perspective, examining developments across the spectrum from fundamental numerical techniques to practical applications in industrial settings.

Specifically, the objectives of this review are to:

1. Provide a systematic overview of the evolution of numerical methods for gas turbine aerodynamics, highlighting key innovations and their impact on the field.
2. Critically assess the state-of-the-art in high-fidelity simulation approaches, including DNS, LES, and hybrid methods, with particular emphasis on their applicability to gas turbine flows.
3. Evaluate advanced turbulence modeling strategies, examining their theoretical foundations, implementation challenges, and performance for different flow regimes encountered in gas turbines.
4. Analyze cutting-edge approaches for aerothermodynamic simulations, focusing on conjugate heat transfer, film cooling, and multi-physics coupling.
5. Examine numerical methods specifically developed for handling complex geometries and phenomena characteristic of modern gas turbine designs.
6. Present illustrative case studies that demonstrate the application of advanced numerical methods to specific gas turbine components and systems.
7. Identify emerging technologies and methodologies that are likely to shape the future of gas turbine aerodynamics research and development.
8. Discuss remaining challenges and promising research directions that could lead to further advancements in the field.

The scope of this review encompasses the entire gas turbine system, including compressors, combustors, and turbines, with particular attention to areas where advanced numerical methods have had the most significant impact. While the primary focus is on aerodynamics, the review acknowledges and addresses the critical interactions with heat transfer, combustion, and structural mechanics that influence overall system performance.

By providing this comprehensive assessment of revolutionary numerical methods in gas turbine aerodynamics, this review aims to serve as both a reference for researchers and practitioners in the field and a roadmap for future developments that could further enhance our understanding and optimization of these critical engineering systems.

2. Fundamental Principles of Gas Turbine Aerodynamics

2.1. Governing Equations and Physical Phenomena

The aerodynamic behavior of flows within gas turbines is governed by the fundamental conservation laws of fluid mechanics, expressed mathematically through the Navier-Stokes equations. For compressible flows characteristic of gas turbines, these equations must account for variations in density and temperature, as well as the coupling between momentum and energy transport [31]. The complete set of governing equations includes the conservation of mass (continuity equation), momentum (Navier-Stokes equations), and energy, which can be written in differential form as:

Conservation of mass:

$$\frac{\partial \rho}{\partial t} + \nabla \cdot (\rho V) = 0$$

Conservation of momentum:

$$\frac{\partial(\rho V)}{\partial t} + \nabla \cdot (\rho V \otimes V) = -\nabla p + \nabla \cdot \tau + \rho g$$

Conservation of energy:

$$\frac{\partial(\rho E)}{\partial t} + \nabla \cdot (\rho V H) = \nabla \cdot (k \nabla T) + \nabla \cdot (\tau \cdot V) + \rho g \cdot V + Q$$

where ρ is the fluid density, V is the velocity vector, p is the pressure, τ is the viscous stress tensor, g represents body forces, E is the total energy per unit mass, H is the total enthalpy per unit mass, k is the thermal conductivity, T is the temperature, and Q represents heat sources or sinks [32].

These equations are supplemented by constitutive relations, including the equation of state for a perfect gas:

$$p = \rho R T$$

where R is the specific gas constant, and expressions for the viscous stress tensor based on Stokes' hypothesis for Newtonian fluids [33].

The physical phenomena described by these equations in gas turbine flows are characterized by several distinctive features. Compressibility effects become significant in many regions of gas turbines, particularly in high-pressure compressors and turbines where local Mach numbers can approach or exceed unity. These effects manifest as density variations, pressure waves, and potentially shock formations that fundamentally alter the flow behavior compared to incompressible approximations [34].

Viscous effects play a crucial role in gas turbine aerodynamics, particularly in boundary layer development along solid surfaces. The boundary layer represents a thin region near walls where velocity gradients are steep and viscous forces dominate. Its behavior—including growth, transition from laminar to turbulent flow, and potential separation under adverse pressure gradients—significantly impacts overall performance through friction losses and flow blockage [35]. The Reynolds numbers in gas turbines typically range from 10^5 to 10^7 , placing most flows in the fully turbulent regime, though transitional flows can occur in specific regions [36].

Turbulence represents one of the most complex and consequential phenomena in gas turbine flows. Characterized by chaotic, three-dimensional, unsteady motions across a wide range of spatial and temporal scales, turbulence enhances mixing and diffusion while increasing skin friction and pressure losses [37]. The smallest turbulent scales (Kolmogorov scales) in gas turbine flows can be orders of magnitude smaller than the characteristic dimensions of components, creating significant challenges for numerical simulations [38].

Secondary flows—three-dimensional flow structures that deviate from the primary flow direction—are ubiquitous in gas turbines due to pressure gradients, curvature, rotation, and geometric features. These include passage vortices, horseshoe vortices, tip leakage vortices, and corner vortices, which contribute substantially to aerodynamic losses and non-uniform temperature distributions [39]. As noted by Acharya and Mahmood in their analysis of turbine blade aerodynamics:

“The aerodynamics of the flow in a turbine stage (stator/rotor) is rather complex and is still the subject of many ongoing research activities in the gas turbine community. The flow is inherently three-dimensional due to the vane/blade passage geometry with features such as twisting of the vane/blade along the span, clearance between the blade tip and the shroud, film cooling holes, and end wall contouring. The passage flow is characterized by boundary layer effects, secondary flows generated by the passage pressure gradients, and vortical flow structures such as the leading edge horse-shoe vortices, tip-leakage flow vortices, and corner vortices.” [40]

Shock waves can form in transonic and supersonic regions of gas turbines, particularly in high-pressure compressors and turbines. These discontinuities in flow properties cause abrupt changes in pressure, temperature, and velocity, leading to increased losses and potential flow separation when interacting with boundary layers [41]. The accurate prediction of shock formation, propagation, and interaction with other flow features remains challenging for numerical methods.

Heat transfer processes are intimately coupled with aerodynamics in gas turbines, particularly in the hot sections where component cooling is critical for durability. The interaction between the main gas path flow and cooling flows introduces complex mixing phenomena that affect both aerodynamic performance and thermal management [42]. The accurate prediction of heat transfer coefficients and cooling effectiveness requires resolving the flow field at very fine scales near walls and cooling features.

2.2. Flow Characteristics in Gas Turbine Components

The aerodynamic phenomena described above manifest differently across the major components of a gas turbine, each presenting unique challenges for analysis and optimization.

2.2.1. Compressor Aerodynamics

Axial compressors in gas turbines consist of alternating rows of rotating blades (rotors) and stationary vanes (stators) that progressively increase the pressure of the working fluid. The flow through these components is characterized by several distinctive features that influence performance and stability [43].

The blade-to-blade flow in compressor passages exhibits complex three-dimensional patterns due to the combined effects of pressure gradients, boundary layers, and secondary flows. The adverse pressure gradient inherent in compressive flow makes boundary layers particularly susceptible to separation, especially on the suction surface of blades [44]. This separation sensitivity necessitates careful aerodynamic design to maintain attached flow across a wide operating range.

Tip clearance flows in compressors result from the pressure difference between the pressure and suction sides of rotor blades, driving flow through the gap between blade tips and the casing. The resulting tip leakage vortices contribute significantly to losses and can limit the stable operating range by promoting the onset of stall and surge [45]. As noted by Denton:

“Tip leakage flows can account for up to 30% of the total loss in a compressor stage, with the magnitude strongly dependent on the clearance-to-chord ratio and loading level.” [46]

Shock waves occur in transonic compressors when the relative flow velocity exceeds the speed of sound, typically near the leading edge of rotor blades at the tip section. These shocks interact with boundary layers and tip leakage flows, potentially triggering separation and increasing losses [47]. The accurate prediction of these shock-boundary layer interactions remains challenging for numerical methods.

Unsteady flow phenomena in compressors arise from rotor-stator interactions, vortex shedding, and potential instabilities such as rotating stall and surge. These time-dependent effects can significantly impact performance, reliability, and aeromechanical behavior [48]. Capturing these unsteady phenomena requires time-accurate simulations that are computationally intensive.

2.2.2. Combustor Flow Dynamics

Combustors in gas turbines present some of the most complex flow physics, combining aerodynamics with heat transfer, chemical reactions, and multiphase phenomena. The flow structure in modern combustors is dominated by swirl-induced recirculation zones that enhance fuel-air mixing and flame stabilization [49].

The primary flow features in combustors include the central recirculation zone created by vortex breakdown of the swirling flow, corner recirculation zones near the combustor walls, and shear layers between these regions and the main flow [50]. These structures govern the residence time distribution, mixing rates, and flame characteristics that ultimately determine combustion efficiency and emissions.

Turbulence-chemistry interactions in combustors present particular challenges for numerical modeling. The wide range of time scales involved—from fast chemical reactions to slower mixing processes—creates stiffness in the governing equations that complicates numerical solutions [51].

Additionally, the strong coupling between turbulence and chemical reactions requires specialized models that can account for these interactions.

Multiphase flows are common in liquid-fueled combustors, where fuel atomization, droplet dispersion, evaporation, and eventual combustion create a complex sequence of interrelated phenomena [52]. The accurate prediction of spray characteristics and their interaction with the gas phase remains an active area of research in combustor aerodynamics.

Combustion instabilities represent a particularly challenging aspect of combustor aerodynamics, involving the coupling between acoustic waves, heat release fluctuations, and flow dynamics [53]. These instabilities can lead to high-amplitude pressure oscillations that threaten the structural integrity of the combustor and adjacent components.

2.2.3. Turbine Blade and Vane Aerodynamics

Turbines extract energy from the high-temperature, high-pressure gas stream exiting the combustor, converting it to mechanical work. The aerodynamics of turbine blades and vanes is characterized by complex three-dimensional flows influenced by strong pressure gradients, curvature, rotation, and cooling features [54].

The primary flow path in turbines experiences strong acceleration due to the favorable pressure gradient, making boundary layers less prone to separation than in compressors. However, the high temperatures necessitate extensive cooling that introduces secondary flows and mixing phenomena [55]. The interaction between the main gas path and cooling flows significantly impacts aerodynamic performance and heat transfer characteristics.

Secondary flows in turbines are particularly pronounced due to the strong pressure gradients and endwall boundary layers. The passage vortex system, formed by the migration of low-momentum fluid from the endwall toward the suction surface, creates non-uniform flow distributions and increased losses [56]. As described by Langston:

“The horseshoe vortex that forms at the leading edge of turbine blades divides into pressure and suction side legs, with the pressure side leg evolving into the passage vortex that dominates the secondary flow field. This vortex system can account for up to 30-40% of the total aerodynamic losses in a turbine stage.” [57]

Tip leakage flows in turbines differ from those in compressors due to the favorable pressure gradient and higher pressure differences across the blade. The resulting tip leakage vortices not only contribute to aerodynamic losses but also create regions of high heat transfer that can limit component durability [58]. Modern turbine designs often incorporate squealer tips or partial shrouds to reduce these effects.

Film cooling flows, injected through discrete holes on blade and vane surfaces, create complex three-dimensional flow structures as they interact with the main gas path [59]. The effectiveness of these cooling schemes depends strongly on the aerodynamic behavior of the coolant jets, including their penetration, spreading, and mixing characteristics. Accurate prediction of film cooling performance requires resolving flow features at the scale of individual cooling holes while accounting for their collective effect on the overall flow field.

Trailing edge flows in turbines present unique challenges due to the finite thickness of blade trailing edges and the mixing of pressure and suction side boundary layers [60]. The resulting wake structures contribute to profile losses and influence the incoming flow conditions for downstream blade rows. In transonic turbines, trailing edge shock systems further complicate this region.

2.2.4. Secondary Flows and Vortical Structures

Secondary flows and vortical structures deserve special attention as they significantly impact performance across all gas turbine components. These three-dimensional flow features result from the interaction of viscous effects with pressure gradients, curvature, rotation, and geometric features [61].

In turbomachinery passages, the classical secondary flow model identifies several key vortical structures:

1. **Horseshoe vortex:** Forms at the junction of blades or vanes with endwalls due to the blockage effect of the leading edge on the incoming endwall boundary layer. This vortex system wraps around the leading edge and divides into pressure and suction side legs [62].
2. **Passage vortex:** Develops from the pressure side leg of the horseshoe vortex as it migrates across the passage toward the suction surface under the influence of the cross-passage pressure gradient. This vortex dominates the secondary flow field in turbine passages [63].
3. **Corner vortices:** Form in the corners between blade surfaces and endwalls due to the interaction of boundary layers and adverse pressure gradients. These vortices contribute to localized flow separation and increased losses [64].
4. **Tip leakage vortex:** Results from the flow driven through the clearance gap between rotating blade tips and the stationary casing by the pressure difference across the blade. This vortex interacts with the passage flow and other secondary flow structures, significantly impacting performance [65].
5. **Trailing edge shed vorticity:** Generated due to the spanwise variation in blade loading and the resulting circulation variation. This vorticity contributes to the three-dimensionality of blade wakes [66].

The combined effect of these vortical structures creates a complex three-dimensional flow field that deviates significantly from idealized two-dimensional models. As noted by Sharma and Butler:

“Secondary flows can account for up to 30-50% of the total aerodynamic losses in turbomachinery, with their relative importance increasing as aspect ratios decrease and loading levels increase.” [67]

The accurate prediction of these secondary flows and their impact on performance requires three-dimensional simulations with adequate resolution of boundary layers and vortical structures. Traditional RANS approaches can capture the mean characteristics of these flows but may struggle with the unsteady aspects and interactions between different vortical systems [68]. Scale-resolving simulations offer improved fidelity but at significantly higher computational cost.

2.3. Aerodynamic Performance Parameters

The assessment of gas turbine aerodynamic performance relies on various parameters that quantify efficiency, losses, flow quality, and overall system behavior. These parameters provide the metrics for evaluating design alternatives and the basis for validation of numerical simulations [69].

2.3.1. Efficiency Metrics

Efficiency metrics quantify how effectively a component or system converts energy from one form to another. In gas turbines, several efficiency definitions are commonly used:

1. **Isentropic efficiency:** Compares the actual work transfer to the ideal isentropic process between the same pressure levels. For compressors, it is defined as:

$$\eta_c = \frac{h_{2s} - h_1}{h_2 - h_1}$$

where h_1 is the inlet enthalpy, h_2 is the actual outlet enthalpy, and h_{2s} is the outlet enthalpy for an isentropic process. For turbines, it is defined as:

$$\eta_t = \frac{h_1 - h_2}{h_1 - h_{2s}}$$

This efficiency metric directly reflects the aerodynamic quality of the component [70].

2. **Polytropic efficiency:** Represents the efficiency of an infinitesimal stage in a multistage process, providing a more consistent measure for comparing components operating at different pressure ratios. It is defined through the relationship:

$$\eta_p = \frac{\ln(p_2/p_1)}{\ln(T_2/T_1)} \cdot \frac{R}{c_p}$$

for a compressor, where p is pressure, T is temperature, R is the gas constant, and c_p is the specific heat at constant pressure [71].

3. **Total-to-total efficiency:** Accounts for both static and dynamic components of energy, appropriate when the kinetic energy at component exit is utilized in downstream components. This is typically used for intermediate stages in multistage turbomachinery [72].
4. **Total-to-static efficiency:** Considers only the static pressure rise or expansion, appropriate when exit kinetic energy is not recovered. This is typically used for the final stage of a turbine exhausting to ambient conditions [73].
5. **Thermal efficiency:** At the system level, represents the ratio of net work output to heat input:

$$\eta_{th} = \frac{W_{net}}{Q_{in}}$$

This metric reflects the combined effect of component efficiencies and cycle parameters [74].

2.3.2. Loss Mechanisms

Aerodynamic losses in gas turbines are typically categorized based on their physical origin and location. Understanding these loss mechanisms is essential for both design optimization and the development of accurate numerical models [75].

1. **Profile losses:** Result from boundary layer development and potential separation on blade and vane surfaces. These losses depend on the airfoil shape, surface roughness, Reynolds number, and inlet turbulence levels [76].
2. **Secondary flow losses:** Arise from the three-dimensional vortical structures discussed earlier, including passage vortices, corner vortices, and trailing edge shed vorticity. These losses increase with loading level and decrease with aspect ratio [77].
3. **Tip leakage losses:** Result from the flow through clearance gaps between rotating blade tips and stationary casings. These losses depend on the clearance size, blade loading, and tip geometry features such as squealer rims [78].
4. **Shock losses:** Occur in transonic and supersonic flow regions due to the irreversible nature of shock waves. These losses increase with Mach number and can be significant in high-pressure ratio compressors and turbines [79].
5. **Mixing losses:** Result from the mixing of streams with different velocities, temperatures, or compositions. Examples include the mixing of blade wakes with the main flow, coolant jets with the hot gas path, and leakage flows with the primary flow [80].
6. **Endwall losses:** Arise from boundary layer development on hub and casing surfaces, often exacerbated by secondary flows and corner separations [81].

These loss mechanisms are often quantified using loss coefficients, which express the reduction in total pressure relative to a reference dynamic pressure:

$$\omega = \frac{p_{t1} - p_{t2}}{p_{t1} - p_1}$$

for turbines, where p_t is total pressure and p is static pressure. Alternative formulations include entropy-based loss coefficients that directly relate to efficiency reduction [82].

2.3.3. Flow Quality Indicators

Beyond efficiency and loss metrics, several parameters are used to assess the quality of flow in gas turbines:

1. **Flow coefficient:** Relates the axial velocity to the blade speed:

$$\phi = \frac{V_a}{U}$$

This non-dimensional parameter influences loading distribution and incidence angles [83].

2. **Loading coefficient:** Expresses the specific work relative to the blade speed:

$$\psi = \frac{\Delta h_0}{U^2}$$

Higher values indicate more aerodynamically challenging conditions with stronger pressure gradients [84].

3. **Degree of reaction:** Represents the fraction of static enthalpy change that occurs in the rotor relative to the total stage enthalpy change:

$$R = \frac{\Delta h_{rotor}}{\Delta h_{stage}}$$

This parameter influences the pressure gradient distribution between stator and rotor [85].

4. **Flow uniformity indices:** Quantify the spatial variation of flow properties at component interfaces, including velocity profiles, temperature distributions, and pressure distortions. These non-uniformities can significantly impact downstream component performance [86].
5. **Blockage factor:** Represents the effective flow area reduction due to boundary layers and separated regions:

$$B = 1 - \frac{A_{eff}}{A_{geom}}$$

where A_{eff} is the effective flow area and A_{geom} is the geometric area [87].

2.3.4. Performance Evaluation Criteria

The evaluation of gas turbine aerodynamic performance ultimately depends on the specific application and design objectives. Common criteria include:

1. **Efficiency at design point:** Maximizing the efficiency at the primary operating condition, which directly impacts fuel consumption and operating costs [88].
2. **Off-design performance:** Maintaining acceptable efficiency and stability across a range of operating conditions, particularly important for applications with variable power requirements [89].
3. **Operating range:** Ensuring adequate margin between design point and aerodynamic stability limits (surge/stall in compressors, choking in turbines) to accommodate transients and deterioration [90].
4. **Durability considerations:** Balancing aerodynamic performance with thermal management to ensure component life meets requirements. This often involves trade-offs between efficiency and cooling effectiveness [91].
5. **Emissions performance:** Particularly for combustors, achieving low pollutant emissions (NO_x, CO, unburned hydrocarbons) while maintaining combustion efficiency and stability [92].
6. **Noise generation:** Minimizing aerodynamically generated noise, which is increasingly important for both industrial and aviation applications due to regulatory requirements [93].

7. **Cost and manufacturability:** Considering the practical aspects of producing aerodynamic designs, including geometric complexity, material requirements, and manufacturing tolerances [94].

The relative importance of these criteria varies by application. For example, aviation gas turbines typically prioritize weight, specific fuel consumption, and reliability, while industrial gas turbines may emphasize absolute efficiency, emissions compliance, and fuel flexibility [95].

The accurate prediction of these performance parameters through numerical simulations requires not only capturing the relevant flow physics but also appropriate post-processing methodologies that account for averaging procedures, reference conditions, and consistent definitions across different analysis tools [96]. The validation of numerical predictions against experimental measurements of these parameters forms a critical aspect of establishing confidence in simulation methodologies for gas turbine aerodynamics.

3. Evolution of Numerical Methods in Gas Turbine Aerodynamics

The development of numerical methods for gas turbine aerodynamics represents a remarkable journey of scientific and technological advancement that has fundamentally transformed how these complex machines are designed, analyzed, and optimized. This evolution has been driven by the continuous pursuit of higher fidelity in flow prediction, enabled by concurrent advances in mathematical formulations, numerical algorithms, and computational hardware.

3.1. Historical Perspective

The earliest attempts to mathematically model flows in turbomachinery date back to the early 20th century, with simplified analytical approaches based on potential flow theory and cascade analysis [97]. These methods, while mathematically elegant, were limited to idealized two-dimensional, inviscid, incompressible flows that could not capture many of the critical phenomena in actual gas turbines.

The 1940s and 1950s saw the development of more sophisticated analytical techniques, including streamline curvature methods and through-flow calculations that could account for radial variations in flow properties [98]. Wu's S1/S2 stream surface method, introduced in 1952, represented a significant advancement by providing a quasi-three-dimensional framework for analyzing turbomachinery flows [99]. As described by Denton and Dawes:

“Wu's S1/S2 method decomposed the three-dimensional flow into two families of stream surfaces: S1 surfaces (blade-to-blade) and S2 surfaces (hub-to-tip). By solving the flow equations on these surfaces iteratively, a quasi-three-dimensional solution could be constructed that captured many important flow features while remaining computationally tractable with the resources available at that time.” [100]

The 1960s marked the beginning of the computational era in fluid dynamics, with the first numerical solutions of simplified forms of the Navier-Stokes equations. These early computational methods typically employed finite difference schemes on structured grids to solve the potential flow or Euler equations [101]. While still limited in their ability to capture viscous effects and turbulence, these methods enabled analysis of more complex geometries than was possible with purely analytical approaches.

The 1970s witnessed significant methodological advances with the introduction of time-marching schemes for solving the Euler equations, allowing for the treatment of transonic flows with shock waves [102]. Jameson's work on finite volume methods and artificial dissipation schemes provided robust approaches for solving the Euler equations that remain influential today [103]. Concurrently, the first Reynolds-Averaged Navier-Stokes (RANS) solvers began to emerge, incorporating algebraic turbulence models that allowed for approximate treatment of turbulent flows [104].

The 1980s saw the maturation of RANS methods with the development of more sophisticated turbulence models, including the k- ϵ model by Launder and Spalding and the Baldwin-Lomax model, which found widespread application in gas turbine analysis [105]. This period also witnessed significant improvements in grid generation techniques, numerical algorithms, and boundary condition treatments that enhanced the robustness and accuracy of computational methods [106].

The 1990s brought several transformative developments, including the widespread adoption of unstructured grid methods that could accommodate complex geometries more readily than structured approaches [107]. The introduction of more advanced turbulence models, such as the k- ω SST model by Menter, provided improved predictions for flows with adverse pressure gradients and separation [108]. This decade also saw the first serious attempts at Large Eddy Simulation (LES) for turbomachinery flows, though limited to simplified configurations due to computational constraints [109].

The early 2000s marked the emergence of hybrid RANS-LES methods, such as Detached Eddy Simulation (DES), that sought to combine the computational efficiency of RANS for boundary layers with the improved accuracy of LES for separated regions [110]. This period also saw increased emphasis on high-order numerical schemes that could provide improved accuracy for a given computational cost, particularly for problems involving acoustic wave propagation and vortex dynamics [111].

The past decade has witnessed an explosion of innovation in numerical methods for gas turbine aerodynamics, driven by the availability of unprecedented computational resources and the integration of data-driven approaches with traditional physics-based models [112]. Direct Numerical Simulation (DNS) of turbulent flows at conditions relevant to gas turbines has become feasible for specific components, providing new insights into fundamental flow physics and validation data for lower-fidelity models [113]. Machine learning techniques have been increasingly incorporated into turbulence modeling, mesh adaptation, and uncertainty quantification, opening new frontiers in computational efficiency and accuracy [114].

3.2. Traditional Numerical Approaches

Traditional numerical approaches for gas turbine aerodynamics encompass a range of methods that have formed the backbone of computational analysis in the field for decades. These approaches vary in their mathematical formulation, discretization strategies, and solution algorithms, each with distinct advantages and limitations for different applications.

3.2.1. Finite Difference Methods

Finite difference methods (FDM) represent one of the earliest numerical approaches applied to fluid dynamics problems. Based on the direct discretization of differential operators using Taylor series expansions, these methods approximate derivatives at discrete points using differences between neighboring points [115]. For example, a second-order central difference approximation of the first derivative can be expressed as:

$$\left(\frac{\partial \phi}{\partial x}\right)_i \approx \frac{\phi_{i+1} - \phi_{i-1}}{2\Delta x}$$

where ϕ is the variable of interest and Δx is the grid spacing.

The primary advantages of finite difference methods include their conceptual simplicity, straightforward implementation for structured grids, and the ability to achieve high-order accuracy relatively easily [116]. However, these methods face significant challenges when applied to complex geometries characteristic of gas turbine components, as they typically require structured grids that conform to component boundaries. Additionally, finite difference schemes do not inherently ensure conservation properties, which can be problematic for compressible flows where conservation of mass, momentum, and energy is critical [117].

Despite these limitations, finite difference methods have found application in specific areas of gas turbine aerodynamics, particularly for fundamental studies of simplified configurations where high-order accuracy is prioritized over geometric flexibility [118]. They have also been used in specialized applications such as direct numerical simulation of transitional flows and aeroacoustic analysis, where the ability to minimize numerical dispersion and dissipation is valuable [119].

3.2.2. Finite Volume Methods

Finite volume methods (FVM) have emerged as the dominant approach for practical gas turbine aerodynamics simulations due to their inherent conservation properties and flexibility in handling complex geometries [120]. These methods are based on the integral form of the conservation laws, dividing the domain into discrete control volumes and ensuring conservation of flow quantities within each volume.

The semi-discrete form of the conservation equation for a general variable ϕ in a finite volume framework can be written as:

$$\frac{d}{dt} \int_{\Omega_i} \phi dV + \oint_{\partial\Omega_i} F \cdot n dS = \int_{\Omega_i} S dV$$

where Ω_i is the control volume, F is the flux vector, n is the outward normal vector, and S represents source terms [121].

The key advantages of finite volume methods include their natural conservation properties, flexibility in accommodating both structured and unstructured grids, and robustness for flows with discontinuities such as shock waves [122]. These characteristics have made FVM the method of choice for commercial and industrial CFD codes used in gas turbine design and analysis.

Various flux discretization schemes have been developed within the finite volume framework, ranging from first-order upwind schemes that prioritize stability to higher-order schemes that reduce numerical diffusion at the expense of increased computational complexity [123]. For transonic and supersonic flows common in gas turbines, flux-splitting schemes such as Roe's approximate Riemann solver and the AUSM (Advection Upstream Splitting Method) family have proven particularly effective in capturing shock waves and contact discontinuities [124].

Time integration in finite volume methods can be performed using explicit schemes such as Runge-Kutta methods or implicit schemes that offer greater stability at the cost of requiring matrix inversions [125]. For steady-state simulations common in gas turbine analysis, pseudo-time marching approaches with local time stepping and multigrid acceleration techniques are often employed to enhance convergence rates [126].

3.2.3. Finite Element Methods

Finite element methods (FEM) approximate the solution within each element using basis functions, typically polynomials, and enforce the governing equations in a weighted residual or variational form [127]. While less common than finite volume methods in traditional gas turbine CFD, finite element approaches have gained traction for specific applications, particularly those involving coupled multi-physics phenomena or complex geometries.

The standard Galerkin finite element formulation for a general transport equation can be expressed as:

$$\int_{\Omega} w \cdot \left(\frac{\partial \phi}{\partial t} + \nabla \cdot F - S \right) d\Omega = 0$$

where w represents the weighting functions [128].

The primary advantages of finite element methods include their strong mathematical foundation, natural handling of complex geometries through unstructured grids, and straightforward extension to higher-order accuracy through higher-degree basis functions [129]. Additionally, FEM provides a consistent framework for solving coupled multi-physics problems,

such as fluid-structure interaction or conjugate heat transfer, which are increasingly important in gas turbine analysis [130].

However, standard Galerkin finite element methods face challenges when applied to convection-dominated flows typical in gas turbines, as they can produce oscillatory solutions without appropriate stabilization techniques [131]. Various stabilized formulations, including Streamline Upwind Petrov-Galerkin (SUPG) and Galerkin Least-Squares (GLS) methods, have been developed to address these issues [132].

In recent years, discontinuous Galerkin (DG) methods have emerged as a promising approach that combines aspects of finite volume and finite element methods [133]. By allowing discontinuities at element interfaces and enforcing conservation through numerical fluxes, DG methods offer high-order accuracy while maintaining local conservation properties. These methods have shown particular promise for scale-resolving simulations of turbulent flows in gas turbines, though their computational cost remains a limiting factor for routine industrial applications [134].

3.2.4. Boundary Element Methods

Boundary element methods (BEM) represent a fundamentally different approach by reformulating the governing partial differential equations as integral equations defined on the domain boundaries [135]. By requiring discretization only of the boundaries rather than the entire domain, these methods can significantly reduce the dimensionality of the problem.

The primary application of boundary element methods in gas turbine aerodynamics has been for potential flow analysis of blade rows, particularly in the early stages of design when rapid evaluation of multiple configurations is required [136]. These methods are well-suited for external aerodynamics problems with large domains but become less advantageous for internal flows with complex geometries and multiple boundaries characteristic of gas turbine components [137].

The limitations of boundary element methods for general gas turbine aerodynamics include their restriction to linear or linearized equations, difficulties in handling viscous effects and turbulence, and computational inefficiency for problems with many boundary elements [138]. Consequently, these methods have largely been supplanted by finite volume and finite element approaches for comprehensive gas turbine flow analysis, though they retain utility for specialized applications such as acoustic analysis and preliminary design studies [139].

3.3. Limitations of Traditional Methods

Despite their widespread application and continuous refinement, traditional numerical methods for gas turbine aerodynamics face several fundamental limitations that constrain their ability to fully capture the complex flow physics and provide truly predictive capabilities across all operating conditions.

3.3.1. Accuracy Constraints

The accuracy of traditional numerical methods is limited by several factors inherent in their formulation and implementation. Discretization errors arise from the approximation of continuous differential operators with discrete algebraic expressions, with the error magnitude typically scaling with grid spacing according to the formal order of accuracy of the scheme [140]. For the second-order schemes commonly used in industrial gas turbine CFD, these errors can be significant in regions with strong gradients or complex flow structures unless prohibitively fine grids are employed [141].

Numerical diffusion represents a particularly problematic form of discretization error for gas turbine flows, where the accurate preservation of vortical structures, shear layers, and mixing phenomena is critical for performance prediction [142]. As noted by Moin and Mahesh:

“Numerical diffusion in low-order schemes can artificially dampen important flow structures such as vortices and shear layers, leading to significant underprediction of mixing rates and turbulence intensities. This artificial dissipation can mask physical

phenomena and lead to erroneous conclusions about flow behavior and performance.” [143]

Geometric approximation errors arise from the discretization of complex component geometries using finite grids. Features such as thin trailing edges, small fillets, and cooling holes may not be adequately resolved, leading to discrepancies between the simulated and actual geometry that can significantly impact flow prediction [144]. While adaptive mesh refinement techniques can partially address this issue, they introduce additional complexity and computational cost [145].

Boundary condition specification presents another source of accuracy limitation, particularly for subsystem simulations where the true conditions at artificial boundaries are not precisely known [146]. Simplified boundary conditions, such as uniform flow assumptions or fixed pressure distributions, may not adequately capture the complex, unsteady nature of actual boundary conditions in an operating gas turbine [147].

3.3.2. Computational Efficiency Issues

The computational cost of traditional numerical methods remains a significant constraint for gas turbine aerodynamics, despite the exponential growth in computing power over recent decades. The multi-scale nature of turbulent flows in gas turbines, with length scales spanning orders of magnitude from the Kolmogorov microscales to component dimensions, necessitates extremely fine grids for adequate resolution [148]. For example, a typical high-pressure turbine stage simulation with reasonable resolution of boundary layers and secondary flows may require grids with tens or hundreds of millions of cells, even with wall function approaches that avoid resolving the viscous sublayer [149].

Time step restrictions further compound the computational challenge for unsteady simulations. Explicit time integration schemes are limited by the Courant-Friedrichs-Lewy (CFL) condition, which constrains the time step based on the smallest grid spacing and maximum flow velocity [150]. While implicit schemes can alleviate this restriction, they introduce additional computational complexity through the need to solve large systems of equations at each time step [151].

Convergence acceleration techniques, including multigrid methods, implicit residual smoothing, and local time stepping, have been developed to improve the efficiency of steady-state simulations [152]. However, these approaches may not be directly applicable to time-accurate simulations required for capturing unsteady phenomena such as vortex shedding, rotor-stator interactions, and flow instabilities [153].

The computational demands of traditional methods have historically necessitated various simplifications and approximations in practical gas turbine simulations, including:

1. Sector simulations that model only a fraction of the full annulus, assuming circumferential periodicity [154]
2. Mixing plane interfaces between blade rows that average flow properties circumferentially, eliminating unsteady interactions [155]
3. Simplified or omitted geometric features such as fillets, cooling holes, and leakage paths [156]
4. Reduced domain simulations that focus on specific components rather than the integrated system [157]

While these simplifications have enabled practical application of CFD to gas turbine design, they inevitably introduce additional modeling uncertainties that limit predictive accuracy.

3.3.3. Turbulence Modeling Challenges

Perhaps the most fundamental limitation of traditional numerical approaches for gas turbine aerodynamics lies in their treatment of turbulence. The Reynolds-Averaged Navier-Stokes (RANS) approach, which forms the basis of most industrial gas turbine CFD, models the effect of all turbulent scales rather than resolving them directly [158]. This modeling introduces significant uncertainties, particularly for complex flows with features such as strong pressure gradients, curvature, rotation, separation, and transition that characterize gas turbine components [159].

Standard two-equation turbulence models, such as $k-\epsilon$ and $k-\omega$ SST, are calibrated primarily for simple canonical flows and may not accurately capture the physics of complex three-dimensional flows in gas turbines [160]. As noted by Durbin:

“RANS models contain empirical constants and functions that are calibrated for specific flow types. When applied to flows that differ significantly from the calibration cases, these models can produce substantial errors. Unfortunately, many flows in gas turbines fall into this category of complex, non-equilibrium turbulence that challenges standard modeling approaches.” [161]

Specific turbulence modeling challenges in gas turbine aerodynamics include:

1. **Transition prediction:** The laminar-to-turbulent transition process significantly impacts performance but is highly sensitive to factors including pressure gradients, freestream turbulence, surface roughness, and curvature. Traditional transition models struggle to accurately predict this process across the range of conditions encountered in gas turbines [162].
2. **Separation prediction:** Flow separation under adverse pressure gradients is notoriously difficult to predict accurately with RANS models, which tend to be overly optimistic about boundary layer attachment. This can lead to significant errors in loss prediction and flow structure identification [163].
3. **Secondary flow prediction:** The complex vortical structures that constitute secondary flows in turbomachinery passages are often inadequately captured by RANS models, which tend to underpredict their strength and dissipate them too rapidly [164].
4. **Rotation and curvature effects:** Standard turbulence models do not inherently account for the effects of strong curvature and rotation on turbulence structure, requiring corrections that introduce additional empiricism and uncertainty [165].
5. **Heat transfer prediction:** Accurate prediction of heat transfer coefficients, critical for thermal analysis of hot section components, remains challenging with RANS approaches, with errors of 30% or more not uncommon even for relatively simple configurations [166].

More advanced RANS approaches, including Reynolds stress models (RSM) that solve transport equations for the individual components of the Reynolds stress tensor, offer improved physical fidelity but at increased computational cost and with persistent challenges in numerical robustness [167]. Even these more sophisticated models retain fundamental limitations due to the inherent closure problem of turbulence and the challenge of developing universal models applicable across the diverse flow regimes in gas turbines [168].

3.3.4. Multi-Physics Coupling Difficulties

Modern gas turbine analysis increasingly requires consideration of coupled multi-physics phenomena, including fluid-structure interaction, conjugate heat transfer, combustion chemistry, and multi-phase flows [169]. Traditional numerical methods face significant challenges in effectively and efficiently coupling these diverse physical processes, which often operate across disparate time and length scales and may be governed by equations with fundamentally different mathematical characteristics [170].

Coupling strategies for multi-physics simulations typically fall into three categories:

1. **Monolithic approaches:** Solve all governing equations simultaneously within a unified framework, providing strong coupling but often resulting in ill-conditioned systems and specialized solvers that lack the optimization of single-physics codes [171].
2. **Partitioned approaches:** Solve each physical domain separately with specialized solvers and exchange information at interfaces, offering modularity and efficiency but potentially introducing splitting errors and stability issues for strongly coupled problems [172].
3. **Field transformation methods:** Map results from one physics domain to another through transfer functions or reduced-order models, providing computational efficiency at the cost of fidelity [173].

Each of these approaches involves trade-offs between accuracy, stability, computational efficiency, and implementation complexity that complicate their application to comprehensive gas turbine simulations [174].

Specific multi-physics coupling challenges in gas turbine aerodynamics include:

1. **Aerothermal coupling:** The interaction between hot gas path aerodynamics and component heat transfer, including the effects of cooling flows, thermal barrier coatings, and material conduction, spans multiple time scales and requires careful treatment of interface conditions [175].
2. **Aeromechanical coupling:** The interaction between aerodynamic forces and structural deformation, critical for predicting phenomena such as flutter and forced response, involves coupling between compressible flow solvers and structural dynamics codes with different numerical characteristics [176].
3. **Combustion-turbulence interaction:** The coupling between chemical reactions and turbulent mixing in combustors involves processes spanning time scales from nanoseconds (fast chemistry) to milliseconds (large-scale turbulence), presenting significant challenges for numerical integration [177].
4. **Particulate flows:** The interaction between the gas phase and particles or droplets in areas such as fuel sprays, erosion, and deposition requires specialized numerical treatments to account for momentum, heat, and mass transfer across phase boundaries [178].

Traditional segregated approaches to these multi-physics problems often involve significant simplifications and one-way coupling assumptions that limit their predictive capability for phenomena where strong bidirectional coupling exists [179].

The limitations discussed above have motivated the development of revolutionary numerical methods that aim to overcome these constraints and provide higher-fidelity simulations of gas turbine aerodynamics. These advanced approaches, including high-fidelity simulation techniques, novel turbulence modeling strategies, and integrated multi-physics frameworks, represent the cutting edge of computational gas turbine analysis and form the focus of subsequent sections of this review.

4. High-Fidelity Simulation Methods

The limitations of traditional numerical approaches have driven the development of high-fidelity simulation methods that aim to resolve, rather than model, a greater portion of the turbulent flow physics in gas turbines. These methods represent a revolutionary advancement in computational gas turbine aerodynamics, offering unprecedented insights into complex flow phenomena while presenting new challenges in terms of computational requirements and practical implementation.

4.1. Direct Numerical Simulation (DNS)

Direct Numerical Simulation (DNS) represents the highest fidelity approach to computational fluid dynamics, directly solving the Navier-Stokes equations without any turbulence modeling [180]. By resolving all relevant spatial and temporal scales of turbulent motion, from the largest energy-containing eddies down to the smallest Kolmogorov scales where viscous dissipation occurs, DNS provides the most complete and accurate representation of turbulent flows possible within the continuum mechanics framework [181].

4.1.1. Theoretical Foundation

The theoretical foundation of DNS lies in the complete, unfiltered, and unaveraged Navier-Stokes equations for compressible flow:

$$\frac{\partial \rho}{\partial t} + \nabla \cdot (\rho u) = 0$$

$$\frac{\partial(\rho u)}{\partial t} + \nabla \cdot (\rho u \otimes u) = -\nabla p + \nabla \cdot \tau$$

$$\frac{\partial(\rho E)}{\partial t} + \nabla \cdot (\rho u H) = \nabla \cdot (k \nabla T) + \nabla \cdot (\tau \cdot u)$$

where ρ is density, u is velocity, p is pressure, τ is the viscous stress tensor, E is total energy per unit mass, H is total enthalpy per unit mass, k is thermal conductivity, and T is temperature [182].

The distinguishing feature of DNS is that these equations are solved on a computational grid fine enough to resolve the smallest scales of turbulent motion, the Kolmogorov microscales, defined as:

$$\eta = \left(\frac{\nu^3}{\epsilon} \right)^{1/4}$$

where ν is the kinematic viscosity and ϵ is the turbulent dissipation rate [183]. The temporal resolution must similarly capture the fastest fluctuations, with time steps typically on the order of $\tau_\eta = (\nu/\epsilon)^{1/2}$.

For a three-dimensional simulation, the number of grid points required scales approximately with $Re^{9/4}$, where Re is the Reynolds number based on characteristic length and velocity scales [184]. This steep scaling relationship explains why DNS has historically been limited to relatively simple geometries and low Reynolds numbers compared to practical gas turbine applications.

4.1.2. Implementation Strategies

Implementing DNS for gas turbine flows requires careful consideration of numerical methods to ensure that the physical phenomena are accurately captured without being contaminated by numerical errors. Several key implementation aspects have been developed and refined over the past decades:

1. **High-order numerical schemes:** DNS typically employs high-order numerical methods (fourth-order or higher) to minimize numerical dispersion and dissipation that could corrupt the smallest scales of motion [185]. Spectral methods, which offer exponential convergence for smooth solutions, have been widely used for canonical configurations, while high-order finite difference and compact schemes are more common for complex geometries [186].
2. **Conservative formulations:** Ensuring discrete conservation of mass, momentum, and energy is critical for accurate DNS, particularly for compressible flows with shock waves or strong gradients [187]. Split forms of the convective terms that maintain kinetic energy conservation properties have proven beneficial for long-time integration stability [188].
3. **Time integration:** Explicit Runge-Kutta schemes of third or fourth order are commonly employed for time advancement in DNS, balancing accuracy and efficiency [189]. For cases with disparate time scales, semi-implicit approaches that treat stiff terms implicitly can alleviate severe time step restrictions [190].
4. **Boundary conditions:** Accurate representation of boundary conditions is crucial for DNS, particularly for wall-bounded flows characteristic of gas turbines [191]. No-slip, isothermal or adiabatic conditions are typically applied at solid boundaries, while carefully designed non-reflecting conditions are needed at artificial boundaries to prevent spurious reflections of acoustic and vortical waves [192].
5. **Initial conditions:** DNS results can be sensitive to initial conditions, particularly for transitional flows [193]. Synthetic turbulence generation methods that reproduce key statistical properties of turbulence have been developed to provide realistic initial conditions that minimize transient periods [194].

6. **Domain decomposition:** Given the enormous computational requirements, DNS codes must be highly parallelized using domain decomposition strategies that minimize communication overhead while maintaining load balance [195]. Hybrid MPI/OpenMP approaches and GPU acceleration have been increasingly adopted to leverage modern high-performance computing architectures [196].

4.1.3. Computational Requirements

The computational requirements for DNS of gas turbine flows are extremely demanding, representing one of the most computationally intensive applications in scientific computing. For a typical turbulent boundary layer at Reynolds numbers relevant to gas turbines, the number of grid points required can easily exceed 10^9 , with time steps on the order of nanoseconds for physical times spanning milliseconds or longer [197].

To illustrate these requirements, consider a DNS of flow over a low-pressure turbine blade at exit Reynolds number of 10^5 , which is at the lower end of the range for practical applications. Such a simulation would require approximately:

- Grid points: $10^9 - 10^{10}$
- Time steps: $10^5 - 10^6$
- Floating-point operations: $10^{19} - 10^{20}$
- Memory requirement: 10 - 100 TB

These estimates highlight why DNS has historically been limited to academic studies of simplified configurations rather than practical design applications [198]. However, the continued exponential growth in computing power, particularly with the advent of exascale systems capable of 10^{18} floating-point operations per second, is gradually expanding the feasibility of DNS for more realistic gas turbine configurations [199].

4.1.4. Applications and Limitations in Gas Turbine Context

Despite its computational demands, DNS has made significant contributions to gas turbine aerodynamics by providing fundamental insights into flow physics and high-fidelity validation data for lower-fidelity models. Key applications include:

1. **Transitional flows:** DNS has been instrumental in elucidating the mechanisms of boundary layer transition under conditions relevant to gas turbines, including the effects of freestream turbulence, pressure gradients, surface roughness, and curvature [200]. These studies have informed the development of improved transition models for RANS simulations used in design.
2. **Turbine blade aerodynamics:** DNS of flow over simplified turbine blade profiles has provided detailed information on loss generation mechanisms, secondary flow development, and heat transfer characteristics that has enhanced understanding of performance-limiting phenomena [201].
3. **Film cooling:** DNS of simplified film cooling configurations has revealed the complex mixing processes between coolant and mainstream flows, informing the development of improved cooling designs and more accurate predictive models for film cooling effectiveness [202].
4. **Combustion dynamics:** DNS of fundamental combustion processes relevant to gas turbine combustors has advanced understanding of turbulence-chemistry interactions, flame stabilization mechanisms, and pollutant formation pathways [203].

Despite these valuable contributions, DNS faces several fundamental limitations in the gas turbine context:

1. **Reynolds number gap:** The Reynolds numbers in practical gas turbines ($10^6 - 10^7$) remain orders of magnitude higher than what is feasible for DNS with current or near-future computing resources [204].

2. **Geometric complexity:** The intricate geometries of real gas turbine components, including cooling passages, fillets, tip clearances, and surface roughness, present significant challenges for the structured grids often preferred for high-order DNS [205].
3. **Multi-component integration:** DNS of isolated components provides limited insight into the system-level interactions that often dominate real gas turbine performance [206].
4. **Parametric studies:** The computational cost of DNS makes comprehensive parametric studies or design optimization impractical, limiting its direct application in the design process [207].

These limitations have motivated the development of alternative high-fidelity approaches that seek to balance physical fidelity with computational tractability, as discussed in the following sections.

4.2. Large Eddy Simulation (LES)

Large Eddy Simulation (LES) represents a compromise between the first-principles accuracy of DNS and the computational efficiency of RANS approaches. By directly resolving the large, energy-containing eddies while modeling the effect of smaller scales, LES provides high-fidelity representation of the dominant unsteady flow structures at a fraction of the computational cost of DNS [208].

4.2.1. Filtering Approach

The conceptual foundation of LES is the application of a spatial filtering operation to the Navier-Stokes equations, separating the resolved scales (large eddies) from the subgrid scales (small eddies). The filtered continuity and momentum equations for incompressible flow can be written as:

$$\frac{\partial \bar{u}_i}{\partial x_i} = 0$$

$$\frac{\partial \bar{u}_i}{\partial t} + \frac{\partial}{\partial x_j} (\bar{u}_i \bar{u}_j) = -\frac{1}{\rho} \frac{\partial \bar{p}}{\partial x_i} + \nu \frac{\partial^2 \bar{u}_i}{\partial x_j \partial x_j} - \frac{\partial \tau_{ij}}{\partial x_j}$$

where the overbar denotes the filtered quantity, and $\tau_{ij} = \overline{u_i u_j} - \bar{u}_i \bar{u}_j$ is the subgrid-scale (SGS) stress tensor that represents the effect of the unresolved scales on the resolved motion [209].

For compressible flows relevant to gas turbines, Favre filtering (density-weighted filtering) is typically employed to simplify the filtered equations:

$$\bar{u}_i = \frac{\overline{\rho u_i}}{\bar{\rho}}$$

This leads to the Favre-filtered Navier-Stokes equations with additional terms representing subgrid-scale effects on mass, momentum, and energy transport [210].

The filtering operation in LES is implicitly defined by the computational grid and numerical scheme in most practical implementations, with the filter width Δ typically proportional to the local grid spacing [211]. This implicit filtering approach simplifies implementation but complicates the theoretical analysis of numerical errors versus modeling errors.

4.2.2. Subgrid-Scale Modeling

The closure of the filtered equations requires modeling of the subgrid-scale stress tensor τ_{ij} to account for the effect of unresolved scales on the resolved flow. Numerous SGS models have been developed, with varying levels of complexity and physical fidelity:

1. **Smagorinsky model:** The classical approach relates the SGS stress tensor to the resolved strain rate tensor through an eddy viscosity formulation:

$$\tau_{ij} - \frac{1}{3} \tau_{kk} \delta_{ij} = -2\nu_{SGS} \dot{S}_{ij}$$

where \hat{S}_{ij} is the resolved strain rate tensor and $\nu_{SGS} = (C_s \Delta)^2 |\hat{S}|$ is the subgrid-scale viscosity, with C_s being the Smagorinsky constant [212]. While simple and robust, this model is overly dissipative in near-wall regions and transitional flows.

2. **Dynamic Smagorinsky model:** Proposed by Germano et al., this approach dynamically computes the model coefficient C_s based on information from the resolved scales using a test filtering operation [213]. This self-adapting feature significantly improves performance across diverse flow regimes but introduces computational overhead and potential numerical instabilities.
3. **Wall-Adapting Local Eddy-viscosity (WALE) model:** Designed to better capture near-wall behavior without dynamic procedures, this model modifies the velocity scale to account for both strain and rotation rates, naturally providing proper scaling near walls [214].
4. **Vreman model:** Offers a good balance between accuracy and computational efficiency, with automatic reduction of eddy viscosity in laminar and transitional regions without requiring test filtering operations [215].
5. **Approximate Deconvolution Model (ADM):** Takes a fundamentally different approach by approximately inverting the filtering operation to reconstruct the unfiltered velocity field, providing a more accurate representation of the SGS stresses with reduced modeling assumptions [216].
6. **Structural models:** Explicitly account for the structure of the SGS stress tensor rather than simply its dissipative effect, potentially capturing energy backscatter from small to large scales that eddy viscosity models cannot represent [217].

For gas turbine applications involving heat transfer and compressibility effects, additional SGS models are required for energy transport and equation of state nonlinearities [218]. These typically follow similar formulations to the momentum SGS models, often employing gradient diffusion hypotheses with turbulent Prandtl numbers [219].

4.2.3. Wall Treatment Methods

The near-wall region presents particular challenges for LES due to the fine grid resolution required to resolve the energetic structures in the boundary layer. The number of grid points needed for wall-resolved LES scales approximately with $Re^{1.8}$, which remains prohibitively expensive for high Reynolds number flows characteristic of gas turbines [220].

To address this challenge, several wall treatment approaches have been developed:

1. **Wall-resolved LES (WRLES):** Directly resolves the near-wall structures by employing sufficiently fine grid resolution, with $\Delta y^{+ \approx 1}$ for the first grid point and streamwise and spanwise resolutions of $\Delta x^{+ \approx 50}$ and $\Delta z^{+ \approx 15}$ [221]. While most accurate, this approach is computationally feasible only for moderate Reynolds numbers or limited domains.
2. **Wall-modeled LES (WMLES):** Uses coarser near-wall resolution and employs a wall model to account for the unresolved portion of the boundary layer [222]. Common approaches include:
 - a. **Equilibrium wall models:** Assume a local balance between pressure gradient, convection, and diffusion, effectively applying a law-of-the-wall formulation to relate wall shear stress to the velocity at the first off-wall grid point [223].
 - b. **Non-equilibrium wall models:** Solve simplified boundary layer equations on an embedded fine grid between the wall and the first LES grid point, accounting for pressure gradients, convection, and history effects [224].
 - c. **Hybrid RANS-LES approaches:** Use RANS in the near-wall region coupled with LES away from walls, discussed in more detail in Section 4.3 [225].
3. **Detached Eddy Simulation (DES):** A specific form of hybrid RANS-LES that treats the entire boundary layer with RANS and switches to LES mode in separated regions, offering significant computational savings for massively separated flows [226].

The choice of wall treatment significantly impacts both the computational cost and accuracy of LES for gas turbine applications. Wall-modeled approaches can reduce the computational cost by orders of magnitude compared to wall-resolved LES, making simulation of realistic configurations feasible, but introduce additional modeling uncertainties that may be significant for complex flows with strong pressure gradients, separation, or heat transfer [227].

4.2.4. Applications to Turbomachinery Flows

Despite its computational demands, LES has been increasingly applied to turbomachinery flows over the past two decades, providing valuable insights into complex flow phenomena that RANS models struggle to capture accurately. Key applications include:

1. **Compressor stall inception:** LES has elucidated the mechanisms of rotating stall inception in axial compressors, capturing the growth and propagation of stall cells and their interaction with tip clearance flows [228]. These simulations have revealed the importance of unsteady flow structures that are averaged out in RANS approaches.
2. **Turbine heat transfer:** LES of turbine blade cooling configurations has provided detailed information on heat transfer enhancement mechanisms, film cooling effectiveness, and thermal mixing processes that impact component durability [229]. The ability to resolve the unsteady mixing between coolant and mainstream flows offers significant advantages over RANS for these applications.
3. **Secondary flows:** LES has captured the development and interaction of secondary flow structures in turbomachinery passages with greater fidelity than RANS approaches, providing insights into loss generation mechanisms and potential design improvements [230].
4. **Combustor dynamics:** LES has become the method of choice for predicting combustion instabilities, flame dynamics, and pollutant formation in gas turbine combustors, where the strong coupling between turbulence, chemistry, and acoustics requires high-fidelity resolution of unsteady phenomena [231].
5. **Rotor-stator interaction:** LES has enabled detailed analysis of the unsteady flow structures generated by rotor-stator interactions, including potential field effects, wake chopping, and shock wave interactions that impact both aerodynamic performance and aeromechanical forcing [232].

Tucker provides a comprehensive assessment of the state of LES for turbomachinery applications:

“LES has matured to the point where it can provide valuable insights into complex turbomachinery flows that are difficult to capture with RANS approaches. However, the computational cost remains a significant barrier to routine application in the design process, particularly for high Reynolds number flows and multi-stage configurations. The development of more efficient wall treatment approaches and adaptive methods that focus computational resources on critical flow regions represents a promising path forward.” [233]

The computational requirements for LES of realistic gas turbine components remain substantial, typically requiring millions to billions of grid points and thousands of CPU-hours even with wall modeling approaches [234]. However, the continued growth in computing power and the development of more efficient numerical methods and wall treatments are gradually expanding the feasibility of LES for practical design applications.

4.3. Hybrid RANS-LES Methods

Hybrid RANS-LES methods represent a pragmatic compromise between the physical fidelity of LES and the computational efficiency of RANS approaches. By employing RANS in regions where it performs adequately (such as attached boundary layers) and LES in regions where unsteady

resolution is critical (such as separated flows and mixing regions), these methods offer a more practical approach to high-fidelity simulation of complex gas turbine flows [235].

4.3.1. Detached Eddy Simulation (DES)

Detached Eddy Simulation (DES), first proposed by Spalart et al. in 1997, represents the pioneering hybrid RANS-LES approach [236]. The original formulation, based on the Spalart-Allmaras turbulence model, modifies the length scale used in the destruction term of the turbulence transport equation:

$$\tilde{\alpha} = \min(d, C_{DES}\Delta)$$

where d is the wall distance, Δ is the local grid spacing (typically the maximum spacing in any direction), and C_{DES} is a calibration constant [237]. This modification causes the model to function as a standard RANS model near walls where $d < C_{DES}\Delta$ and as a subgrid-scale model away from walls where $d > C_{DES}\Delta$.

The original DES formulation encountered issues with “grid-induced separation,” where the model could prematurely switch to LES mode within attached boundary layers if the grid was refined for reasons other than capturing turbulent structures [238]. This led to the development of Delayed DES (DDES) and Improved DDES (IDDES), which incorporate shielding functions to ensure that attached boundary layers are treated with RANS regardless of grid spacing [239].

DES has been successfully applied to various gas turbine components, including:

1. **Compressor tip clearance flows:** Capturing the unsteady dynamics of tip leakage vortices and their role in loss generation and stall inception [240].
2. **Turbine blade trailing edge flows:** Resolving the vortex shedding and wake dynamics that impact profile losses and aeromechanical forcing [241].
3. **Combustor-turbine interaction:** Simulating the transport of temperature non-uniformities (hot streaks) from combustors to turbine sections and their impact on heat transfer and aerodynamics [242].

The primary advantages of DES include its relatively straightforward implementation within existing RANS frameworks and its significant computational savings compared to wall-resolved LES. However, challenges remain in the treatment of the RANS-LES interface region, where the sudden change in modeling approach can lead to artificial behavior in the resolved turbulence [243].

4.3.2. Scale-Adaptive Simulation (SAS)

Scale-Adaptive Simulation (SAS), developed by Menter and Egorov, takes a fundamentally different approach to hybridization by introducing additional source terms in the turbulence transport equations that are sensitive to resolved unsteadiness [244]. Unlike DES, which explicitly switches between RANS and LES based on grid spacing, SAS dynamically adjusts its behavior based on the detected flow instabilities.

The key innovation in SAS is the introduction of the von Kármán length scale into the turbulence scale equation:

$$L_{vK} = \kappa \frac{|\nabla U|}{|\nabla^2 U|}$$

where κ is the von Kármán constant, ∇U is the velocity gradient, and $\nabla^2 U$ is the second derivative of velocity [245]. This length scale provides information about the local flow structure that allows the model to reduce eddy viscosity in regions where resolved unsteadiness is detected.

The advantages of SAS include its reduced sensitivity to grid spacing compared to DES and its ability to smoothly transition between RANS and LES-like behavior based on the resolved flow physics rather than explicit grid-based switching [246]. This makes it particularly suitable for flows with varying degrees of instability, such as those encountered in different components of gas turbines.

Applications of SAS to gas turbine flows include:

1. **Compressor blade row interactions:** Capturing the unsteady wake transport and its impact on downstream blade rows without requiring excessively fine grids in the entire domain [247].
2. **Combustor flow dynamics:** Resolving the large-scale unsteady structures in swirl-stabilized combustors while maintaining computational efficiency [248].
3. **Turbine secondary flows:** Simulating the development of passage vortices and their interaction with blade boundary layers with improved accuracy compared to pure RANS approaches [249].

4.3.3. Zonal Approaches

Zonal hybrid approaches explicitly define different regions of the computational domain where either RANS or LES is applied, with special treatment at the interfaces between these regions [250]. This approach offers maximum flexibility in allocating computational resources but requires a priori knowledge of where high-fidelity resolution is needed.

Common zonal approaches include:

1. **Two-layer models:** Apply RANS in the near-wall region up to a specified distance and LES beyond that, with matching conditions at the interface [251].
2. **Domain decomposition:** Use RANS in certain components or regions (e.g., attached boundary layers) and LES in others (e.g., wakes, mixing regions), with interpolation at the interfaces [252].
3. **Embedded LES:** Apply LES in specific regions of interest within a larger RANS domain, with special treatment at the boundaries to generate resolved turbulence entering the LES region [253].

Zonal approaches have been applied to various gas turbine configurations, including:

1. **Film cooling:** Using LES to resolve the complex mixing between coolant and mainstream flows while treating the supply passages and far-field regions with RANS [254].
2. **Combustor-turbine interface:** Applying LES to the combustor and first turbine stage where unsteady interactions are critical, with RANS for downstream stages [255].
3. **Tip clearance flows:** Focusing LES resolution on the tip gap region while using RANS for the main passage flow [256].

The primary challenge in zonal approaches lies in the treatment of the RANS-LES interfaces, particularly when the flow crosses from a RANS region to an LES region. The RANS solution provides only mean flow information, lacking the resolved turbulent fluctuations needed for a proper LES inflow [257]. Various techniques have been developed to address this issue, including:

1. **Synthetic turbulence generation:** Creating artificial turbulent fluctuations at the RANS-LES interface based on the RANS turbulence quantities [258].
2. **Recycling methods:** Extracting turbulent fluctuations from a downstream location in the LES domain and reintroducing them at the interface, modified to match the local RANS statistics [259].
3. **Precursor simulations:** Running separate LES of canonical flows (e.g., channel flow, boundary layer) to generate realistic turbulent inflow conditions [260].

4.3.4. Interface Treatment Strategies

The treatment of interfaces between RANS and LES regions represents one of the most challenging aspects of hybrid methods, particularly for non-zonal approaches where these interfaces may not be explicitly defined [261]. Several strategies have been developed to address the issues that arise at these interfaces:

1. **Grey area mitigation:** Techniques to accelerate the development of resolved turbulence in the transition region from RANS to LES, reducing the extent of the “grey area” where neither model provides accurate predictions [262]. These include synthetic turbulence generation, controlled forcing, and enhanced SGS models in the transition region.

2. **Blending functions:** Smooth blending of RANS and LES contributions to avoid sharp discontinuities in the modeled stresses [263]. These approaches typically define a blending parameter that varies continuously from 0 (pure RANS) to 1 (pure LES) based on grid resolution, wall distance, or flow properties.
3. **Dynamic hybrid methods:** Approaches that dynamically adjust the RANS-LES blending based on the resolved turbulent content, grid resolution, and modeling error estimates [264]. These methods aim to optimize the distribution of computational resources by applying LES only where it provides significant benefits over RANS.
4. **Shielding functions:** Techniques to prevent the premature switching from RANS to LES within attached boundary layers, addressing the grid-induced separation issue encountered in early DES formulations [265].

The effectiveness of these interface treatment strategies significantly impacts the overall accuracy and reliability of hybrid RANS-LES simulations for gas turbine flows, particularly for cases involving complex geometries and multiple interacting flow features [266].

4.4. Multi-Fidelity Simulation Frameworks

The diverse components and flow regimes in gas turbines, coupled with varying requirements for physical fidelity and computational efficiency across different design stages, have motivated the development of multi-fidelity simulation frameworks that integrate multiple levels of modeling sophistication within a unified approach [267].

4.4.1. Coupling Methodologies

Multi-fidelity frameworks employ various coupling methodologies to integrate simulations of different fidelity levels:

1. **One-way coupling:** Information flows unidirectionally from higher-fidelity to lower-fidelity models or vice versa [268]. For example, RANS simulations of an entire gas turbine might provide boundary conditions for LES of specific components, or high-fidelity simulations of canonical configurations might inform the development of improved models for lower-fidelity approaches.
2. **Two-way coupling:** Information flows bidirectionally between models of different fidelity, allowing mutual influence [269]. This approach is particularly valuable for capturing feedback effects, such as the impact of downstream components on upstream flow conditions.
3. **Concurrent coupling:** Different fidelity models are executed simultaneously with regular exchange of information at their interfaces [270]. This approach provides the most consistent treatment of interactions between regions but requires careful synchronization of time steps and interface conditions.
4. **Sequential coupling:** Higher-fidelity simulations are used to calibrate or enhance lower-fidelity models, which are then applied to the full system [271]. This approach is computationally efficient but may not capture dynamic interactions between components.

4.4.2. Domain Decomposition Strategies

The decomposition of the computational domain for multi-fidelity simulations can follow various strategies:

1. **Component-based decomposition:** Different components of the gas turbine (compressor, combustor, turbine) are simulated with different fidelity levels based on their physical complexity and importance [272]. For example, LES might be applied to the combustor where turbulence-chemistry interactions are critical, while RANS is used for the compressor and turbine.

2. **Region-based decomposition:** Different regions within a single component are treated with different fidelity levels based on local flow complexity [273]. For example, near-wall regions might use RANS while free shear layers and separated regions use LES.
3. **Feature-based decomposition:** The fidelity level is adapted based on identified flow features such as vortices, shear layers, or shock waves [274]. This approach requires dynamic identification of these features during the simulation.
4. **Hierarchical decomposition:** A nested hierarchy of models with increasing fidelity is applied to progressively smaller regions of interest [275]. For example, a system-level reduced-order model might provide boundary conditions for a RANS simulation of a component, which in turn provides boundary conditions for LES of a critical subregion.

4.4.3. Information Transfer Techniques

The accurate and consistent transfer of information between regions of different fidelity represents a critical aspect of multi-fidelity frameworks. Several techniques have been developed:

1. **Conservative interpolation:** Ensures conservation of integral quantities (mass, momentum, energy) across interfaces between regions of different resolution or modeling approach [276].
2. **Characteristic-based coupling:** Decomposes the flow variables into characteristic waves at interfaces to prevent spurious reflections, particularly important for compressible flows [277].
3. **Overlapping grids:** Uses overlapping regions where both high and low fidelity models are applied, with gradual blending to smooth the transition [278].
4. **Dynamic downscaling:** Generates synthetic small-scale fluctuations when transferring information from low to high fidelity regions, based on the resolved larger scales and modeled turbulence quantities [279].
5. **Statistical coupling:** Transfers statistical information rather than instantaneous values, appropriate for interfaces between RANS and LES regions where time-averaging may be needed [280].

4.4.4. Computational Efficiency Considerations

The primary motivation for multi-fidelity frameworks is to optimize computational efficiency while maintaining adequate physical fidelity. Several strategies are employed to achieve this balance:

1. **Adaptive fidelity:** Dynamically adjusts the fidelity level based on error estimates, solution gradients, or other indicators of where higher resolution is needed [281].
2. **Reduced-order modeling:** Incorporates simplified models derived from high-fidelity simulations to efficiently represent certain components or phenomena [282].
3. **Machine learning augmentation:** Uses machine learning algorithms trained on high-fidelity data to enhance the accuracy of lower-fidelity models without their full computational cost [283].
4. **Time-scale bridging:** Employs different time steps or time-averaging approaches in different regions based on the characteristic time scales of the relevant phenomena [284].
5. **Hardware-aware implementation:** Optimizes the distribution of computational tasks across heterogeneous computing resources, assigning high-fidelity calculations to the most powerful processors [285].

Multi-fidelity simulation frameworks represent a promising approach for comprehensive analysis of gas turbine systems, potentially enabling high-fidelity simulation of critical phenomena while maintaining computational tractability. As noted by Deng et al.:

“Multi-fidelity simulation frameworks offer a pathway to leverage the strengths of different modeling approaches while mitigating their individual weaknesses. By applying high-fidelity methods selectively where they provide the greatest benefit, these frameworks can achieve an optimal balance between physical accuracy and computational efficiency for complex systems like gas turbines.” [286]

The continued development of these frameworks, coupled with advances in computational hardware and algorithms, is gradually expanding the scope and fidelity of comprehensive gas turbine simulations, bridging the gap between component-level analysis and system-level performance prediction.

5. Advanced Turbulence Modeling Approaches

Turbulence modeling remains one of the most challenging aspects of computational gas turbine aerodynamics, with profound implications for the accuracy and reliability of performance predictions. While high-fidelity simulation methods like DNS and LES offer improved physical fidelity, their computational demands limit their application to specific components or simplified configurations. Consequently, advanced turbulence modeling approaches that enhance the capabilities of more computationally efficient frameworks continue to be actively developed and refined for practical gas turbine applications.

5.1. Reynolds-Averaged Navier-Stokes (RANS) Models

Despite the emergence of higher-fidelity approaches, Reynolds-Averaged Navier-Stokes (RANS) models remain the workhorse of industrial gas turbine CFD due to their computational efficiency and robustness. Significant advancements have been made in RANS turbulence modeling to address the specific challenges of gas turbine flows, including strong pressure gradients, curvature, rotation, and transition.

5.1.1. Eddy Viscosity Models

Eddy viscosity models (EVMs) represent the most widely used class of RANS turbulence models, relating the Reynolds stresses to the mean strain rate through the Boussinesq approximation:

$$-\overline{\rho u'_i u'_j} = \mu_t \left(\frac{\partial U_i}{\partial x_j} + \frac{\partial U_j}{\partial x_i} \right) - \frac{2}{3} \rho k \delta_{ij}$$

where μ_t is the turbulent (eddy) viscosity and k is the turbulent kinetic energy [287]. The primary difference between various EVMs lies in how they determine the eddy viscosity.

k- ϵ Models

The standard k- ϵ model, developed by Launder and Spalding, solves transport equations for the turbulent kinetic energy (k) and its dissipation rate (ϵ), with the eddy viscosity defined as:

$$\mu_t = C_\mu \rho \frac{k^2}{\epsilon}$$

where C_μ is a model constant [288]. While widely used due to its robustness and reasonable accuracy for free shear flows, the standard k- ϵ model has well-documented deficiencies for flows with adverse pressure gradients, strong curvature, and rotation—all common features in gas turbines.

Several variants have been developed to address these limitations:

1. **RNG k- ϵ model:** Derived using renormalization group theory, this variant modifies the production term in the ϵ -equation to better account for rapid strain effects, improving predictions for flows with strong streamline curvature [289].
2. **Realizable k- ϵ model:** Ensures mathematical consistency by making C_μ variable rather than constant, preventing non-physical values of Reynolds stresses under certain strain conditions [290]. This modification improves predictions for separated flows and round jets relevant to combustor simulations.
3. **Low-Reynolds number k- ϵ models:** Incorporate damping functions to enable integration through the viscous sublayer without wall functions, improving heat transfer predictions critical for turbine cooling analysis [291].

Despite these improvements, k- ϵ models generally overpredict the turbulence kinetic energy in stagnation regions (leading to excessive heat transfer on leading edges) and struggle with accurate prediction of separation under adverse pressure gradients [292].

k- ω Models

The k- ω model family, pioneered by Wilcox, solves transport equations for turbulent kinetic energy (k) and specific dissipation rate ($\omega = \epsilon/k$), with the eddy viscosity defined as:

$$\mu_t = \rho \frac{k}{\omega}$$

The standard k- ω model offers improved performance for adverse pressure gradient flows and does not require damping functions for near-wall treatment, making it attractive for boundary layer flows in turbomachinery [293]. However, it exhibits high sensitivity to freestream values of ω , limiting its reliability for free shear flows.

The k- ω SST (Shear Stress Transport) model developed by Menter addresses this limitation by blending the k- ω formulation near walls with a transformed k- ϵ formulation in the free stream [294]. Additionally, it incorporates a limiter on the eddy viscosity to account for the transport of turbulent shear stress, improving separation prediction under adverse pressure gradients:

$$\mu_t = \frac{\rho a_1 k}{\max(a_1 \omega, \Omega F_2)}$$

where Ω is the vorticity magnitude and F_2 is a blending function [295].

The k- ω SST model has demonstrated superior performance for many gas turbine flows, particularly those involving separation, and has become the de facto standard for many industrial applications [296]. As noted by Menter et al.:

“The SST model combines the robust and accurate formulation of the k- ω model in the near-wall region with the free-stream independence of the k- ϵ model in the far field. This makes it particularly suitable for aerodynamic applications with adverse pressure gradients and separating flow, which are common features in turbomachinery.” [297]

Further refinements to the k- ω SST model for gas turbine applications include:

1. **SST-SAS (Scale-Adaptive Simulation)**: Incorporates additional source terms that enable the model to dynamically adjust its behavior based on resolved unsteadiness, providing LES-like behavior in unstable flow regions while maintaining RANS behavior in stable regions [298].
2. **SST-CC (Curvature Correction)**: Modifies the production term based on local flow curvature and rotation rate, improving predictions for the highly curved flows characteristic of turbomachinery passages [299].
3. **SST-RC (Rotation Correction)**: Accounts for system rotation effects on turbulence, critical for centrifugal compressors and rotating turbine passages [300].

Spalart-Allmaras Model

The Spalart-Allmaras (SA) model takes a different approach by solving a single transport equation for a modified eddy viscosity parameter ν , with the actual eddy viscosity given by:

$$\mu_t = \rho \nu f_{v1}$$

where f_{v1} is a damping function [301]. Originally developed for aerodynamic applications, the SA model offers good performance for attached boundary layers and mild separations with significantly lower computational cost than two-equation models.

The baseline SA model has been extended with various corrections for specific flow phenomena relevant to gas turbines:

1. **SA-RC (Rotation/Curvature)**: Incorporates a correction term that accounts for the effects of system rotation and streamline curvature [302].
2. **SA-DES (Detached Eddy Simulation)**: Modifies the length scale to enable LES-like behavior away from walls, forming the basis for the original DES approach [303].

3. **SA-neg:** Improves robustness for complex geometries by allowing negative values of the working variable during the solution process [304].

The SA model and its variants are particularly popular for external aerodynamics but have also found application in gas turbine simulations where computational efficiency is prioritized over capturing complex secondary flows [305].

5.1.2. Reynolds Stress Models

Reynolds Stress Models (RSMs) represent a higher level of closure by solving transport equations for each component of the Reynolds stress tensor rather than employing the Boussinesq approximation [306]. This approach naturally accounts for anisotropy of turbulence, streamline curvature, rotation, and complex strain fields—all important features in gas turbine flows.

The transport equation for the Reynolds stress tensor can be written as:

$$\frac{D}{Dt}(\overline{\rho u'_i u'_j}) = D_{ij} + P_{ij} + \Phi_{ij} - \varepsilon_{ij} + \Omega_{ij}$$

where D_{ij} represents diffusion, P_{ij} is production, Φ_{ij} is pressure-strain correlation, ε_{ij} is dissipation, and Ω_{ij} accounts for rotation effects [307]. The primary modeling challenge lies in the closure of the pressure-strain correlation term, which redistributes energy among the Reynolds stress components.

Several RSM variants have been applied to gas turbine flows:

1. **SSG (Speziale-Sarkar-Gatski) model:** Uses a quadratic form for the pressure-strain correlation, providing improved predictions for complex strain fields and rotating flows [308].
2. **LRR (Launder-Reece-Rodi) model:** Employs a simpler linear pressure-strain model but has been widely validated for engineering flows [309].
3. **Omega-based RSM:** Combines the Reynolds stress transport equations with an ω -equation for length scale determination, improving near-wall behavior without damping functions [310].

RSMs have demonstrated superior performance for flows with strong curvature, rotation, and secondary flows characteristic of turbomachinery passages [311]. As noted by Leschziner:

“Reynolds stress transport models offer clear advantages for flows dominated by anisotropic turbulence, strong streamline curvature, and system rotation. Their ability to naturally account for these effects without ad hoc corrections makes them particularly valuable for complex turbomachinery flows where secondary flows and stress-driven phenomena dominate.” [312]

However, the adoption of RSMs in industrial gas turbine CFD has been limited by several factors:

1. **Computational cost:** Solving for six Reynolds stress components plus a length scale equation increases computational requirements by 2-3 times compared to two-equation models [313].
2. **Numerical stability:** RSMs are generally less robust than eddy viscosity models, requiring careful initialization and solution strategies, particularly for complex geometries [314].
3. **Wall treatment:** Near-wall modeling remains challenging, with many implementations requiring complex damping functions or wall functions similar to eddy viscosity models [315].
4. **Limited improvement:** For certain flows, the practical improvement in accuracy over well-calibrated eddy viscosity models may not justify the increased computational cost and complexity [316].

Despite these challenges, RSMs continue to be developed and refined for gas turbine applications, particularly for cases where accurate prediction of secondary flows and anisotropic turbulence effects is critical for performance assessment [317].

5.1.3. Transition Modeling

The prediction of laminar-to-turbulent transition represents a particular challenge for RANS approaches, as the underlying physics involves complex, often bypass mechanisms triggered by factors including pressure gradients, freestream turbulence, surface roughness, and curvature [318]. Accurate transition prediction is critical for gas turbine aerodynamics, particularly for low-pressure turbine blades where significant portions of the boundary layer may be transitional at cruise conditions [319].

Several approaches have been developed for transition modeling within the RANS framework:

1. **Empirical correlation-based methods:** Apply criteria based on local momentum thickness Reynolds number and pressure gradient to trigger transition at specified locations [320]. While computationally efficient, these methods lack generality and struggle with complex geometries and three-dimensional flows.
2. **Intermittency transport models:** Solve an additional transport equation for intermittency (γ), which represents the fraction of time the flow is turbulent at a given location [321]. The intermittency is then used to modulate the turbulence production terms in the underlying turbulence model.
3. **γ - $Re\theta$ model:** Developed by Menter et al., this approach solves transport equations for both intermittency (γ) and transition momentum thickness Reynolds number ($Re\theta$), incorporating empirical correlations while maintaining local formulation suitable for modern CFD codes [322].
4. **Algebraic intermittency models:** Specify the intermittency distribution based on empirical functions of boundary layer parameters, offering computational efficiency with reasonable accuracy for attached flows [323].

The γ - $Re\theta$ model and its variants have gained particular traction for gas turbine applications due to their ability to handle various transition mechanisms relevant to turbomachinery, including:

1. **Natural transition:** Driven by the growth of Tollmien-Schlichting waves in low-turbulence environments [324].
2. **Bypass transition:** Triggered by high freestream turbulence levels typical in gas turbines, bypassing the linear instability phase [325].
3. **Separation-induced transition:** Occurring in the shear layer of laminar separation bubbles common on low-pressure turbine blades at off-design conditions [326].
4. **Wake-induced transition:** Caused by periodic impingement of upstream blade wakes, creating a distinctive pattern of transitional strips on downstream blades [327].

Recent advancements in transition modeling for gas turbines include:

1. **Local correlation-based models:** Reformulated to eliminate non-local operations, enabling application on unstructured grids and in parallel computing environments [328].
2. **Crossflow transition prediction:** Extended models that account for crossflow instabilities relevant to highly three-dimensional flows in turbomachinery [329].
3. **Roughness-induced transition:** Modifications to account for the effect of surface roughness, which can significantly impact transition location in real engine environments [330].
4. **Laminar kinetic energy models:** Incorporate the development of pre-transitional fluctuations through a laminar kinetic energy transport equation, improving prediction of bypass transition [331].

As noted by Langtry and Menter:

“Transition modeling represents one of the most challenging aspects of turbomachinery CFD, as it involves complex, often bypass mechanisms that traditional turbulence models cannot capture. The development of transport equation-based transition models has significantly improved the practical applicability of transition prediction in industrial CFD, enabling more accurate performance predictions for components where transitional effects are significant.” [332]

5.1.4. Rotation and Curvature Corrections

The effects of system rotation and streamline curvature on turbulence are particularly important in gas turbine flows, influencing both the mean flow development and turbulence structure in compressor and turbine passages [333]. Standard eddy viscosity models, based on the Boussinesq approximation, do not inherently account for these effects, leading to significant prediction errors for strongly curved or rotating flows [334].

Several correction approaches have been developed to address this limitation:

1. **Spalart-Shur rotation/curvature correction:** Introduces a multiplier to the production term based on the strain rate tensor, rotation rate tensor, and their material derivatives [335]. This correction has been implemented in various models including SA and SST, with the general form:

$$f_r = \max[\min(f_r, 1.25), 0.0]$$

where f_r is a function of strain rate, rotation rate, and their gradients [336].

2. **Richardson number corrections:** Modify the turbulent viscosity based on the gradient Richardson number, which quantifies the ratio of buoyancy effects (analogous to curvature) to shear production [337].
3. **Bifurcation approach:** Identifies the bifurcation surface in the phase space of the invariants of the anisotropy tensor and modifies model coefficients to account for stabilizing or destabilizing effects of rotation and curvature [338].
4. **Realizability-based corrections:** Ensure that model predictions remain physically realizable under strong rotation and curvature by limiting certain model coefficients based on local flow invariants [339].

These corrections have demonstrated significant improvements for specific gas turbine flows, including:

1. **Centrifugal compressor impellers:** Where strong curvature and rotation effects dominate the flow development and significantly impact performance prediction [340].
2. **Turbine blade passages:** Where the combination of strong convex and concave curvature affects secondary flow development and loss generation [341].
3. **Rotating cavities:** Where Coriolis and centrifugal forces create complex flow structures critical for internal cooling system performance [342].

As noted by Durbin:

“Rotation and curvature effects represent a fundamental challenge for eddy viscosity models due to their inherent limitations in accounting for frame-rotation effects on turbulence anisotropy. While various corrections have improved predictions for specific cases, they remain semi-empirical in nature and may require case-specific calibration for optimal performance.” [343]

The development of more general and physically consistent approaches to rotation and curvature effects remains an active area of research in turbulence modeling for gas turbine applications.

5.2. Scale-Resolving Simulation (SRS) Models

Scale-Resolving Simulation (SRS) models occupy the middle ground between fully-resolved approaches like DNS and LES and purely statistical approaches like RANS. These models aim to resolve the dominant, energy-containing turbulent structures while modeling the effect of smaller scales, offering improved physical fidelity compared to RANS with lower computational cost than wall-resolved LES [344].

5.2.1. Very Large Eddy Simulation (VLES)

Very Large Eddy Simulation (VLES) represents a class of approaches that resolve only the largest, most energetic eddies while modeling a greater portion of the turbulence spectrum compared to traditional LES [345]. This is typically achieved through a resolution control function that adjusts the model contribution based on the local grid resolution relative to the turbulent length scales.

The key concept in VLES is the introduction of a resolution control function F_r that modifies the subgrid-scale viscosity:

$$\nu_{sgs}^{VLES} = F_r \nu_{sgs}^{LES}$$

where F_r varies between 0 (DNS limit) and 1 (LES limit) based on the ratio of grid size to turbulent length scale [346]. As the grid becomes coarser relative to the turbulent scales, F_r increases, providing more modeling contribution to compensate for the reduced resolution.

Several VLES formulations have been proposed and applied to gas turbine flows:

1. **k- ϵ based VLES:** Modifies the standard k- ϵ model with a resolution function based on the ratio of grid size to turbulent length scale, enabling a smooth transition between RANS-like and LES-like behavior based on local grid resolution [347].
2. **Limited Numerical Scales (LNS):** Blends RANS and LES contributions based on the ratio of grid size to turbulent length scale, with a limiter function that ensures appropriate asymptotic behavior in both fine and coarse grid limits [348].
3. **Flow Simulation Methodology (FSM):** Applies a damping function to the turbulent length scale in a RANS model, with the damping dependent on the ratio of grid size to RANS length scale [349].

VLES approaches have shown promise for complex gas turbine flows where traditional LES would be prohibitively expensive, including:

1. **Combustor flows:** Where large-scale unsteady structures dominate mixing and flame dynamics, but near-wall resolution requirements would make wall-resolved LES impractical [350].
2. **Turbine blade cooling:** Where complex geometric features and multiple length scales characterize the flow, requiring selective resolution of dominant structures [351].
3. **Compressor tip clearance flows:** Where the interaction between tip leakage vortices and passage flow involves both large-scale structures and fine-scale turbulence [352].

The primary advantage of VLES approaches is their ability to automatically adapt the level of resolution based on local grid density, potentially offering a more continuous and physically consistent transition between resolved and modeled scales compared to hybrid RANS-LES methods with explicit switching mechanisms [353].

5.2.2. Partially-Averaged Navier-Stokes (PANS)

Partially-Averaged Navier-Stokes (PANS) represents a bridging approach between RANS and DNS, based on partial averaging of the Navier-Stokes equations [354]. Unlike VLES, which typically modifies existing LES models, PANS starts from RANS formulations and reduces the modeled contribution by specifying the unresolved-to-total ratios of turbulent kinetic energy (f_k) and dissipation (f_ϵ):

$$f_k = \frac{k_u}{k}$$

$$f_\epsilon = \frac{\epsilon_u}{\epsilon}$$

where subscript u denotes unresolved quantities [355]. These ratios can be specified as constants for the entire domain or, more effectively, as functions of local grid resolution and turbulence scales.

The PANS approach has been implemented with various underlying RANS models, including:

1. **PANS k- ϵ** : Modifies the standard k- ϵ equations by adjusting the model coefficients based on f_k and f_ϵ [356].
2. **PANS k- ω** : Adapts the k- ω framework to the partially-averaged approach, offering improved near-wall behavior [357].
3. **PANS SST**: Combines the SST blending approach with PANS methodology, providing robust performance across a range of flow regimes [358].

Applications of PANS to gas turbine flows include:

1. **Turbine blade trailing edge flows**: Where vortex shedding and wake dynamics significantly impact profile losses and heat transfer [359].
2. **Film cooling configurations**: Where the interaction between coolant jets and mainstream flow involves complex mixing processes across multiple scales [360].
3. **Combustor swirl flows**: Where large-scale precessing vortex cores interact with smaller-scale turbulence to influence flame stability and mixing [361].

The PANS approach offers several advantages for gas turbine applications:

1. **Physical consistency**: The formulation provides a theoretically consistent bridge between RANS and DNS, with well-defined limiting behaviors [362].
2. **Computational efficiency**: By selectively resolving only the portion of the turbulence spectrum that can be adequately captured by the grid, PANS optimizes computational resources [363].
3. **Flexibility**: The approach can be implemented with various underlying RANS models, leveraging their respective strengths for different flow regimes [364].

However, challenges remain in the specification of the unresolved-to-total ratios, particularly for complex geometries and flows with varying turbulence characteristics [365].

5.2.3. Limited Numerical Scales (LNS)

Limited Numerical Scales (LNS) represents another bridging approach that blends RANS and LES contributions based on the local grid resolution relative to the turbulent length scales [366]. The key concept is a blending function that determines the relative contribution of RANS and LES stresses:

$$\tau_{ij} = f_{LNS}\tau_{ij}^{RANS} + (1 - f_{LNS})\tau_{ij}^{LES}$$

where f_{LNS} is a function of the ratio between the grid size and the turbulent length scale [367].

The LNS approach differs from other bridging methods in its explicit blending of stress contributions rather than modification of model coefficients or length scales. This provides a more direct control over the transition between RANS and LES behaviors [368].

Applications of LNS to gas turbine flows include:

1. **Compressor blade boundary layers**: Where selective resolution of near-wall structures can improve prediction of separation and transition [369].
2. **Turbine internal cooling passages**: Where complex geometric features create a range of turbulent scales that benefit from adaptive resolution [370].
3. **Combustor liner flows**: Where the interaction between cooling films and mainstream flow involves multiple scale structures [371].

The LNS approach offers a conceptually simple framework for bridging between RANS and LES, with the potential for smooth transitions based on local grid resolution. However, the specification of appropriate blending functions remains challenging, particularly for flows with strong inhomogeneity and anisotropy [372].

5.2.4. Dynamic Hybrid RANS-LES Methods

Dynamic hybrid RANS-LES methods represent the latest evolution in scale-resolving approaches, incorporating dynamic procedures that automatically adjust the RANS-LES blending

based on local flow conditions and grid resolution [373]. Unlike earlier hybrid methods with fixed or grid-dependent switching criteria, these approaches continuously optimize the distribution of resolved and modeled turbulence based on solution-dependent parameters.

Key concepts in dynamic hybrid methods include:

1. **Dynamic resolution control:** Adjusts the resolved-to-modeled ratio based on estimates of the resolved turbulent kinetic energy and its dissipation, ensuring optimal use of available grid resolution [374].
2. **Error-driven adaptation:** Modifies the RANS-LES blending based on indicators of modeling error, directing computational resources to regions where improved resolution would most benefit solution accuracy [375].
3. **Scale-dependent dynamic procedures:** Extends the dynamic Smagorinsky concept to hybrid RANS-LES frameworks, using test filtering to optimize model coefficients locally [376].

Several dynamic hybrid formulations have been applied to gas turbine flows:

1. **Dynamic Hybrid RANS-LES (DHRL):** Dynamically adjusts the RANS-LES blending based on the resolved turbulence activity, with minimal resolved fluctuations triggering RANS mode and significant resolved activity promoting LES mode [377].
2. **Locally Dynamic k-equation Model (LDKM):** Solves a transport equation for subgrid kinetic energy with dynamically computed coefficients, providing a seamless transition between RANS and LES regions [378].
3. **Dynamic Delayed Detached Eddy Simulation (DDES):** Incorporates dynamic procedures into the DDES framework to optimize the RANS-LES interface location based on local flow conditions [379].

Applications of dynamic hybrid methods to gas turbine flows include:

1. **Multi-stage turbomachinery:** Where varying flow conditions across different components benefit from adaptive resolution strategies [380].
2. **Combustor-turbine interaction:** Where the transition from highly unsteady combustor flows to more structured turbine flows requires adaptive modeling approaches [381].
3. **Off-design operation:** Where changing flow regimes under different operating conditions benefit from dynamic adaptation of modeling strategy [382].

As noted by Simmonds:

“Dynamic hybrid RANS-LES turbulence models can help optimize turbulence simulations by using RANS modeling where there are relatively low amounts of resolved turbulent fluctuations, and LES modeling where significant turbulent fluctuations are resolved. This adaptive approach ensures computational resources are focused where they provide the greatest benefit to solution accuracy.” [383]

Dynamic hybrid methods represent a promising direction for scale-resolving simulations of gas turbine flows, potentially offering improved accuracy and efficiency compared to fixed-parameter approaches. However, they introduce additional complexity and computational overhead that must be balanced against their benefits for practical applications.

5.3. Machine Learning Enhanced Turbulence Models

The emergence of machine learning (ML) techniques has opened new frontiers in turbulence modeling for gas turbine aerodynamics. By leveraging data from high-fidelity simulations and experiments, ML approaches can potentially overcome limitations of traditional physics-based models while maintaining computational efficiency [384]. These methods represent a paradigm shift from purely analytical formulations to data-driven or hybrid approaches that combine physical constraints with statistical learning.

5.3.1. Data-Driven Turbulence Modeling

Data-driven turbulence modeling encompasses approaches that use machine learning algorithms to develop improved closure models based on high-fidelity data, typically from DNS or experiments [385]. These approaches can be categorized based on their integration with existing modeling frameworks:

1. **Field inversion:** Uses optimization techniques to infer spatial distributions of model discrepancies by minimizing differences between RANS predictions and high-fidelity data [386]. These discrepancies are then used to train machine learning algorithms that can predict similar corrections for new flows.
2. **Direct replacement:** Substitutes traditional algebraic or differential closures with machine learning models trained to predict Reynolds stresses or other closure terms directly from mean flow features [387].
3. **Augmentation:** Enhances existing models with machine learning corrections that account for effects not captured by the baseline formulation, such as pressure gradients, curvature, or non-equilibrium effects [388].

Several machine learning techniques have been applied to turbulence modeling for gas turbine flows:

1. **Random forests:** Ensemble learning methods that construct multiple decision trees during training and output the mean prediction of individual trees, offering good performance with relatively small training datasets [389].
2. **Neural networks:** Multi-layer perceptron or deep learning architectures that can capture complex nonlinear relationships between flow features and turbulence quantities [390].
3. **Gaussian process regression:** Probabilistic models that provide not only predictions but also uncertainty estimates, valuable for reliability assessment in critical applications [391].

Applications of data-driven turbulence modeling to gas turbine flows include:

1. **Compressor blade boundary layers:** Improving prediction of separation under adverse pressure gradients by learning from high-fidelity data of similar configurations [392].
2. **Turbine secondary flows:** Enhancing the representation of anisotropic turbulence in passage vortices and corner separations [393].
3. **Film cooling:** Improving mixing predictions between coolant and mainstream flows by learning from detailed experimental or DNS data [394].

The primary advantages of data-driven approaches include their ability to capture complex, non-linear relationships that may be difficult to express in analytical form and their potential to improve predictions without increasing computational cost once trained [395]. However, challenges remain in ensuring physical consistency, generalizability beyond training cases, and integration with existing CFD frameworks [396].

5.3.2. Physics-Informed Neural Networks

Physics-informed neural networks (PINNs) represent a hybrid approach that embeds physical constraints directly into the neural network architecture or loss function [397]. Unlike purely data-driven methods, PINNs incorporate known physical laws—such as conservation principles, realizability constraints, or dimensional consistency—to ensure that predictions remain physically meaningful even with limited training data.

Key concepts in physics-informed neural networks for turbulence modeling include:

1. **Invariance enforcement:** Ensuring that model predictions respect fundamental invariance properties, such as Galilean invariance, rotational invariance, and reflectional symmetry [398].
2. **Realizability constraints:** Incorporating constraints that ensure predictions satisfy mathematical properties required for physical consistency, such as positive definiteness of the Reynolds stress tensor [399].

3. **Conservation enforcement:** Including conservation laws as soft or hard constraints in the network formulation to ensure that predictions do not violate fundamental physical principles [400].

Several physics-informed approaches have been developed for turbulence modeling:

1. **Tensor basis neural networks:** Construct Reynolds stress predictions as expansions in a tensor basis, ensuring frame invariance while using neural networks to predict the scalar coefficients [401].
2. **Invariant embedding:** Transform input features into invariant scalars before processing with neural networks, ensuring that the resulting model respects fundamental symmetries [402].
3. **Constrained optimization:** Formulate the training process as a constrained optimization problem where physical constraints are enforced explicitly [403].

Applications of physics-informed neural networks to gas turbine flows include:

1. **Non-equilibrium boundary layers:** Improving predictions for rapidly changing flows such as those in transitional regions or after shock-boundary layer interactions [404].
2. **Strongly curved flows:** Enhancing models for flows with significant streamline curvature, such as in turbine blade passages [405].
3. **Rotating flows:** Developing improved representations of rotation effects on turbulence structure in centrifugal compressors and turbine disk cavities [406].

As noted by Duraisamy:

“Physics-informed machine learning approaches offer a promising path forward for turbulence modeling by combining the flexibility and expressive power of neural networks with the reliability and generalizability of physics-based constraints. This hybrid approach has the potential to overcome limitations of purely analytical models while avoiding the pitfalls of black-box data fitting.” [407]

5.3.3. Uncertainty Quantification Approaches

Uncertainty quantification (UQ) in turbulence modeling aims to characterize and quantify the uncertainties associated with model predictions, providing confidence intervals rather than single-point estimates [408]. Machine learning techniques have been increasingly integrated with UQ approaches to develop probabilistic turbulence models that provide not only improved predictions but also estimates of prediction reliability.

Key concepts in uncertainty quantification for turbulence modeling include:

1. **Aleatoric uncertainty:** Represents inherent variability in the physical system that cannot be reduced by improved modeling, such as cycle-to-cycle variations in combustion processes [409].
2. **Epistemic uncertainty:** Stems from limited knowledge or data and can potentially be reduced through improved models or additional information [410]. This includes model form uncertainty, parameter uncertainty, and numerical uncertainty.
3. **Ensemble methods:** Use multiple model formulations or parameter sets to generate a distribution of predictions, providing a measure of model-form uncertainty [411].

Several machine learning approaches have been integrated with UQ for turbulence modeling:

1. **Bayesian neural networks:** Replace deterministic weights with probability distributions, providing prediction intervals that reflect parameter uncertainty [412].
2. **Dropout as Bayesian approximation:** Uses dropout during inference to generate multiple predictions, approximating a Bayesian neural network at lower computational cost [413].
3. **Gaussian process regression:** Inherently provides uncertainty estimates along with predictions, making it particularly suitable for UQ applications [414].

Applications of uncertainty quantification to gas turbine flows include:

1. **Design margin assessment:** Quantifying the uncertainty in performance predictions to inform appropriate design margins for new components [415].

2. **Reliability analysis:** Estimating the probability of critical events such as compressor surge or excessive turbine blade temperatures [416].
3. **Experimental design:** Identifying regions of high uncertainty where additional experimental data would most effectively improve model reliability [417].

The integration of machine learning with uncertainty quantification offers significant potential for gas turbine aerodynamics, where design decisions often involve trade-offs between performance, reliability, and cost. By providing not only predictions but also confidence levels, these approaches enable more informed decision-making in the design process [418].

5.3.4. Model Form Uncertainty

Model form uncertainty represents a fundamental challenge in turbulence modeling, stemming from the inherent limitations of mathematical formulations in capturing the complex physics of turbulent flows [419]. Machine learning approaches offer new pathways for quantifying and reducing this uncertainty by identifying structural inadequacies in existing models and suggesting improvements.

Key approaches for addressing model form uncertainty include:

1. **Eigenspace perturbation:** Introduces perturbations to the eigenvalues and eigenvectors of the Reynolds stress tensor to explore the impact of structural uncertainties in the turbulence anisotropy [420].
2. **Transport equation augmentation:** Adds machine-learning-derived source terms to transport equations to compensate for missing physics in the baseline formulation [421].
3. **Discrepancy modeling:** Directly models the difference between RANS predictions and high-fidelity data, using machine learning to identify patterns in these discrepancies [422].

Applications of model form uncertainty analysis to gas turbine flows include:

1. **Secondary flow prediction:** Quantifying uncertainties in the prediction of passage vortices and corner separations due to limitations in turbulence anisotropy representation [423].
2. **Heat transfer forecasting:** Assessing the reliability of heat transfer predictions for turbine cooling design, where model form uncertainties can significantly impact component life estimates [424].
3. **Transition modeling:** Characterizing uncertainties in transition location prediction due to simplified representations of complex transition mechanisms [425].

As noted by Iaccarino et al.:

“Model form uncertainty represents the most challenging aspect of uncertainty quantification for turbulence modeling, as it stems from fundamental limitations in our mathematical representation of turbulent physics. Machine learning approaches offer a promising pathway for systematically identifying and addressing these structural inadequacies, potentially leading to more reliable and accurate predictions for complex flows.” [426]

The continued development of machine learning approaches for quantifying and reducing model form uncertainty represents a critical direction for improving the reliability of computational predictions for gas turbine aerodynamics.

5.4. Validation and Verification Methodologies

The development and application of advanced turbulence models for gas turbine aerodynamics require robust validation and verification methodologies to establish confidence in their predictions and define their range of applicability [427]. These methodologies have evolved significantly with the increasing sophistication of both computational approaches and experimental techniques.

5.4.1. Benchmark Cases

Benchmark cases provide standardized test problems for evaluating turbulence models, enabling consistent comparison across different formulations and implementations [428]. For gas turbine applications, several categories of benchmark cases have been established:

1. **Canonical flows:** Simple geometries with well-defined boundary conditions that isolate specific flow phenomena relevant to gas turbines, such as:
 - Flat plate boundary layers with pressure gradients [429]
 - Curved channel flows to evaluate curvature effects [430]
 - Rotating channel flows to assess rotation effects [431]
 - Backward-facing steps to test separation prediction [432]
2. **Simplified component geometries:** Idealized representations of gas turbine components that capture key flow features while maintaining well-defined conditions:
 - Linear and annular cascades of turbine or compressor airfoils [433]
 - Simplified film cooling configurations (flat plate with cooling holes) [434]
 - Model combustor geometries with well-characterized boundary conditions [435]
3. **Full component test cases:** Actual gas turbine components tested under controlled laboratory conditions:
 - Single-stage compressor or turbine rigs [436]
 - Combustor sector rigs with optical access [437]
 - Cooling system test facilities with detailed instrumentation [438]

The selection of appropriate benchmark cases depends on the specific aspects of turbulence modeling being evaluated and the intended application. A hierarchical approach often proves most effective, starting with canonical flows to isolate fundamental model behaviors before progressing to more complex configurations [439].

5.4.2. Experimental Validation Techniques

Experimental validation techniques for turbulence models have advanced significantly, providing increasingly detailed and accurate data for model assessment [440]. Modern experimental methods employed for gas turbine aerodynamics include:

1. **Particle Image Velocimetry (PIV):** Provides instantaneous velocity fields in a plane or volume, enabling statistical analysis of mean flows and turbulence quantities [441]. Stereoscopic and tomographic variants offer three-component velocity measurements critical for assessing complex three-dimensional flows in turbomachinery.
2. **Laser Doppler Velocimetry (LDV):** Offers high temporal resolution point measurements of velocity components and turbulence statistics, valuable for boundary layer and shear layer characterization [442].
3. **Hot-wire anemometry:** Provides high-frequency velocity measurements for spectral analysis and turbulence characterization, particularly useful for transition studies [443].
4. **Pressure-Sensitive Paint (PSP):** Enables surface pressure distribution measurements with high spatial resolution, valuable for validating pressure predictions on complex geometries [444].
5. **Temperature-Sensitive Paint (TSP):** Provides surface temperature distributions for heat transfer validation, critical for cooling system assessment [445].
6. **Infrared thermography:** Offers non-intrusive surface temperature measurements for heat transfer validation with high spatial resolution [446].
7. **Magnetic Resonance Velocimetry (MRV):** Provides three-dimensional, three-component mean velocity fields in complex internal geometries, particularly valuable for cooling passage flows [447].

The integration of multiple experimental techniques provides complementary data that can more comprehensively validate different aspects of turbulence model predictions [448]. Additionally,

uncertainty quantification in experimental measurements has become increasingly important for meaningful model validation, with modern techniques providing not only measured values but also confidence intervals [449].

5.4.3. Uncertainty Assessment

Uncertainty assessment in turbulence model validation involves quantifying and distinguishing between various sources of uncertainty that affect the comparison between computational predictions and experimental or high-fidelity numerical data [450]. Key aspects include:

1. **Numerical uncertainty:** Arises from discretization errors, iterative convergence limitations, and other numerical approximations [451]. Systematic grid refinement studies, convergence analysis, and code verification procedures are essential for quantifying these uncertainties.
2. **Input uncertainty:** Results from imperfect knowledge of boundary conditions, geometry details, material properties, and other simulation inputs [452]. Sensitivity analyses and uncertainty propagation techniques help assess the impact of these uncertainties on predictions.
3. **Model form uncertainty:** Stems from structural inadequacies in the turbulence model formulation, as discussed in Section 5.3.4 [453]. Ensemble approaches, eigenspace perturbation, and machine learning techniques provide frameworks for quantifying these uncertainties.
4. **Experimental uncertainty:** Includes measurement errors, limited spatial and temporal resolution, and intrusive effects of instrumentation [454]. Modern experimental techniques increasingly provide uncertainty estimates along with measured values.
5. **Aleatory uncertainty:** Represents inherent variability in the physical system, such as cycle-to-cycle variations in combustion processes or manufacturing variations in geometric details [455].

Comprehensive validation approaches account for these various uncertainty sources when comparing model predictions with reference data, often employing statistical frameworks that consider both simulation and experimental uncertainties [456]. Validation metrics that incorporate uncertainty information provide more meaningful assessments of model performance than simple error measures [457].

5.4.4. Best Practices for Turbulence Model Selection

The selection of appropriate turbulence models for gas turbine aerodynamics applications requires careful consideration of the specific flow physics, accuracy requirements, and computational constraints [458]. Several best practices have emerged from extensive experience in the field:

1. **Physics-based selection:** Choose models based on the dominant flow phenomena in the application rather than defaulting to a single “general-purpose” model [459]. For example:
 - $k-\omega$ SST for adverse pressure gradient flows and separation prediction
 - RSM for flows dominated by anisotropic turbulence and strong secondary flows
 - Scale-resolving approaches for flows where unsteady features significantly impact performance
2. **Hierarchical validation:** Validate model performance across a range of relevant test cases with increasing complexity, from canonical flows to component geometries [460].
3. **Sensitivity analysis:** Assess the sensitivity of critical outputs to turbulence model selection and parameters, identifying where model choice significantly impacts design decisions [461].
4. **Uncertainty-aware comparison:** When comparing different models, consider not only their absolute accuracy but also the uncertainty in their predictions, favoring models that provide reliable uncertainty estimates [462].
5. **Application-specific calibration:** For critical applications, consider calibrating model parameters using relevant experimental or high-fidelity data, while ensuring physical consistency is maintained [463].
6. **Multi-model approaches:** For high-consequence decisions, employ multiple turbulence models to generate a range of predictions, providing insight into model-form uncertainty [464].

7. **Continuous assessment:** Regularly reevaluate model performance as new validation data becomes available and new model formulations are developed [465].

As noted by Menter:

“No single turbulence model is optimal for all flow situations encountered in gas turbine aerodynamics. The selection of appropriate models should be guided by a thorough understanding of their theoretical foundations, validated range of applicability, and the specific flow physics relevant to the application. A systematic validation process using relevant test cases is essential for establishing confidence in model predictions.” [466]

The continued advancement of turbulence modeling for gas turbine aerodynamics will likely involve not only the development of improved models but also more sophisticated frameworks for model selection, validation, and uncertainty quantification that can guide the application of these models in practical design and analysis workflows.

6. Advanced Aerothermodynamic Analyses

The aerothermodynamic analysis of gas turbines represents one of the most challenging aspects of computational fluid dynamics, requiring the simultaneous consideration of complex flow physics, heat transfer mechanisms, and their intricate interactions. Modern gas turbines operate at increasingly demanding conditions, with turbine inlet temperatures exceeding 1700 K and pressure ratios approaching 50:1, necessitating sophisticated cooling strategies and advanced analytical capabilities to ensure component durability and optimal performance [467]. The revolutionary numerical methods discussed in previous sections have enabled unprecedented insights into these coupled phenomena, transforming our understanding of aerothermodynamic processes in gas turbines.

6.1. Conjugate Heat Transfer Modeling

Conjugate heat transfer (CHT) modeling represents a fundamental advancement in gas turbine thermal analysis, simultaneously solving the fluid flow equations in the gas and coolant domains coupled with heat conduction in the solid components [468]. This approach provides a more physically realistic representation of thermal processes compared to traditional methods that impose simplified boundary conditions or use heat transfer correlations derived from idealized configurations.

6.1.1. Fluid-Solid Thermal Interaction

The mathematical foundation of conjugate heat transfer modeling lies in the simultaneous solution of the energy equation in both fluid and solid domains, coupled through interface conditions that ensure continuity of temperature and heat flux [469]. In the fluid domain, the energy equation accounts for convective and diffusive transport:

$$\frac{\partial(\rho h)}{\partial t} + \nabla \cdot (\rho u h) = \nabla \cdot (k \nabla T) + \Phi + S_h$$

where h is enthalpy, k is thermal conductivity, Φ represents viscous dissipation, and S_h includes heat sources [470]. In the solid domain, the heat conduction equation governs temperature distribution:

$$\rho c_p \frac{\partial T}{\partial t} = \nabla \cdot (k_s \nabla T) + Q_s$$

where c_p is specific heat, k_s is solid thermal conductivity, and Q_s represents internal heat generation [471].

The coupling between fluid and solid domains occurs through interface boundary conditions that enforce:

1. **Temperature continuity:** $T_f = T_s$ at the interface
2. **Heat flux continuity:** $k_f \frac{\partial T_f}{\partial n} = k_s \frac{\partial T_s}{\partial n}$ at the interface

where subscripts f and s denote fluid and solid properties, respectively, and n is the normal direction to the interface [472].

The implementation of CHT modeling in gas turbine applications presents several unique challenges:

1. **Multi-scale heat transfer:** Gas turbine components involve heat transfer processes spanning multiple length scales, from millimeter-scale cooling holes to meter-scale component dimensions, requiring careful grid design and numerical treatment [473].
2. **Material property variations:** The extreme temperature ranges in gas turbines cause significant variations in material properties, particularly thermal conductivity and specific heat, which must be accurately represented in the solid domain [474].
3. **Complex geometries:** Modern gas turbine components incorporate intricate internal cooling passages, film cooling holes, and thermal barrier coatings that create complex thermal boundary conditions requiring sophisticated meshing strategies [475].
4. **Transient effects:** The thermal response of solid components is typically much slower than fluid processes, creating disparate time scales that complicate time-accurate simulations [476].

Recent advances in CHT modeling for gas turbines include the development of efficient coupling algorithms that minimize computational overhead while maintaining accuracy. Partitioned approaches that solve fluid and solid domains separately with interface data exchange have proven particularly effective for complex geometries [477]. As noted by Bohn et al.:

“Conjugate heat transfer modeling has revolutionized thermal analysis of gas turbine components by providing a physically consistent treatment of fluid-solid thermal interactions. This approach eliminates the need for empirical heat transfer correlations and enables accurate prediction of metal temperatures under realistic operating conditions, which is critical for component life assessment and cooling system optimization.” [478]

6.1.2. Interface Treatment Methods

The accurate treatment of fluid-solid interfaces represents a critical aspect of CHT modeling, particularly for gas turbine applications where complex geometries and disparate material properties create challenging numerical conditions [479]. Several interface treatment approaches have been developed to address these challenges:

1. **Conforming mesh approaches:** Use matching grids at fluid-solid interfaces, ensuring exact geometric representation and straightforward implementation of interface conditions [480]. While conceptually simple, this approach can be challenging for complex geometries and may require significant mesh generation effort.
2. **Non-conforming mesh methods:** Allow independent meshing of fluid and solid domains with interpolation procedures to transfer information across non-matching interfaces [481]. This approach offers greater flexibility in mesh generation but requires careful treatment of conservation properties and interface accuracy.
3. **Immersed boundary methods:** Represent solid boundaries implicitly within a Cartesian fluid grid, using forcing terms to impose boundary conditions [482]. These methods simplify mesh generation for complex geometries but may introduce accuracy limitations near interfaces.
4. **Overset grid techniques:** Employ overlapping grids for different components, with interpolation in overlap regions to exchange information [483]. This approach is particularly useful for moving boundaries or complex multi-component assemblies.

The choice of interface treatment method significantly impacts both computational efficiency and solution accuracy. For gas turbine applications, conforming mesh approaches are often preferred

for critical heat transfer regions, while non-conforming methods may be used for less critical areas to reduce mesh complexity [484].

Advanced interface treatment techniques for gas turbine CHT include:

1. **Adaptive interface refinement:** Dynamically refines the mesh near interfaces based on temperature gradients or heat flux distributions, optimizing computational resources [485].
2. **Multi-physics coupling:** Extends CHT to include additional physics such as thermal stress, phase change, or chemical reactions relevant to specific gas turbine applications [486].
3. **Uncertainty quantification:** Incorporates uncertainty in material properties, boundary conditions, and geometric tolerances into the CHT analysis, providing confidence bounds on thermal predictions [487].

6.1.3. Temporal Coupling Strategies

The temporal coupling of fluid and solid domains in CHT simulations presents unique challenges due to the disparate time scales involved [488]. Fluid processes typically occur on time scales of microseconds to milliseconds, while solid thermal diffusion occurs on time scales of seconds to minutes. This disparity necessitates specialized temporal coupling strategies to achieve computational efficiency while maintaining accuracy.

Several temporal coupling approaches have been developed:

1. **Explicit coupling:** Advances fluid and solid solutions simultaneously using the same time step, ensuring strong coupling but potentially requiring very small time steps to maintain stability [489].
2. **Implicit coupling:** Solves fluid and solid equations simultaneously at each time step, providing unconditional stability but requiring solution of large coupled systems [490].
3. **Subcycling:** Uses different time steps for fluid and solid domains, with multiple fluid time steps for each solid time step, balancing accuracy and efficiency [491].
4. **Quasi-steady approaches:** Assumes the solid domain reaches thermal equilibrium instantaneously with respect to fluid boundary conditions, appropriate for applications where solid thermal response is much faster than fluid transients [492].
5. **Periodic coupling:** For applications with periodic boundary conditions, couples domains only at specific phases of the cycle, reducing computational cost for cyclic processes [493].

The selection of appropriate temporal coupling strategies depends on the specific application and the relative importance of transient effects. For gas turbine startup and shutdown simulations, explicit or implicit coupling may be necessary to capture thermal transients accurately [494]. For steady-state or quasi-steady applications, subcycling or quasi-steady approaches may provide adequate accuracy with significant computational savings [495].

6.1.4. Applications to Cooled Turbine Components

Conjugate heat transfer modeling has found extensive application in the analysis of cooled turbine components, where accurate thermal prediction is critical for component life and performance [496]. Key applications include:

1. **Turbine blade cooling:** CHT analysis of turbine blades with internal cooling passages and film cooling provides detailed temperature distributions that inform cooling system design and life assessment [497]. Modern turbine blades incorporate complex internal geometries including serpentine passages, impingement cooling, and pin fin arrays that create intricate heat transfer patterns requiring high-fidelity CHT analysis.
2. **Combustor liner cooling:** The extreme thermal environment in combustors necessitates sophisticated cooling strategies that can be optimized using CHT modeling [498]. Applications include effusion cooling, impingement cooling, and transpiration cooling systems where the interaction between coolant and hot gas flows significantly impacts thermal performance.

3. **Turbine vane cooling:** Stationary turbine vanes often incorporate complex internal cooling circuits that can be analyzed using CHT to optimize coolant distribution and minimize thermal gradients [499].
4. **Disk and rotor cooling:** The thermal management of turbine disks and rotors involves complex interactions between hot gas ingestion, cooling air flows, and centrifugal effects that require CHT analysis for accurate prediction [500].

Recent advances in CHT modeling for cooled turbine components include:

1. **Multi-scale modeling:** Techniques that couple detailed CHT analysis of local features (such as cooling holes) with system-level thermal models to provide comprehensive component analysis [501].
2. **Optimization integration:** Coupling CHT solvers with optimization algorithms to automatically design cooling systems that meet thermal constraints while minimizing coolant usage [502].
3. **Uncertainty propagation:** Methods that propagate uncertainties in operating conditions, material properties, and geometric tolerances through CHT analysis to provide robust design margins [503].

As noted by Hylton et al.:

“Conjugate heat transfer modeling has become indispensable for modern gas turbine thermal design, enabling engineers to predict metal temperatures with unprecedented accuracy and optimize cooling systems for maximum efficiency. The ability to simultaneously consider fluid dynamics, heat transfer, and solid conduction has revolutionized our approach to thermal management in high-temperature turbomachinery.” [504]

6.2. Film Cooling and Internal Cooling Simulation

Film cooling represents one of the most critical thermal protection technologies in modern gas turbines, involving the injection of relatively cool air through discrete holes or slots to form a protective layer between hot combustion gases and component surfaces [505]. The effectiveness of film cooling depends on complex aerodynamic and thermal interactions that are challenging to predict accurately using traditional methods, making advanced numerical simulation essential for optimization and design.

6.2.1. Hole Geometry Effects

The geometry of film cooling holes significantly influences the aerodynamic behavior of coolant jets and their thermal protection effectiveness [506]. Traditional cylindrical holes, while simple to manufacture, often exhibit poor performance due to jet separation and kidney-shaped vortices that reduce surface coverage. Advanced hole geometries have been developed to improve cooling effectiveness:

1. **Shaped holes:** Feature expanded exits that reduce jet momentum and promote better surface attachment [507]. Common configurations include fan-shaped, laidback fan-shaped, and console holes that provide improved lateral spreading and reduced jet penetration.
2. **Compound angle holes:** Inject coolant at angles to both the surface normal and streamwise direction, enhancing lateral spreading and surface coverage [508].
3. **Micro-holes:** Use very small diameter holes with high density to create more uniform cooling films while reducing aerodynamic losses [509].
4. **Anti-vortex holes:** Incorporate secondary holes or geometric features designed to counteract the formation of kidney-shaped vortices that degrade cooling effectiveness [510].

The numerical simulation of these complex geometries requires high-resolution grids capable of resolving the detailed flow structures within and downstream of cooling holes. Large Eddy

Simulation has proven particularly valuable for capturing the unsteady mixing processes that govern film cooling effectiveness [511]. As noted by Bogard and Thole:

“The complex three-dimensional flow structures generated by film cooling holes, including counter-rotating vortex pairs, shear layer instabilities, and jet-crossflow interactions, require high-fidelity numerical methods to predict accurately. The development of advanced hole geometries has been greatly facilitated by detailed CFD analysis that can capture these complex flow phenomena.” [512]

Recent advances in film cooling hole design have been enabled by sophisticated numerical optimization techniques that can explore large design spaces while accounting for manufacturing constraints [513]. These approaches often couple high-fidelity CFD with surrogate modeling and genetic algorithms to identify optimal hole configurations for specific applications.

6.2.2. Blowing Ratio Influence

The blowing ratio, defined as the ratio of coolant mass flux to mainstream mass flux ($M = \rho_c u_c / \rho_\infty u_\infty$), represents a critical parameter governing film cooling performance [514]. The relationship between blowing ratio and cooling effectiveness is complex and non-monotonic, with optimal values depending on hole geometry, mainstream conditions, and surface curvature.

At low blowing ratios ($M < 0.5$), coolant jets typically remain attached to the surface, providing good thermal protection but limited downstream coverage [515]. As blowing ratio increases, jet momentum increases, leading to greater penetration into the mainstream and potential separation from the surface. At high blowing ratios ($M > 2.0$), jets may completely separate from the surface, creating regions of poor cooling effectiveness despite high coolant flow rates [516].

The numerical prediction of blowing ratio effects requires accurate modeling of:

1. **Jet-crossflow interaction:** The complex three-dimensional flow field created by the interaction between coolant jets and mainstream flow, including the formation of counter-rotating vortex pairs and horseshoe vortices [517].
2. **Turbulent mixing:** The mixing between coolant and mainstream flows, which determines the thermal boundary layer development and heat transfer characteristics [518].
3. **Surface curvature effects:** The influence of surface curvature on jet trajectory and mixing, particularly important for turbine blade applications where significant curvature is present [519].
4. **Compressibility effects:** At high mainstream Mach numbers, compressibility can significantly influence jet behavior and mixing characteristics [520].

Advanced numerical methods, particularly LES and hybrid RANS-LES approaches, have provided new insights into the physics of blowing ratio effects. These methods can capture the unsteady flow structures and mixing processes that govern film cooling effectiveness across the full range of blowing ratios [521].

6.2.3. Density Ratio Effects

The density ratio between coolant and mainstream flows ($DR = \rho_c / \rho_\infty$) significantly influences film cooling aerodynamics and thermal performance [522]. In actual gas turbines, density ratios typically range from 1.5 to 2.5 due to the temperature difference between coolant air and hot combustion gases. However, most experimental studies are conducted at unity density ratio due to practical limitations, creating a significant gap between laboratory data and engine conditions.

Density ratio effects manifest in several ways:

1. **Jet trajectory modification:** Higher density coolant exhibits reduced penetration into the mainstream due to lower momentum for a given mass flow rate [523].
2. **Mixing enhancement:** Density differences create additional instabilities that can enhance mixing between coolant and mainstream flows [524].

3. **Buoyancy effects:** In the presence of body forces or acceleration, density differences can create buoyancy-driven flows that influence cooling effectiveness [525].
4. **Shock interactions:** At high Mach numbers, density differences can influence shock formation and propagation in the cooling jet region [526].

The accurate numerical simulation of density ratio effects requires:

1. **Compressible flow formulation:** Proper treatment of density variations and their coupling with momentum and energy transport [527].
2. **Real gas properties:** Accurate representation of thermodynamic properties across the temperature range encountered in gas turbines [528].
3. **High-resolution schemes:** Numerical methods capable of accurately capturing density interfaces and mixing layers without excessive numerical diffusion [529].

Recent studies using DNS and LES have provided detailed insights into density ratio effects on film cooling, revealing complex interactions between density stratification, turbulent mixing, and heat transfer that were not captured by earlier RANS-based studies [530].

6.2.4. Advanced Cooling Configurations

Modern gas turbines employ increasingly sophisticated cooling configurations that go beyond simple film cooling to achieve the thermal protection required for high-temperature operation [531]. These advanced configurations often combine multiple cooling mechanisms and require sophisticated numerical analysis for optimization:

1. **Double-wall cooling:** Combines impingement cooling on the inner surface with film cooling on the outer surface, creating a complex thermal environment with multiple interacting flows [532]. The numerical simulation of double-wall systems requires modeling of:
 - Impingement jet arrays with complex crossflow interactions
 - Heat conduction through perforated walls with variable thickness
 - Film cooling effectiveness with non-uniform surface temperature distributions
 - Thermal stress distributions due to temperature gradients
2. **Transpiration cooling:** Involves the injection of coolant through porous walls, creating a distributed cooling effect that can be more effective than discrete film cooling [533]. Numerical modeling challenges include:
 - Porous media flow modeling with appropriate permeability and inertial resistance
 - Coupling between porous wall flow and external boundary layer development
 - Heat transfer enhancement due to distributed injection
 - Manufacturing constraints on pore size and distribution
3. **Effusion cooling:** Uses high-density arrays of small holes to create quasi-transpiration cooling effects while maintaining structural integrity [534]. Simulation requirements include:
 - High-resolution grids to resolve individual cooling holes
 - Interaction effects between closely spaced jets
 - Cumulative cooling effects downstream of hole arrays
 - Aerodynamic losses due to coolant injection
4. **Hybrid cooling systems:** Combine multiple cooling technologies in optimized configurations tailored to specific thermal environments [535]. Examples include:
 - Leading edge showerhead cooling combined with pressure surface film cooling
 - Internal serpentine cooling with trailing edge ejection
 - Thermal barrier coatings integrated with film cooling systems

The numerical analysis of these advanced cooling configurations often requires multi-scale modeling approaches that can capture both local heat transfer phenomena and system-level thermal performance [536]. As noted by Han et al.:

“Advanced cooling configurations in modern gas turbines require sophisticated numerical analysis that can capture the complex interactions between multiple cooling mechanisms. The development of these systems has been greatly facilitated by high-fidelity CFD that can predict the detailed thermal and aerodynamic performance of complex cooling geometries.” [537]

6.3. Multiphase Flow Modeling

Multiphase flows are prevalent throughout gas turbine systems, from fuel atomization and combustion in the combustor to particle ingestion and deposition in the compressor and turbine sections [538]. The accurate prediction of multiphase phenomena is critical for performance optimization, emissions reduction, and component durability assessment. Revolutionary numerical methods have significantly advanced our capability to model these complex flows with unprecedented fidelity.

6.3.1. Particle-Laden Flows

Particle-laden flows in gas turbines arise from various sources, including atmospheric dust ingestion, combustion products, and wear debris from component surfaces [539]. These particles can significantly impact performance through several mechanisms:

1. **Aerodynamic effects:** Particles modify the flow field through momentum exchange with the gas phase, potentially altering pressure distributions and boundary layer development [540].
2. **Heat transfer modification:** Particles can enhance or degrade heat transfer depending on their size, concentration, and thermal properties [541].
3. **Erosion and deposition:** Particle impacts on component surfaces can cause material removal (erosion) or accumulation (deposition), both of which degrade performance and reduce component life [542].

The numerical modeling of particle-laden flows employs several approaches depending on particle concentration and size distribution:

1. **Eulerian-Lagrangian methods:** Treat the gas phase as a continuum (Eulerian) while tracking individual particles or particle parcels (Lagrangian) [543]. This approach is well-suited for dilute particle flows where particle-particle interactions are negligible.
2. **Eulerian-Eulerian methods:** Treat both gas and particle phases as interpenetrating continua, solving conservation equations for each phase [544]. This approach is more efficient for dense particle flows but requires closure models for inter-phase interactions.
3. **Direct Numerical Simulation:** Resolves the flow around individual particles, providing the highest fidelity but limited to very small computational domains and particle numbers [545].
4. **Immersed boundary methods:** Represent particles as moving boundaries within the gas phase grid, offering a compromise between accuracy and computational efficiency [546].

For gas turbine applications, Eulerian-Lagrangian methods are most commonly employed due to the typically dilute nature of particle flows and the need to track particle trajectories for erosion and deposition prediction [547]. The particle equation of motion includes various forces:

$$m_p \frac{dv_p}{dt} = F_D + F_G + F_B + F_{VM} + F_{other}$$

where F_D is drag force, F_G is gravitational force, F_B is buoyancy force, F_{VM} is virtual mass force, and F_{other} includes additional forces such as thermophoresis and electrostatic effects [548].

Recent advances in particle-laden flow modeling for gas turbines include:

1. **High-fidelity particle tracking:** LES-based approaches that capture the effect of turbulent fluctuations on particle dispersion and deposition patterns [549].

2. **Particle-turbulence interaction:** Models that account for the two-way coupling between particles and turbulence, including turbulence modulation and preferential concentration effects [550].
3. **Non-spherical particle modeling:** Methods that account for particle shape effects on drag, lift, and orientation, important for realistic particle behavior prediction [551].
4. **Polydisperse modeling:** Techniques for handling particle size distributions rather than monodisperse assumptions, critical for realistic ingestion scenarios [552].

6.3.2. Droplet Evaporation and Combustion

Liquid fuel injection and combustion in gas turbine combustors involve complex multiphase processes including atomization, droplet transport, evaporation, and combustion [553]. The accurate modeling of these processes is critical for predicting combustion efficiency, emissions formation, and combustor durability.

The modeling of droplet-laden flows involves several key phenomena:

1. **Primary atomization:** The breakup of liquid jets into droplets, governed by complex instability mechanisms and influenced by injection conditions and ambient flow [554].
2. **Secondary atomization:** Further breakup of droplets due to aerodynamic forces, particularly important in high-velocity crossflow environments [555].
3. **Droplet evaporation:** Mass transfer from liquid droplets to the gas phase, coupled with heat transfer and influenced by ambient temperature, pressure, and composition [556].
4. **Droplet combustion:** Chemical reactions involving evaporated fuel, often occurring in the gas phase surrounding droplets or in the wake of evaporating droplets [557].

The mathematical modeling of droplet evaporation typically employs the D^2 law for spherical droplets:

$$\frac{d(D^2)}{dt} = -K$$

where D is droplet diameter, t is time, and K is the evaporation constant that depends on ambient conditions and fuel properties [558]. More sophisticated models account for non-spherical droplet shapes, internal circulation, and multi-component fuel effects.

Advanced numerical methods for droplet-laden combustion flows include:

1. **Large Eddy Simulation with Lagrangian particle tracking:** Captures the unsteady interactions between turbulent flow structures and droplet dynamics [559].
2. **Adaptive mesh refinement:** Dynamically refines the grid in regions of high droplet concentration or steep gradients to improve accuracy [560].
3. **Stochastic modeling:** Accounts for the random nature of turbulent dispersion and droplet breakup through Monte Carlo methods [561].
4. **Multi-scale modeling:** Couples detailed droplet-scale physics with system-level combustor performance models [562].

Recent developments in droplet combustion modeling include:

1. **Machine learning enhanced models:** Use data-driven approaches to improve submodels for droplet breakup, evaporation, and combustion [563].
2. **High-pressure effects:** Account for supercritical conditions that can occur in high-pressure combustors where traditional evaporation models break down [564].
3. **Alternative fuel modeling:** Extend models to handle biofuels, synthetic fuels, and hydrogen that have different physical and chemical properties than conventional jet fuel [565].

6.3.3. Erosion Prediction

Erosion of gas turbine components due to particle impact represents a significant operational concern, particularly for engines operating in dusty environments [566]. Accurate erosion prediction is essential for maintenance planning, component design, and operational decision-making.

The prediction of erosion involves several steps:

1. **Particle trajectory calculation:** Determining the paths of particles through the gas turbine, accounting for aerodynamic forces and turbulent dispersion [567].
2. **Impact parameter determination:** Calculating impact velocity, angle, and frequency for particles striking component surfaces [568].
3. **Erosion rate modeling:** Relating impact parameters to material removal rates using empirical or mechanistic models [569].
4. **Cumulative damage assessment:** Integrating erosion rates over time and particle size distributions to predict component life [570].

Erosion rate models typically take the form:

$$E = f(V, \alpha, d_p, \rho_p, H_t, \dots)$$

where E is erosion rate, V is impact velocity, α is impact angle, d_p is particle diameter, ρ_p is particle density, and H_t is target material hardness [571]. Various functional forms have been proposed, ranging from simple power laws to complex mechanistic models based on material science principles.

Advanced erosion prediction methods include:

1. **Probabilistic modeling:** Accounts for uncertainties in particle properties, operating conditions, and material behavior [572].
2. **Multi-scale approaches:** Couple molecular dynamics simulations of individual impacts with continuum-scale erosion prediction [573].
3. **Real-time monitoring integration:** Combine computational predictions with sensor data to update erosion models based on actual operating experience [574].
4. **Machine learning applications:** Use data-driven approaches to improve erosion models based on extensive experimental and operational databases [575].

6.3.4. Deposition Modeling

Particle deposition on gas turbine components can significantly degrade performance by altering surface roughness, blocking cooling holes, and changing aerodynamic shapes [576]. Unlike erosion, which removes material, deposition involves particle adhesion and accumulation on surfaces, creating complex feedback effects on flow and heat transfer.

The modeling of particle deposition involves several mechanisms:

1. **Thermophoresis:** Movement of particles due to temperature gradients, typically driving particles toward cooler surfaces [577].
2. **Impaction:** Direct collision of particles with surfaces due to their inertia in curved flow paths [578].
3. **Diffusion:** Random motion of small particles due to Brownian motion, important for submicron particles [579].
4. **Electrostatic effects:** Attraction or repulsion of charged particles by electric fields, which can be significant in certain operating conditions [580].

The sticking probability of particles upon impact depends on various factors:

$$P_{stick} = f(V_{impact}, T_{surface}, T_{particle}, \phi, \sigma, \dots)$$

where ϕ represents particle composition, σ is surface properties, and other variables influence the adhesion process [581].

Advanced deposition modeling approaches include:

1. **Dynamic surface evolution:** Tracks the evolution of surface geometry as deposition progresses, accounting for feedback effects on flow and further deposition [582].
2. **Multi-component modeling:** Considers the deposition of different particle types with varying sticking probabilities and thermal properties [583].
3. **Sintering and aging effects:** Models the evolution of deposited material properties over time due to high-temperature exposure [584].
4. **Cleaning mechanisms:** Incorporates natural cleaning processes such as particle re-entrainment and thermal spallation [585].

As noted by Dunn:

“Particle deposition in gas turbines represents a complex multiphase phenomenon that significantly impacts performance and operability. Advanced numerical modeling that can predict deposition patterns and their evolution over time is essential for developing effective mitigation strategies and optimizing maintenance schedules.” [586]

6.4. Combustion-Turbulence Interaction

The interaction between combustion and turbulence represents one of the most complex and challenging aspects of gas turbine aerothermodynamics [587]. In modern gas turbine combustors, turbulent mixing controls fuel-air preparation, flame stabilization, heat release rates, and pollutant formation, while combustion-generated heat release modifies the turbulent flow field through density changes, acceleration, and baroclinic effects [588]. Revolutionary numerical methods have provided unprecedented insights into these coupled phenomena, enabling the development of cleaner, more efficient combustion systems.

6.4.1. Flamelet Models

Flamelet models represent a powerful approach for modeling turbulent combustion by assuming that the local flame structure can be characterized by one-dimensional laminar flame solutions (flamelets) that are embedded within the turbulent flow field [589]. This approach separates the complex chemistry from the turbulent mixing, enabling efficient treatment of detailed chemical kinetics while maintaining computational tractability.

The fundamental assumption of flamelet modeling is that the local flame structure is determined by a small number of parameters, typically the mixture fraction (Z) and its dissipation rate (χ) [590]. The flamelet equations are derived from the full combustion equations by transforming to mixture fraction space:

$$\rho \frac{\partial Y_i}{\partial t} = \rho \frac{\chi}{2} \frac{\partial^2 Y_i}{\partial Z^2} + \dot{\omega}_i$$

where Y_i is the mass fraction of species i , and $\dot{\omega}_i$ is the chemical source term [591].

Several flamelet model variants have been developed for gas turbine applications:

1. **Steady flamelet model:** Assumes local chemical equilibrium with respect to mixing time scales, appropriate for fast chemistry regimes [592].
2. **Unsteady flamelet model:** Includes transient effects in the flamelet equations, capturing finite-rate chemistry effects important for pollutant formation [593].
3. **Flamelet/Progress Variable (FPV) model:** Introduces an additional progress variable to track reaction progress, enabling modeling of partially premixed and premixed flames [594].
4. **Conditional Source-term Estimation (CSE):** Uses conditional averaging to close chemical source terms, providing improved accuracy for complex chemistry [595].

The application of flamelet models to gas turbine combustors has provided significant insights into:

1. **Flame stabilization mechanisms:** Understanding how swirl-induced recirculation zones and pilot flames stabilize the main combustion process [596].

2. **Pollutant formation:** Predicting NO_x, CO, and unburned hydrocarbon emissions through detailed chemistry modeling [597].
3. **Combustion instabilities:** Analyzing the coupling between heat release fluctuations and acoustic modes that can lead to destructive oscillations [598].
4. **Fuel flexibility:** Assessing the impact of alternative fuels on combustion characteristics and emissions [599].

Recent advances in flamelet modeling include:

1. **Machine learning enhancement:** Using neural networks to accelerate chemistry tabulation and improve interpolation accuracy [600].
2. **Multi-regime modeling:** Extending flamelet approaches to handle transitions between different combustion regimes within a single combustor [601].
3. **Soot modeling integration:** Coupling flamelet models with detailed soot formation and oxidation mechanisms [602].

As noted by Peters:

“Flamelet models have revolutionized turbulent combustion modeling by enabling the treatment of detailed chemistry within computationally tractable frameworks. Their application to gas turbine combustors has provided fundamental insights into flame stabilization, pollutant formation, and combustion efficiency that have guided the development of cleaner, more efficient combustion systems.” [603]

6.4.2. Transported PDF Methods

Transported Probability Density Function (PDF) methods represent the most theoretically rigorous approach to turbulent combustion modeling, solving transport equations for the joint PDF of composition and enthalpy [604]. This approach provides exact treatment of chemical source terms without requiring closure models, making it particularly valuable for complex chemistry applications.

The transport equation for the joint PDF of composition and enthalpy can be written as:

$$\frac{\partial \rho \bar{f}}{\partial t} + \frac{\partial \rho \bar{u}_j \bar{f}}{\partial x_j} = - \frac{\partial}{\partial \psi_\alpha} [\rho \langle S_\alpha \rangle \psi \bar{f}] + \frac{\partial}{\partial x_j} [\rho \langle u_j'' \rangle \psi \bar{f}]$$

where \bar{f} is the Favre-averaged PDF, ψ is the composition vector, and S_α represents chemical source terms [605].

The key advantage of PDF methods is that chemical source terms appear in closed form, eliminating the need for turbulence-chemistry interaction models. However, the molecular mixing term requires closure, typically through models such as:

1. **Interaction by Exchange with the Mean (IEM):** Assumes mixing occurs through interaction with the mean composition [606].
2. **Modified Curl's model:** Models mixing as a coalescence-dispersion process between fluid particles [607].
3. **Euclidean Minimum Spanning Tree (EMST):** Uses geometric algorithms to determine mixing pairs based on composition space proximity [608].

The numerical solution of PDF transport equations is typically performed using Monte Carlo methods, where the PDF is represented by an ensemble of computational particles that evolve according to stochastic differential equations [609]. This approach naturally handles complex chemistry but requires careful treatment of statistical convergence and computational efficiency.

Applications of transported PDF methods to gas turbine combustion include:

1. **Autoignition modeling:** Predicting ignition delay times and autoignition locations in lean premixed combustors [610].
2. **Extinction and reignition:** Modeling local flame extinction and subsequent reignition processes that affect combustion stability [611].

3. **Pollutant formation:** Detailed prediction of NO_x formation pathways, including prompt, thermal, and fuel-bound nitrogen mechanisms [612].
4. **Supercritical combustion:** Modeling combustion at pressures above the critical point where traditional gas-phase assumptions break down [613].

Recent developments in PDF methods include:

1. **Sparse-Lagrangian approaches:** Reduce computational cost by using adaptive particle distributions that concentrate computational effort in important regions [614].
2. **Hybrid PDF-LES methods:** Combine the advantages of LES for turbulence resolution with PDF methods for chemistry treatment [615].
3. **Machine learning acceleration:** Use neural networks to accelerate mixing models and improve computational efficiency [616].

6.4.3. Chemical Kinetics Integration

The integration of detailed chemical kinetics into turbulent combustion simulations represents a significant computational challenge due to the wide range of time scales involved and the stiffness of the resulting differential equation systems [617]. Gas turbine combustion involves hundreds of chemical species and thousands of elementary reactions, creating systems of ordinary differential equations that are computationally expensive to solve.

Several approaches have been developed to address these challenges:

1. **Operator splitting:** Separates the chemistry integration from the flow solution, allowing specialized solvers for each process [618].
2. **Chemistry tabulation:** Pre-computes chemical states and stores them in lookup tables, reducing runtime chemistry calculations [619].
3. **Reduced mechanisms:** Simplifies detailed mechanisms by eliminating unimportant species and reactions while preserving essential combustion characteristics [620].
4. **Adaptive chemistry:** Dynamically adjusts the chemical mechanism complexity based on local conditions and accuracy requirements [621].

Modern chemistry integration methods for gas turbine applications include:

1. **In-Situ Adaptive Tabulation (ISAT):** Dynamically builds chemistry tables during the simulation, balancing accuracy and efficiency [622].
2. **Flamelet Generated Manifolds (FGM):** Uses flamelet solutions to construct low-dimensional manifolds that capture the essential chemistry [623].
3. **Principal Component Analysis (PCA):** Reduces the dimensionality of composition space by identifying the most important chemical modes [624].
4. **Artificial Neural Networks:** Train neural networks to approximate chemical source terms, providing fast evaluation during simulations [625].

The selection of appropriate chemistry integration methods depends on the specific application requirements:

1. **Accuracy requirements:** Applications requiring detailed pollutant predictions may necessitate full chemistry integration [626].
2. **Computational resources:** Limited computational budgets may require reduced mechanisms or tabulation approaches [627].
3. **Fuel composition:** Alternative fuels may require specialized mechanisms not available in reduced form [628].
4. **Operating conditions:** Extreme conditions (high pressure, low temperature) may require detailed chemistry to capture important phenomena [629].

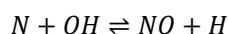
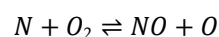
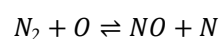
6.4.4. Emissions Prediction

The prediction of pollutant emissions from gas turbine combustors represents a critical application of advanced combustion modeling, driven by increasingly stringent environmental regulations and the need for cleaner propulsion and power generation systems [630]. The formation of major pollutants—nitrogen oxides (NO_x), carbon monoxide (CO), and unburned hydrocarbons (UHC)—involves complex chemical pathways that are strongly coupled with turbulent mixing and heat transfer processes.

Nitrogen Oxides (NO_x) Formation

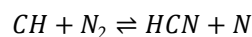
NO_x formation in gas turbine combustors occurs through several mechanisms:

1. **Thermal NO_x**: Formed through the extended Zeldovich mechanism at high temperatures:



This mechanism dominates in high-temperature regions and is strongly temperature-dependent [631].

2. **Prompt NO_x**: Formed through reactions involving hydrocarbon radicals:



This mechanism is important in fuel-rich regions and near flame fronts [632].

3. **Fuel NO_x**: Results from the oxidation of nitrogen-containing compounds in the fuel, important for certain alternative fuels [633].

The accurate prediction of NO_x formation requires detailed chemistry models that can capture the temperature and species concentration histories experienced by fluid elements as they pass through the combustor [634]. Advanced modeling approaches include:

1. **Conditional moment closure**: Provides detailed chemistry treatment while accounting for turbulent fluctuations [635].
2. **Large eddy simulation with detailed chemistry**: Resolves the large-scale mixing structures that control NO_x formation [636].
3. **Lagrangian particle tracking**: Follows fluid element histories to capture the integrated effect of temperature and composition variations [637].

Carbon Monoxide and Unburned Hydrocarbons

CO and UHC emissions result from incomplete combustion due to insufficient residence time, low temperatures, or poor mixing [638]. These emissions are particularly challenging to predict because they depend on the detailed flow patterns and mixing characteristics in the combustor, especially in regions where combustion is quenched or incomplete.

Key factors affecting CO and UHC formation include:

1. **Mixing quality**: Poor fuel-air mixing leads to locally rich or lean regions where combustion is incomplete [639].
2. **Residence time**: Insufficient time for complete oxidation, particularly important in compact combustor designs [640].
3. **Wall quenching**: Heat loss to combustor walls can quench reactions and increase CO and UHC emissions [641].
4. **Combustion instabilities**: Oscillatory combustion can create regions of incomplete burning [642].

Advanced modeling approaches for CO and UHC prediction include:

1. **Large eddy simulation with finite-rate chemistry:** Captures the unsteady mixing processes that control incomplete combustion [643].
2. **Conjugate heat transfer modeling:** Accounts for wall heat loss effects on local combustion efficiency [644].
3. **Multi-scale modeling:** Couples detailed combustor simulations with simplified system models to predict overall emissions [645].

Recent advances in emissions prediction include:

1. **Machine learning applications:** Use data-driven approaches to improve emissions models based on extensive experimental databases [646].
2. **Uncertainty quantification:** Provide confidence bounds on emissions predictions to account for modeling and operational uncertainties [647].
3. **Real-time optimization:** Integrate emissions models with control systems to optimize combustor operation for minimum emissions [648].

As noted by Lefebvre and Ballal:

“The prediction of pollutant emissions from gas turbine combustors requires sophisticated modeling that can capture the complex interactions between turbulent mixing, chemical kinetics, and heat transfer. Advanced numerical methods have significantly improved our ability to predict emissions, enabling the development of cleaner combustion systems that meet increasingly stringent environmental requirements.” [649]

The continued development of advanced combustion-turbulence interaction models, coupled with increasing computational resources and improved experimental validation data, promises further improvements in our ability to predict and control emissions from gas turbine combustors.

7. Practical Applications and Case Studies

The revolutionary numerical methods and advanced aerothermodynamic analyses discussed in previous sections have found extensive practical applications in gas turbine design, optimization, and operation. This section examines specific case studies that demonstrate the transformative impact of these technologies on real-world gas turbine development and performance enhancement.

7.1. Next-Generation Turbine Design

The application of high-fidelity simulation methods to next-generation turbine design has enabled unprecedented levels of performance optimization while meeting increasingly stringent efficiency and emissions requirements [650]. Modern turbine design processes integrate multiple advanced numerical techniques to achieve optimal aerodynamic and thermal performance.

7.1.1. Multi-Objective Design Optimization

Contemporary turbine design employs sophisticated multi-objective optimization frameworks that simultaneously consider aerodynamic efficiency, heat transfer characteristics, mechanical integrity, and manufacturing constraints [651]. These frameworks typically integrate:

1. **High-fidelity CFD analysis:** LES or hybrid RANS-LES simulations provide detailed flow field information for performance assessment [652].
2. **Conjugate heat transfer modeling:** Simultaneous solution of fluid flow and solid heat conduction enables accurate thermal design [653].
3. **Structural analysis:** Finite element analysis of thermal and mechanical stresses ensures component durability [654].
4. **Manufacturing constraint integration:** Geometric constraints based on manufacturing capabilities and tolerances [655].
5. **Multi-disciplinary optimization algorithms:** Advanced optimization techniques that can handle multiple objectives and constraints simultaneously [656].

A notable example is the development of the next-generation low-pressure turbine for the Rolls-Royce Trent XWB engine, where advanced CFD analysis enabled a 15% reduction in part count while maintaining aerodynamic performance [657]. The design process employed:

- Large eddy simulation to optimize blade loading distributions and minimize profile losses
- Conjugate heat transfer analysis to optimize cooling air usage
- Multi-objective genetic algorithms to explore the design space efficiently
- Uncertainty quantification to ensure robust performance across operating conditions

The integration of these advanced methods resulted in significant improvements in specific fuel consumption and reduced manufacturing complexity compared to previous generation designs [658].

7.1.2. Advanced Cooling System Design

The design of cooling systems for high-temperature turbine components represents one of the most challenging applications of advanced aerothermodynamic analysis [659]. Modern cooling system design employs sophisticated numerical methods to optimize thermal protection while minimizing coolant usage and aerodynamic penalties.

Recent developments in turbine cooling include:

1. **Additive manufacturing-enabled designs:** Complex internal cooling geometries that were previously impossible to manufacture, optimized using high-fidelity CHT analysis [660].
2. **Micro-channel cooling:** Arrays of small cooling channels that provide enhanced heat transfer with reduced coolant requirements [661].
3. **Impingement-film cooling integration:** Optimized combinations of impingement and film cooling that maximize thermal protection efficiency [662].
4. **Thermal barrier coating integration:** Coupled analysis of TBC thermal performance with underlying cooling systems [663].

A case study of advanced cooling system design is the development of the ceramic matrix composite (CMC) turbine vanes for the GE9X engine [664]. The design process involved:

- Detailed conjugate heat transfer analysis to predict temperature distributions in the CMC material
- Optimization of cooling hole patterns using genetic algorithms coupled with CFD
- Uncertainty quantification to account for manufacturing variations and material property uncertainties
- Multi-scale modeling to couple component-level thermal analysis with system-level performance models

The resulting design achieved a 200°F reduction in cooling air requirements compared to metallic designs while maintaining acceptable stress levels in the CMC material [665].

7.1.3. Aerodynamic Shape Optimization

Advanced numerical methods have revolutionized aerodynamic shape optimization for turbine components, enabling the exploration of complex three-dimensional geometries that would be impossible to evaluate using traditional methods [666]. Modern shape optimization approaches include:

1. **Adjoint-based optimization:** Efficient gradient computation for high-dimensional design spaces [667].
2. **Topology optimization:** Systematic exploration of optimal material distributions within design domains [668].
3. **Multi-fidelity optimization:** Integration of different fidelity levels to balance accuracy and computational efficiency [669].

4. **Robust design optimization:** Optimization under uncertainty to ensure performance robustness [670].

A significant application is the development of the transonic turbine blades for the Pratt & Whitney GTF engine, where advanced shape optimization techniques enabled:

- 3% improvement in stage efficiency through optimized blade loading distributions
- Reduced secondary flow losses through three-dimensional blade shaping
- Improved off-design performance through robust optimization techniques
- Integration of aerodynamic and mechanical constraints in the optimization process [671]

The optimization process employed high-fidelity RANS and LES simulations coupled with adjoint-based gradient computation, enabling the exploration of design spaces with hundreds of design variables [672].

7.2. Combustor Development

Advanced combustion modeling has played a crucial role in the development of next-generation combustors that meet stringent emissions requirements while maintaining high combustion efficiency and operability [673]. The integration of detailed chemistry modeling with high-fidelity turbulence simulation has enabled fundamental advances in combustor design.

7.2.1. Lean Burn Combustor Design

The development of lean burn combustors for reduced NO_x emissions represents a major application of advanced combustion-turbulence interaction modeling [674]. Lean burn combustors operate with excess air to reduce peak temperatures and thermal NO_x formation, but this creates challenges for flame stability and combustion efficiency.

Key design challenges addressed through advanced modeling include:

1. **Flame stabilization:** Ensuring stable combustion across the operating envelope while maintaining lean conditions [675].
2. **Mixing optimization:** Achieving rapid and uniform fuel-air mixing to prevent local hot spots [676].
3. **Autoignition control:** Preventing uncontrolled autoignition in the premixing section [677].
4. **Pattern factor optimization:** Achieving uniform temperature distributions at the combustor exit [678].

The development of the LEAP engine combustor by CFM International exemplifies the application of advanced combustion modeling [679]. The design process employed:

- Large eddy simulation with detailed chemistry to predict NO_x formation mechanisms
- Transported PDF methods to model autoignition and extinction phenomena
- Conjugate heat transfer analysis to optimize liner cooling
- Multi-objective optimization to balance emissions, efficiency, and operability

The resulting combustor achieved a 50% reduction in NO_x emissions compared to previous generation designs while maintaining excellent operability characteristics [680].

7.2.2. Alternative Fuel Compatibility

The increasing interest in sustainable aviation fuels (SAF) and hydrogen combustion has driven the development of advanced modeling capabilities for alternative fuel combustion [681]. These fuels present unique challenges due to their different physical and chemical properties compared to conventional jet fuel.

Key modeling challenges for alternative fuels include:

1. **Fuel property variations:** Accounting for different volatility, density, and chemical composition [682].

2. **Combustion kinetics:** Developing and validating chemical mechanisms for new fuel compositions [683].
3. **Emissions characteristics:** Predicting how alternative fuels affect pollutant formation pathways [684].
4. **Operability impacts:** Assessing effects on ignition, lean blowout, and combustion stability [685].
Recent applications include the development of hydrogen combustion systems for zero-emission aviation [686]. Advanced modeling approaches have been essential for:
 - Predicting hydrogen-air mixing and combustion characteristics
 - Assessing NO_x formation mechanisms specific to hydrogen combustion
 - Optimizing injector designs for hydrogen fuel systems
 - Evaluating safety considerations related to hydrogen combustion

The modeling efforts have employed detailed chemistry simulations with hundreds of species and thousands of reactions to capture the unique characteristics of hydrogen combustion [687].

7.2.3. Combustion Instability Mitigation

Combustion instabilities represent a major challenge in modern gas turbine combustors, potentially causing catastrophic damage if not properly controlled [688]. Advanced numerical methods have been instrumental in understanding and mitigating these instabilities.

Key aspects of combustion instability modeling include:

1. **Acoustic-flame coupling:** Understanding how acoustic waves interact with heat release fluctuations [689].
2. **Flame dynamics:** Predicting how flames respond to flow perturbations [690].
3. **System acoustics:** Modeling the acoustic characteristics of the entire combustor system [691].
4. **Control strategies:** Developing active and passive control methods to suppress instabilities [692].

A notable application is the development of instability mitigation strategies for the Siemens SGT-800 industrial gas turbine [693]. The analysis employed:

- Large eddy simulation to capture unsteady flame dynamics
- Acoustic analysis to identify resonant modes
- Flame transfer function modeling to quantify acoustic-flame coupling
- Control system design to implement active instability suppression

The resulting control system reduced instability amplitudes by over 90% while maintaining combustion efficiency and emissions performance [694].

7.3. Compressor Performance Enhancement

Advanced numerical methods have enabled significant improvements in compressor performance through better understanding of complex flow phenomena and optimization of component geometries [695]. Modern compressor design integrates high-fidelity simulation with sophisticated optimization techniques to achieve maximum efficiency and operability.

7.3.1. Stall and Surge Mitigation

Compressor stall and surge represent fundamental limitations on compressor performance and operability [696]. Advanced numerical methods have provided new insights into these phenomena and enabled the development of effective mitigation strategies.

Key applications include:

1. **Stall inception prediction:** Understanding the mechanisms that trigger rotating stall [697].
2. **Tip clearance optimization:** Minimizing losses while maintaining adequate clearances [698].
3. **Casing treatment design:** Developing passive flow control devices to extend the operating range [699].

4. **Active flow control:** Implementing active control systems to suppress stall inception [700].

The development of the advanced compressor for the Pratt & Whitney GTF engine employed extensive LES analysis to understand tip clearance flows and their role in stall inception [701]. The analysis revealed:

- Detailed structure of tip leakage vortices and their interaction with the main flow
- Mechanisms of stall cell formation and propagation
- Effectiveness of different casing treatment configurations
- Optimal control strategies for active stall suppression

The resulting compressor design achieved a 15% improvement in stall margin while maintaining high efficiency across the operating range [702].

7.3.2. Multi-Stage Interaction Effects

The interaction between multiple compressor stages creates complex unsteady flow phenomena that significantly impact performance [703]. Advanced numerical methods have enabled detailed analysis of these interactions and optimization of multi-stage configurations.

Key aspects of multi-stage interaction modeling include:

1. **Wake transport:** Tracking the evolution of upstream blade wakes through downstream stages [704].
2. **Potential field interactions:** Understanding how pressure fields from different blade rows interact [705].
3. **Secondary flow interactions:** Analyzing how secondary flows from different stages interact and accumulate [706].
4. **Clocking effects:** Optimizing the circumferential positioning of blade rows to minimize interactions [707].

A comprehensive study of the 10-stage compressor for the Rolls-Royce Trent 1000 engine employed time-accurate RANS simulations to analyze multi-stage interactions [708]. The analysis revealed:

- Optimal clocking positions that reduced unsteady loading by 20%
- Mechanisms of wake-shock interactions in transonic stages
- Accumulation of secondary flows through multiple stages
- Strategies for minimizing inter-stage flow distortions

The insights from this analysis led to design modifications that improved overall compressor efficiency by 1.2% [709].

7.3.3. Advanced Materials Integration

The integration of advanced materials such as ceramic matrix composites (CMCs) and titanium aluminides in compressor components has been enabled by sophisticated numerical analysis capabilities [710]. These materials offer significant weight and temperature advantages but require careful analysis to ensure structural integrity and performance.

Key modeling challenges include:

1. **Material property characterization:** Accounting for anisotropic and temperature-dependent properties [711].
2. **Thermal stress analysis:** Predicting stress distributions due to temperature gradients [712].
3. **Fatigue life prediction:** Assessing component durability under cyclic loading [713].
4. **Manufacturing constraint integration:** Accounting for material-specific manufacturing limitations [714].

The development of CMC compressor vanes for the GE9X engine required extensive multidisciplinary analysis [715]. The design process involved:

- Conjugate heat transfer analysis to predict temperature distributions

- Structural analysis with anisotropic material properties
- Probabilistic analysis to account for material property uncertainties
- Manufacturing process simulation to optimize fiber orientations

The resulting design achieved a 30% weight reduction compared to metallic alternatives while maintaining structural integrity under all operating conditions [716].

7.4. System-Level Integration

The integration of advanced numerical methods at the system level has enabled comprehensive analysis of entire gas turbine engines, providing insights into component interactions and overall performance optimization [717]. System-level modeling approaches combine high-fidelity component analysis with reduced-order models to achieve computational tractability while maintaining physical fidelity.

7.4.1. Component Interaction Modeling

Modern gas turbines involve complex interactions between components that significantly impact overall performance [718]. Advanced numerical methods have enabled detailed analysis of these interactions and optimization of system-level performance.

Key interaction phenomena include:

1. **Combustor-turbine interaction:** Transport of temperature and pressure disturbances from combustor to turbine [719].
2. **Compressor-combustor coupling:** Effects of compressor exit conditions on combustor performance [720].
3. **Turbine-exhaust system interaction:** Impact of exhaust system backpressure on turbine performance [721].
4. **Secondary air system integration:** Interaction between main gas path and cooling/sealing air systems [722].

The development of the integrated propulsion system for the Boeing 787 employed comprehensive system-level modeling [723]. The analysis included:

- Coupled combustor-turbine simulations to predict hot streak transport
- Compressor-combustor interface modeling to optimize pressure recovery
- Secondary air system analysis to minimize performance penalties
- Exhaust system optimization to reduce noise and emissions

The integrated analysis led to system-level optimizations that improved overall engine efficiency by 2.5% compared to component-optimized designs [724].

7.4.2. Digital Twin Development

The development of digital twins for gas turbine engines represents a major application of advanced numerical methods, enabling real-time performance monitoring and predictive maintenance [725]. Digital twins integrate high-fidelity physics-based models with real-time sensor data to provide accurate predictions of engine performance and health.

Key components of gas turbine digital twins include:

1. **Physics-based performance models:** Reduced-order models derived from high-fidelity CFD analysis [726].
2. **Component degradation models:** Models that predict how performance changes due to wear, fouling, and damage [727].
3. **Sensor data integration:** Algorithms that combine model predictions with real-time measurements [728].
4. **Uncertainty quantification:** Methods that provide confidence bounds on predictions [729].

The development of digital twins for the Rolls-Royce Trent series engines has employed extensive CFD analysis to create accurate reduced-order models [730]. The digital twin capabilities include:

- Real-time performance monitoring with 1% accuracy
- Predictive maintenance scheduling based on component health assessment
- Optimization of operating parameters for maximum efficiency
- Early detection of performance anomalies and potential failures

The digital twin implementation has resulted in 10% reduction in maintenance costs and 5% improvement in fuel efficiency through optimized operation [731].

7.4.3. Environmental Impact Assessment

Advanced numerical methods have enabled comprehensive assessment of the environmental impact of gas turbine engines, supporting the development of cleaner and more sustainable propulsion systems [732]. Environmental impact assessment involves detailed modeling of emissions formation, noise generation, and lifecycle effects.

Key aspects of environmental impact modeling include:

1. **Emissions prediction:** Detailed modeling of NO_x, CO, UHC, and particulate emissions [733].
2. **Noise modeling:** Prediction of combustion noise, jet noise, and fan noise [734].
3. **Lifecycle assessment:** Analysis of environmental impacts throughout the engine lifecycle [735].
4. **Alternative fuel assessment:** Evaluation of sustainable aviation fuels and hydrogen combustion [736].

The environmental impact assessment for the LEAP engine family employed comprehensive modeling approaches [737]. The analysis included:

- Detailed chemistry modeling to predict emissions across the flight envelope
- Acoustic analysis to predict noise characteristics
- Lifecycle assessment to evaluate overall environmental impact
- Alternative fuel compatibility analysis for sustainable aviation fuels

The assessment demonstrated significant environmental benefits, including 50% reduction in NO_x emissions and 15% reduction in fuel consumption compared to previous generation engines [738].

As noted by Cumpsty:

“The integration of advanced numerical methods at the system level has transformed gas turbine development from a component-centric approach to a truly integrated system optimization process. This holistic approach has enabled unprecedented improvements in performance, efficiency, and environmental impact while reducing development time and cost.” [739]

The continued advancement of system-level integration capabilities, coupled with increasing computational resources and improved modeling techniques, promises further improvements in gas turbine performance and environmental compatibility.

8. Discussion

The revolutionary numerical methods and advanced aerothermodynamic analyses presented in this review represent a paradigm shift in gas turbine aerodynamics research and development. The evolution from simplified analytical models to high-fidelity computational approaches has fundamentally transformed our understanding of complex flow phenomena and enabled unprecedented levels of design optimization and performance prediction.

8.1. Synthesis of Revolutionary Advances

The integration of high-fidelity simulation methods, advanced turbulence modeling, and sophisticated aerothermodynamic analyses has created a synergistic effect that extends far beyond the sum of individual technological advances [740]. This synthesis has enabled several breakthrough capabilities that were previously unattainable:

Multi-Physics Integration: The ability to simultaneously model fluid dynamics, heat transfer, combustion, and structural mechanics within unified frameworks has revealed complex coupling effects that were previously overlooked [741]. For example, the interaction between combustor temperature non-uniformities and turbine blade cooling effectiveness can now be predicted with sufficient accuracy to inform design decisions, leading to more robust and efficient cooling systems.

Scale-Bridging Capabilities: Modern numerical methods can now bridge multiple length and time scales, from molecular-level combustion processes to system-level performance characteristics [742]. This capability has been particularly transformative for understanding phenomena such as autoignition in lean premixed combustors, where molecular-scale chemistry couples with turbulent mixing at much larger scales.

Uncertainty Quantification Integration: The incorporation of uncertainty quantification into high-fidelity simulations has provided a more realistic assessment of prediction reliability, enabling risk-informed design decisions [743]. This advancement has been crucial for developing robust designs that maintain performance across manufacturing tolerances and operational variations.

Real-Time Optimization: The development of reduced-order models derived from high-fidelity simulations has enabled real-time optimization and control, bridging the gap between fundamental research and practical implementation [744]. Digital twin technologies exemplify this capability, providing continuous optimization of gas turbine operation based on real-time performance data.

8.2. Impact on Design Philosophy

The revolutionary numerical methods discussed in this review have fundamentally altered the design philosophy for gas turbine development, shifting from experience-based iterative approaches to physics-informed optimization strategies [745].

From Component to System Optimization: Traditional design approaches focused on optimizing individual components in isolation, often leading to suboptimal system-level performance [746]. Advanced numerical methods now enable true system-level optimization that accounts for complex component interactions and trade-offs. The development of the Pratt & Whitney GTF engine exemplifies this approach, where system-level optimization led to the revolutionary geared turbofan architecture that would not have been discovered through component-level optimization alone [747].

Predictive Rather Than Reactive Design: Historical design practices relied heavily on extensive testing and iterative refinement to address performance shortfalls discovered during development [748]. Modern high-fidelity simulation capabilities enable predictive design approaches that can identify and address potential issues before hardware fabrication, significantly reducing development time and cost while improving final performance.

Physics-Informed Design Exploration: Advanced numerical methods have expanded the design space that can be practically explored, enabling the investigation of unconventional configurations and operating strategies [749]. Additive manufacturing technologies, combined with high-fidelity thermal analysis, have enabled cooling system designs with complex internal geometries that would have been impossible to analyze using traditional methods.

Robust Design Under Uncertainty: The integration of uncertainty quantification with optimization has enabled the development of robust designs that maintain performance across a range of operating conditions and manufacturing variations [750]. This capability has been particularly important for developing gas turbines that can operate efficiently across diverse fuel compositions and environmental conditions.

8.3. Computational Challenges and Solutions

Despite the remarkable advances in numerical methods, significant computational challenges remain that continue to drive innovation in algorithms, hardware, and software architectures [751].

Scale Separation Challenges: Gas turbine flows involve phenomena spanning multiple orders of magnitude in both spatial and temporal scales, from turbulent eddies measured in micrometers to system-level flows spanning meters, and from acoustic oscillations occurring in microseconds to thermal transients lasting hours [752]. Current computational approaches often require compromises in scale resolution that can impact prediction accuracy for certain phenomena.

Recent advances in multi-scale modeling approaches have begun to address these challenges through adaptive mesh refinement, temporal subcycling, and hybrid modeling strategies that apply different levels of fidelity to different scales [753]. Machine learning techniques are also being explored to develop scale-bridging models that can capture the essential physics of unresolved scales without the computational cost of direct resolution.

Computational Resource Requirements: High-fidelity simulations of realistic gas turbine configurations continue to push the boundaries of available computational resources [754]. A wall-resolved LES of a complete gas turbine engine remains beyond current computational capabilities, requiring compromises in geometric fidelity, Reynolds number, or temporal resolution.

The emergence of exascale computing systems and specialized hardware architectures, including graphics processing units (GPUs) and tensor processing units (TPUs), is gradually expanding the feasible scope of high-fidelity simulations [755]. Additionally, cloud computing platforms are democratizing access to high-performance computing resources, enabling smaller organizations to leverage advanced simulation capabilities.

Algorithm Efficiency and Scalability: The development of efficient algorithms that can effectively utilize modern parallel computing architectures remains an active area of research [756]. Traditional CFD algorithms were developed for serial or modestly parallel computers and often do not scale efficiently to the massively parallel systems now available.

Recent advances in algorithm development include asynchronous communication strategies, task-based parallelism, and adaptive load balancing techniques that can better utilize modern computing architectures [757]. Machine learning approaches are also being explored to accelerate traditional algorithms through learned approximations of expensive computational kernels.

8.4. Validation and Verification Challenges

The increasing sophistication of numerical methods has created new challenges for validation and verification, particularly as simulations begin to provide insights into phenomena that are difficult or impossible to measure experimentally [758].

Experimental Validation Limitations: Many of the advanced phenomena that can now be predicted numerically occur under conditions that are challenging to replicate in laboratory experiments [759]. For example, the detailed structure of turbulent combustion at gas turbine operating pressures and temperatures is difficult to measure with sufficient spatial and temporal resolution to validate high-fidelity simulations.

The development of advanced experimental techniques, including high-speed diagnostics, non-intrusive measurement methods, and specialized test facilities, continues to expand the range of phenomena that can be experimentally validated [760]. Additionally, the use of simplified canonical configurations that isolate specific physical phenomena has proven valuable for validating individual aspects of complex numerical models.

Code Verification Challenges: The increasing complexity of numerical codes makes comprehensive verification increasingly challenging [761]. Modern CFD codes may contain millions of lines of code implementing numerous physical models, numerical schemes, and coupling algorithms, making it difficult to ensure that the code correctly implements the intended mathematical models.

Systematic code verification approaches, including the method of manufactured solutions, convergence studies, and comparison with analytical solutions, remain essential for establishing confidence in numerical implementations [762]. Additionally, the development of standardized test cases and benchmark problems has facilitated code comparison and verification across the research community.

Uncertainty Quantification Validation: The validation of uncertainty quantification methods presents unique challenges, as it requires not only that the mean predictions be accurate but also that the predicted uncertainty bounds correctly represent the actual uncertainty in the predictions [763]. This requires extensive validation studies with well-characterized experimental uncertainty and multiple independent measurements.

8.5. Industrial Implementation Challenges

The transition of advanced numerical methods from research tools to industrial design and analysis capabilities faces several practical challenges that continue to influence the pace of adoption [764].

Integration with Existing Workflows: Industrial gas turbine development involves complex workflows that integrate design, analysis, testing, and manufacturing processes [765]. The introduction of new numerical methods must be carefully integrated with existing processes to avoid disrupting established development timelines and quality assurance procedures.

Successful industrial implementation often requires the development of specialized interfaces, automated workflows, and training programs that enable engineers to effectively utilize advanced numerical capabilities [766]. The development of user-friendly software interfaces and automated analysis procedures has been crucial for enabling widespread adoption of advanced methods.

Computational Resource Management: Industrial organizations must balance the computational cost of advanced numerical methods against their benefits for specific applications [767]. This requires careful assessment of when high-fidelity methods provide sufficient additional value to justify their computational cost compared to lower-fidelity alternatives.

The development of adaptive fidelity approaches that automatically adjust the level of modeling sophistication based on local flow characteristics and accuracy requirements represents a promising direction for optimizing computational resource utilization [768].

Skill and Knowledge Requirements: The effective application of advanced numerical methods requires specialized knowledge and skills that may not be widely available within industrial organizations [769]. This creates challenges for recruiting and training personnel capable of effectively utilizing these advanced capabilities.

Educational initiatives, professional development programs, and collaboration with academic institutions have been important for developing the workforce capabilities needed to effectively utilize advanced numerical methods in industrial settings [770].

8.6. Emerging Paradigms

Several emerging paradigms are beginning to reshape the landscape of gas turbine aerodynamics research and development, building upon the revolutionary advances discussed in this review [771].

Physics-Informed Machine Learning: The integration of machine learning with physics-based models represents a promising direction for developing more efficient and accurate numerical methods [772]. Physics-informed neural networks that embed conservation laws and other physical constraints into their architecture can potentially provide the accuracy of high-fidelity methods with significantly reduced computational cost.

Early applications of physics-informed machine learning to gas turbine aerodynamics have shown promise for accelerating turbulence modeling, improving combustion chemistry integration, and developing real-time optimization algorithms [773]. However, significant challenges remain in

ensuring the generalizability and reliability of machine learning approaches for safety-critical applications.

Digital Twin Integration: The concept of digital twins that continuously update their predictions based on real-time sensor data represents a fundamental shift toward predictive rather than reactive maintenance and operation strategies [774]. Advanced numerical methods provide the physics-based foundation for digital twins, while machine learning techniques enable the integration of real-time data and adaptive model updating.

The development of comprehensive digital twins for gas turbine engines requires the integration of multiple physical models, uncertainty quantification, and real-time data processing capabilities [775]. This represents a significant systems engineering challenge that extends beyond the development of individual numerical methods.

Autonomous Design Optimization: The combination of advanced numerical methods with artificial intelligence and optimization algorithms is enabling increasingly autonomous design processes [776]. These systems can explore vast design spaces, identify optimal configurations, and even discover novel design concepts without direct human intervention.

The development of autonomous design systems requires careful consideration of design constraints, safety requirements, and manufacturing limitations [777]. Additionally, the integration of human expertise and judgment remains important for ensuring that autonomous systems produce practical and implementable designs.

Quantum Computing Applications: While still in early stages of development, quantum computing technologies may eventually provide new capabilities for solving certain classes of problems relevant to gas turbine aerodynamics [778]. Quantum algorithms for optimization, machine learning, and simulation of quantum mechanical systems could potentially address some of the computational challenges that currently limit the scope of high-fidelity simulations.

The practical application of quantum computing to gas turbine aerodynamics will likely require the development of hybrid classical-quantum algorithms that leverage the strengths of both computing paradigms [779]. Additionally, the development of quantum error correction and fault-tolerant quantum computers will be necessary for practical applications to complex engineering problems.

9. Conclusions

This comprehensive review has examined the revolutionary numerical methods that have transformed gas turbine aerodynamics research and development over the past several decades. The evolution from simplified analytical approaches to sophisticated high-fidelity simulations has fundamentally altered our understanding of complex flow phenomena and enabled unprecedented levels of design optimization and performance prediction.

9.1. Key Findings and Contributions

The analysis presented in this review reveals several key findings that highlight the transformative impact of revolutionary numerical methods on gas turbine aerodynamics:

Paradigm Shift in Modeling Capability: The transition from Reynolds-Averaged Navier-Stokes (RANS) approaches to scale-resolving methods such as Large Eddy Simulation (LES) and hybrid RANS-LES techniques has enabled the resolution of unsteady flow phenomena that were previously inaccessible [780]. This capability has been particularly transformative for understanding combustion instabilities, transition mechanisms, and complex secondary flows that significantly impact gas turbine performance.

Integration of Multi-Physics Phenomena: Advanced numerical methods have enabled the simultaneous modeling of fluid dynamics, heat transfer, combustion, and structural mechanics within unified frameworks [781]. This integration has revealed complex coupling effects that were previously overlooked, leading to more accurate performance predictions and more robust design strategies.

Unprecedented Design Optimization Capabilities: The combination of high-fidelity simulation with advanced optimization algorithms has enabled the exploration of design spaces that were previously inaccessible [782]. This capability has led to breakthrough designs such as additive manufacturing-enabled cooling systems and unconventional combustor configurations that achieve superior performance through physics-informed optimization.

Real-Time Operational Optimization: The development of reduced-order models derived from high-fidelity simulations has enabled real-time optimization and control capabilities [783]. Digital twin technologies exemplify this advancement, providing continuous optimization of gas turbine operation based on real-time performance data and predictive analytics.

Quantified Uncertainty and Risk Assessment: The integration of uncertainty quantification with high-fidelity simulations has provided more realistic assessments of prediction reliability [784]. This advancement has enabled risk-informed design decisions and the development of robust designs that maintain performance across manufacturing tolerances and operational variations.

9.2. Impact on Gas Turbine Technology

The revolutionary numerical methods examined in this review have had profound impacts on gas turbine technology development across multiple domains:

Performance Improvements: Advanced numerical methods have enabled performance improvements that would have been impossible using traditional design approaches [785]. Examples include the 15% fuel consumption reduction achieved by the Pratt & Whitney GTF engine through system-level optimization and the 50% NO_x reduction achieved by advanced lean burn combustors through detailed combustion modeling.

Accelerated Development Cycles: High-fidelity simulation capabilities have significantly reduced the time and cost required for gas turbine development by enabling predictive design approaches that minimize the need for extensive hardware testing [786]. This acceleration has been crucial for responding to rapidly evolving environmental regulations and market demands.

Enhanced Reliability and Durability: Advanced thermal and structural analysis capabilities have enabled the development of more reliable and durable gas turbine components [787]. Conjugate heat transfer modeling and life prediction algorithms have been particularly important for ensuring component integrity under increasingly demanding operating conditions.

Environmental Impact Reduction: Sophisticated combustion modeling has been instrumental in developing cleaner gas turbine technologies that meet stringent emissions requirements [788]. The ability to predict pollutant formation mechanisms with high fidelity has enabled the development of combustion systems that achieve ultra-low emissions while maintaining high efficiency.

9.3. Broader Scientific and Technological Implications

The advances in gas turbine aerodynamics reviewed in this paper have implications that extend beyond the specific domain of turbomachinery:

Computational Fluid Dynamics Advancement: Many of the numerical methods developed for gas turbine applications have found broader application in other fields of computational fluid dynamics [789]. Scale-resolving simulation methods, advanced turbulence models, and multi-physics coupling techniques developed for gas turbines have been adapted for applications ranging from automotive aerodynamics to renewable energy systems.

High-Performance Computing Utilization: The computational demands of gas turbine simulations have driven advances in high-performance computing algorithms and software architectures [790]. These advances have benefited the broader scientific computing community and have contributed to the effective utilization of emerging computing technologies such as GPU acceleration and exascale systems.

Machine Learning Integration: The integration of machine learning with physics-based modeling in gas turbine applications has pioneered approaches that are now being adopted across many engineering disciplines [791]. Physics-informed neural networks and other hybrid approaches

developed for turbomachinery applications are finding application in diverse fields from materials science to climate modeling.

Digital Twin Methodologies: The development of digital twin technologies for gas turbine engines has established methodologies and best practices that are being adapted for other complex engineering systems [792]. The integration of high-fidelity physics-based models with real-time data and uncertainty quantification represents a general framework for predictive maintenance and operational optimization.

9.4. Limitations and Ongoing Challenges

Despite the remarkable advances documented in this review, several limitations and challenges remain that continue to drive research and development efforts:

Computational Scale Limitations: Current computational capabilities still impose significant limitations on the scale and fidelity of simulations that can be practically performed [793]. Wall-resolved LES of complete gas turbine engines remains beyond current computational reach, requiring continued advances in both algorithms and hardware.

Model Validation Challenges: The increasing sophistication of numerical models has created new challenges for experimental validation, particularly for phenomena that occur under conditions that are difficult to replicate in laboratory settings [794]. This limitation necessitates continued investment in advanced experimental techniques and validation methodologies.

Industrial Implementation Barriers: The transition of advanced numerical methods from research tools to routine industrial use continues to face practical barriers related to computational cost, workflow integration, and workforce capabilities [795]. Addressing these barriers requires continued collaboration between research institutions and industrial organizations.

Uncertainty Quantification Maturity: While significant progress has been made in uncertainty quantification for gas turbine applications, many aspects of this field remain immature [796]. Improved methods for characterizing and propagating uncertainties, particularly model form uncertainties, are needed to fully realize the potential of uncertainty-aware design and operation.

9.5. Transformative Potential

The revolutionary numerical methods examined in this review possess transformative potential that extends beyond current applications:

Sustainable Aviation: Advanced numerical methods are essential for developing the next generation of sustainable aviation technologies, including hydrogen-powered aircraft, electric propulsion systems, and sustainable aviation fuels [797]. The ability to accurately model these emerging technologies will be crucial for achieving aviation industry sustainability goals.

Adaptive and Autonomous Systems: The integration of advanced numerical methods with artificial intelligence and machine learning is enabling the development of adaptive and autonomous gas turbine systems [798]. These systems can continuously optimize their performance based on changing operating conditions and mission requirements.

Revolutionary Design Concepts: The combination of high-fidelity simulation with advanced manufacturing technologies is enabling the exploration of revolutionary design concepts that were previously impossible to implement [799]. Examples include bio-inspired designs, metamaterial structures, and multi-functional components that integrate multiple capabilities.

System-of-Systems Integration: Advanced numerical methods are enabling the analysis and optimization of gas turbines as components within larger systems-of-systems, including aircraft, power plants, and energy networks [800]. This capability is essential for optimizing overall system performance and enabling new operational paradigms.

As noted by Cumpsty in his seminal work on gas turbine aerodynamics:

“The revolution in numerical methods has not merely improved our ability to analyze existing designs; it has fundamentally changed what is possible in gas turbine technology.

We are now limited more by our imagination and manufacturing capabilities than by our ability to predict and optimize performance.” [801]

The revolutionary numerical methods reviewed in this paper represent a foundation for continued innovation in gas turbine technology. As computational capabilities continue to advance and new methodologies are developed, we can expect further transformative advances that will enable cleaner, more efficient, and more capable gas turbine systems. The integration of these advanced numerical capabilities with emerging technologies such as artificial intelligence, quantum computing, and advanced manufacturing will likely produce innovations that are difficult to envision from our current perspective.

The journey from the early potential flow methods of the 1970s to the sophisticated multi-physics simulations of today represents one of the most remarkable technological transformations in engineering history. This transformation has not only revolutionized gas turbine technology but has also established methodologies and capabilities that continue to drive innovation across numerous engineering disciplines. The future promises even more dramatic advances as these revolutionary numerical methods continue to evolve and mature.

10. Future Directions and Research Opportunities

The revolutionary numerical methods examined in this review have established a strong foundation for continued innovation in gas turbine aerodynamics. However, emerging challenges and opportunities are creating new research directions that promise to further transform the field over the coming decades.

10.1. Next-Generation Computational Paradigms

The evolution of computational paradigms continues to create new opportunities for advancing gas turbine aerodynamics research and development [802].

Exascale Computing Integration: The emergence of exascale computing systems capable of performing 10^{18} floating-point operations per second is creating unprecedented opportunities for high-fidelity simulation of complete gas turbine systems [803]. These systems will enable wall-resolved LES of entire engines, multi-physics simulations that capture all relevant coupling effects, and ensemble simulations that provide comprehensive uncertainty quantification.

The effective utilization of exascale systems will require the development of new algorithms that can efficiently utilize millions of processing cores while maintaining numerical accuracy and stability [804]. This includes the development of asynchronous communication strategies, fault-tolerant algorithms, and adaptive load balancing techniques that can handle the complexity of exascale architectures.

Quantum Computing Applications: While still in early stages of development, quantum computing technologies offer potential advantages for certain classes of problems relevant to gas turbine aerodynamics [805]. Quantum algorithms for optimization, machine learning, and simulation of quantum mechanical systems could address some of the computational challenges that currently limit the scope of high-fidelity simulations.

Near-term applications of quantum computing to gas turbine aerodynamics may include quantum-enhanced optimization algorithms for design problems and quantum machine learning approaches for developing improved turbulence models [806]. Longer-term applications could include quantum simulation of combustion chemistry and quantum algorithms for solving large-scale linear systems arising in CFD applications.

Neuromorphic Computing: Neuromorphic computing architectures that mimic the structure and function of biological neural networks offer potential advantages for certain types of computational problems [807]. These architectures could be particularly valuable for real-time control applications, adaptive mesh refinement, and machine learning-enhanced turbulence modeling.

The development of neuromorphic computing applications for gas turbine aerodynamics will require new algorithmic approaches that can effectively utilize the unique capabilities of these architectures [808]. This includes the development of spiking neural network models for turbulence prediction and event-driven algorithms for adaptive simulation control.

10.2. Artificial Intelligence and Machine Learning Integration

The integration of artificial intelligence and machine learning with traditional numerical methods represents one of the most promising directions for future advancement [809].

Physics-Informed Deep Learning: The development of deep learning architectures that embed physical constraints and conservation laws represents a promising approach for developing more efficient and accurate numerical methods [810]. Physics-informed neural networks (PINNs) that can solve partial differential equations while respecting physical constraints offer potential advantages for both forward simulation and inverse design problems.

Future developments in physics-informed deep learning may include the development of neural network architectures specifically designed for turbulent flow problems, multi-scale neural networks that can handle the scale separation challenges in gas turbine flows, and uncertainty-aware neural networks that provide reliable confidence estimates [811].

Automated Model Discovery: Machine learning techniques for automated discovery of mathematical models from data offer potential for developing improved turbulence models and combustion chemistry mechanisms [812]. These approaches could identify new functional forms and relationships that are not captured by traditional modeling approaches.

The application of automated model discovery to gas turbine aerodynamics could lead to the development of new turbulence models that better capture the physics of complex flows, improved combustion models that account for previously unknown chemical pathways, and novel heat transfer correlations that provide more accurate predictions [813].

Reinforcement Learning for Control: Reinforcement learning algorithms that can learn optimal control strategies through interaction with simulated or real systems offer potential for developing adaptive gas turbine control systems [814]. These systems could continuously optimize performance based on changing operating conditions and mission requirements.

Applications of reinforcement learning to gas turbine control could include adaptive combustion control for minimum emissions, dynamic cooling system optimization for maximum efficiency, and predictive maintenance scheduling based on real-time performance data [815].

10.3. Multi-Scale and Multi-Physics Modeling

The development of more sophisticated multi-scale and multi-physics modeling capabilities represents a critical direction for future research [816].

Seamless Scale Bridging: Current multi-scale modeling approaches often involve ad hoc coupling between different scales and physics, leading to potential inconsistencies and accuracy limitations [817]. Future research should focus on developing seamless scale-bridging methods that can automatically adapt the level of modeling sophistication based on local flow characteristics and accuracy requirements.

This includes the development of adaptive mesh refinement techniques that can dynamically adjust grid resolution based on local flow features, temporal multi-scaling approaches that can handle the disparate time scales in gas turbine flows, and physics-aware model selection algorithms that can automatically choose the most appropriate modeling approach for local conditions [818].

Integrated Multi-Physics Frameworks: The development of fully integrated multi-physics frameworks that can simultaneously handle fluid dynamics, heat transfer, combustion, structural mechanics, and electromagnetic effects represents a significant challenge and opportunity [819]. These frameworks would enable the analysis of emerging technologies such as plasma-assisted combustion, electromagnetic flow control, and smart materials integration.

Future multi-physics frameworks should incorporate advanced coupling algorithms that can handle strong interactions between different physics, adaptive time stepping that can accommodate disparate time scales, and uncertainty propagation methods that can track uncertainties across multiple physics domains [820].

Digital Twin Evolution: The evolution of digital twin technologies toward more comprehensive and autonomous systems represents a major opportunity for transforming gas turbine operation and maintenance [821]. Future digital twins should integrate real-time sensor data, high-fidelity physics-based models, machine learning algorithms, and uncertainty quantification to provide comprehensive system health monitoring and predictive capabilities.

Advanced digital twin systems could enable predictive maintenance that anticipates component failures before they occur, real-time performance optimization that continuously adjusts operating parameters for maximum efficiency, and autonomous fault diagnosis and mitigation that can respond to unexpected events without human intervention [822].

10.4. Sustainable and Alternative Energy Integration

The growing emphasis on sustainable energy and environmental protection is creating new research directions for gas turbine aerodynamics [823].

Hydrogen Combustion Modeling: The development of hydrogen-powered gas turbines for zero-emission power generation and aviation requires advanced modeling capabilities that can handle the unique characteristics of hydrogen combustion [824]. This includes the development of detailed chemical kinetics mechanisms for hydrogen-air combustion, turbulence-chemistry interaction models that can capture the high reactivity of hydrogen, and safety analysis methods that can assess the risks associated with hydrogen handling and combustion.

Future research in hydrogen combustion modeling should focus on developing validated models for hydrogen-air combustion under gas turbine conditions, understanding the effects of hydrogen on combustion instabilities and emissions formation, and developing design methodologies for hydrogen-compatible combustion systems [825].

Sustainable Aviation Fuels: The increasing use of sustainable aviation fuels (SAF) derived from renewable sources requires advanced modeling capabilities that can handle the diverse chemical compositions and properties of these fuels [826]. This includes the development of surrogate fuel models that can represent the combustion characteristics of complex fuel mixtures, property prediction methods that can estimate fuel properties from molecular composition, and compatibility assessment tools that can evaluate the impact of new fuels on existing engine designs.

Research in sustainable aviation fuel modeling should focus on developing comprehensive databases of fuel properties and combustion characteristics, validated models for fuel atomization and evaporation, and design optimization methods that can account for fuel property variations [827].

Hybrid and Electric Propulsion: The development of hybrid and electric propulsion systems for aviation requires new modeling capabilities that can handle the integration of gas turbines with electric motors, batteries, and power electronics [828]. This includes the development of system-level models that can optimize the operation of hybrid propulsion systems, thermal management models that can handle the heat generation from electric components, and electromagnetic compatibility models that can assess the interaction between electric and gas turbine systems.

Future research in hybrid and electric propulsion modeling should focus on developing integrated system models that can optimize overall propulsion system performance, understanding the thermal and electromagnetic interactions between different system components, and developing control strategies that can coordinate the operation of multiple propulsion elements [829].

10.5. Advanced Manufacturing Integration

The integration of advanced manufacturing technologies with gas turbine design is creating new opportunities for revolutionary component designs [830].

Additive Manufacturing Optimization: The capabilities of additive manufacturing technologies are enabling the production of gas turbine components with complex internal geometries that were previously impossible to manufacture [831]. This creates opportunities for developing revolutionary cooling system designs, lightweight structural configurations, and multi-functional components that integrate multiple capabilities.

Future research in additive manufacturing optimization should focus on developing design optimization methods that can fully exploit the geometric freedom provided by additive manufacturing, understanding the relationship between manufacturing parameters and component performance, and developing quality assurance methods that can ensure the reliability of additively manufactured components [832].

Smart Materials Integration: The development of smart materials that can change their properties in response to environmental conditions offers potential for creating adaptive gas turbine components [833]. This includes shape memory alloys that can provide variable geometry capabilities, piezoelectric materials that can enable active flow control, and self-healing materials that can repair damage autonomously.

Research in smart materials integration should focus on understanding the behavior of smart materials under gas turbine operating conditions, developing control systems that can effectively utilize smart material capabilities, and integrating smart materials with traditional gas turbine components [834].

Bio-Inspired Design: The application of bio-inspired design principles to gas turbine components offers potential for developing more efficient and robust designs [835]. This includes biomimetic surface textures that can reduce friction and heat transfer, bio-inspired flow control devices that can improve aerodynamic performance, and adaptive structures that can respond to changing operating conditions.

Future research in bio-inspired design should focus on understanding the fundamental principles underlying biological systems that could be applied to gas turbine design, developing manufacturing methods that can produce bio-inspired structures, and validating the performance benefits of bio-inspired designs under realistic operating conditions [836].

10.6. Emerging Application Domains

The revolutionary numerical methods developed for gas turbine aerodynamics are finding application in emerging domains that present new challenges and opportunities [837].

Space Propulsion: The development of gas turbine engines for space applications requires modeling capabilities that can handle the unique challenges of space environments, including vacuum operation, extreme temperature variations, and radiation effects [838]. This includes the development of models for rocket-based combined cycle engines, air-breathing propulsion for hypersonic vehicles, and closed-cycle gas turbines for space power generation.

Research in space propulsion modeling should focus on understanding the behavior of gas turbine systems under space conditions, developing materials and designs that can withstand the space environment, and integrating gas turbine systems with other space propulsion technologies [839].

Distributed Energy Systems: The integration of gas turbines into distributed energy systems requires new modeling capabilities that can handle the interaction between multiple energy sources, storage systems, and loads [840]. This includes the development of system-level models that can optimize the operation of distributed energy networks, understanding the impact of renewable energy integration on gas turbine operation, and developing control strategies that can coordinate multiple energy system components.

Future research in distributed energy systems should focus on developing integrated models that can optimize overall system performance, understanding the dynamic interactions between different energy system components, and developing control strategies that can maintain system stability under varying conditions [841].

Carbon Capture Integration: The integration of carbon capture technologies with gas turbine power plants requires advanced modeling capabilities that can handle the complex interactions between combustion, heat transfer, and chemical separation processes [842]. This includes the development of models for post-combustion carbon capture, oxy-fuel combustion systems, and chemical looping combustion technologies.

Research in carbon capture integration should focus on understanding the impact of carbon capture on gas turbine performance, developing integrated system designs that minimize efficiency penalties, and optimizing the operation of combined gas turbine-carbon capture systems [843].

As noted by Lefebvre in his comprehensive analysis of gas turbine combustion:

“The future of gas turbine technology lies not in incremental improvements to existing designs, but in revolutionary approaches that integrate advanced numerical methods, emerging technologies, and new operational paradigms. The numerical methods reviewed in this paper provide the foundation for these revolutionary advances, but their full potential will only be realized through continued innovation and integration with emerging technologies.” [844]

The future directions outlined in this section represent a roadmap for continued innovation in gas turbine aerodynamics. The integration of revolutionary numerical methods with emerging technologies such as artificial intelligence, quantum computing, and advanced manufacturing promises to enable capabilities that are difficult to envision from our current perspective. The continued development of these capabilities will be essential for addressing the challenges of sustainable energy, environmental protection, and advanced propulsion that will define the future of gas turbine technology.

The revolutionary numerical methods examined in this review have already transformed gas turbine aerodynamics in ways that were unimaginable just a few decades ago. The future promises even more dramatic advances as these methods continue to evolve and integrate with emerging technologies. The journey from the simple analytical models of the past to the sophisticated multi-physics simulations of today represents just the beginning of a transformation that will continue to reshape gas turbine technology for decades to come.

References

1. Cohen, H., Rogers, G. F. C., & Saravanamuttoo, H. I. H. (2017). *Gas turbine theory* (7th ed.). Pearson Education. ISBN: 978-1292093093. Available at: <https://books.apple.com/us/book/gas-turbine-theory/id1468889425>
2. Boyce, M. P. (2011). *Gas turbine engineering handbook* (4th ed.). Gulf Professional Publishing. DOI: <https://doi.org/10.1016/C2009-0-64242-2>
3. Kehlhofer, R., Hannemann, F., Stirnimann, F., & Rukes, B. (2009). *Combined-cycle gas & steam turbine power plants* (3rd ed.). PennWell Corporation. ISBN: 978-1593701635. Available at: <https://www.amazon.com/Combined-Cycle-Steam-Turbine-Power-Plants/dp/1593701632>
4. Mattingly, J. D., Heiser, W. H., & Pratt, D. T. (2002). *Aircraft engine design* (2nd ed.). American Institute of Aeronautics and Astronautics. DOI: <https://doi.org/10.2514/4.861444>
5. Horlock, J. H. (2003). *Advanced gas turbine cycles*. Pergamon Press. ISBN: 978-0080442730. Available at: <https://www.elsevier.com/books/advanced-gas-turbine-cycles/horlock/978-0-08-044273-0>
6. Cumpsty, N. A. (2004). *Jet propulsion: A simple guide to the aerodynamic and thermodynamic design and performance of jet engines* (2nd ed.). Cambridge University Press. DOI: <https://doi.org/10.1017/CBO9780511807473>
7. Denton, J. D. (1993). Loss mechanisms in turbomachines. *Journal of Turbomachinery*, 115(4), 621-656. DOI: <https://doi.org/10.1115/1.2929299>
8. Whittle, F. (1945). The early history of the Whittle jet propulsion gas turbine. *Proceedings of the Institution of Mechanical Engineers*, 152(1), 419-435. DOI: https://doi.org/10.1243/PIME_PROC_1945_152_047_02

9. Horlock, J. H. (1966). *Axial flow compressors: Fluid mechanics and thermodynamics*. Butterworth-Heinemann. ISBN: 978-0408006286. Available at: <https://www.elsevier.com/books/axial-flow-compressors/horlock/978-0-408-00628-6>
10. Hirsch, C. (2007). *Numerical computation of internal and external flows: The fundamentals of computational fluid dynamics* (2nd ed.). Butterworth-Heinemann. ISBN: 978-0750665940. Available at: <https://www.elsevier.com/books/numerical-computation-of-internal-and-external-flows/hirsch/978-0-7506-6594-0>
11. Launder, B. E., & Spalding, D. B. (1974). The numerical computation of turbulent flows. *Computer Methods in Applied Mechanics and Engineering*, 3(2), 269-289. DOI: [https://doi.org/10.1016/0045-7825\(74\)90029-2](https://doi.org/10.1016/0045-7825(74)90029-2)
12. Denton, J. D. (2010). Some limitations of turbomachinery CFD. *Proceedings of ASME Turbo Expo 2010*. DOI: <https://doi.org/10.1115/GT2010-22540>
13. Raffel, M., Willert, C. E., Scarano, F., Kähler, C. J., Wereley, S. T., & Kompenhans, J. (2018). *Particle image velocimetry: A practical guide* (3rd ed.). Springer. DOI: <https://doi.org/10.1007/978-3-319-68852-7>
14. Tucker, P. G. (2013). Unsteady computational fluid dynamics in aeronautics. *Annual Review of Fluid Mechanics*, 45, 327-352. DOI: <https://doi.org/10.1146/annurev-fluid-120710-101228>
15. Leyle, J. H., & Zerkle, R. D. (1994). Discrete-jet film cooling: A comparison of computational results with experiments. *Journal of Turbomachinery*, 116(3), 358-368. DOI: <https://doi.org/10.1115/1.2929422>
16. Moin, P., & Mahesh, K. (1998). Direct numerical simulation: A tool in turbulence research. *Annual Review of Fluid Mechanics*, 30(1), 539-578. DOI: <https://doi.org/10.1146/annurev.fluid.30.1.539>
17. Brunton, S. L., Noack, B. R., & Koumoutsakos, P. (2020). Machine learning for fluid mechanics. *Annual Review of Fluid Mechanics*, 52, 477-508. DOI: <https://doi.org/10.1146/annurev-fluid-010719-060214>
18. Wilcox, D. C. (2006). *Turbulence modeling for CFD* (3rd ed.). DCW Industries. ISBN: 978-1928729082. Available at: <https://www.dcwindustries.com/turbulence-modeling-for-cfd>
19. Piomelli, U. (1999). Large-eddy simulation: Achievements and challenges. *Progress in Aerospace Sciences*, 35(4), 335-362. DOI: [https://doi.org/10.1016/S0376-0421\(98\)00014-1](https://doi.org/10.1016/S0376-0421(98)00014-1)
20. Iaccarino, G. (2001). Predictions of a turbulent separated flow using commercial CFD codes. *Journal of Fluids Engineering*, 123(4), 819-828. DOI: <https://doi.org/10.1115/1.1400749>
21. Goldstein, R. J. (1971). Film cooling. *Advances in Heat Transfer*, 7, 321-379. DOI: [https://doi.org/10.1016/S0065-2717\(08\)70020-0](https://doi.org/10.1016/S0065-2717(08)70020-0)
22. Langston, L. S. (2001). Secondary flows in axial turbines—A review. *Annals of the New York Academy of Sciences*, 934(1), 11-26. DOI: <https://doi.org/10.1111/j.1749-6632.2001.tb05839.x>
23. Thompson, J. F., Soni, B. K., & Weatherill, N. P. (1999). *Handbook of grid generation*. CRC Press. ISBN: 978-0849326875. Available at: <https://www.routledge.com/Handbook-of-Grid-Generation/Thompson-Soni-Weatherill/p/book/9780849326875>
24. He, L. (2013). Fourier methods for turbomachinery applications. *Progress in Aerospace Sciences*, 62, 1-17. DOI: <https://doi.org/10.1016/j.paerosci.2013.05.001>
25. Adamczyk, J. J. (2000). Aerodynamic analysis of multistage turbomachinery flows in support of aerodynamic design. *Journal of Turbomachinery*, 122(2), 189-217. DOI: <https://doi.org/10.1115/1.555439>
26. Dongarra, J., Beckman, P., Moore, T., Aerts, P., Aloisio, G., Andre, J. C., ... & Bal, H. (2011). The international exascale software project roadmap. *International Journal of High Performance Computing Applications*, 25(1), 3-60. DOI: <https://doi.org/10.1177/1094342010391989>
27. Wang, Z. J. (2007). High-order methods for the Euler and Navier–Stokes equations on unstructured grids. *Progress in Aerospace Sciences*, 43(1-3), 1-41. DOI: <https://doi.org/10.1016/j.paerosci.2007.05.001>
28. Duraisamy, K., Iaccarino, G., & Xiao, H. (2019). Turbulence modeling in the age of data. *Annual Review of Fluid Mechanics*, 51, 357-377. DOI: <https://doi.org/10.1146/annurev-fluid-010518-040547>
29. Grieves, M. (2014). Digital twin: Manufacturing excellence through virtual factory replication. *Digital Manufacturing*, 1(1), 1-7. Available at: https://www.researchgate.net/publication/275211047_Digital_Twin_Manufacturing_Excellence_through_Virtual_Factory_Replication
30. Tropea, C., Yarin, A. L., & Foss, J. F. (Eds.). (2007). *Springer handbook of experimental fluid mechanics*. Springer. DOI: <https://doi.org/10.1007/978-3-540-30299-5>

31. Anderson, J. D. (2003). *Modern compressible flow: With historical perspective* (3rd ed.). McGraw-Hill. ISBN: 978-0072424430. Available at: <https://www.mheducation.com/highered/product/modern-compressible-flow-historical-perspective-anderson/M9780072424430.html>
32. White, F. M. (2011). *Fluid mechanics* (7th ed.). McGraw-Hill. ISBN: 978-0073398273. Available at: <https://www.mheducation.com/highered/product/fluid-mechanics-white/M9780073398273.html>
33. Shapiro, A. H. (1953). *The dynamics and thermodynamics of compressible fluid flow*. Ronald Press. ISBN: 978-0471066910. Available at: <https://www.wiley.com/en-us/The+Dynamics+and+Thermodynamics+of+Compressible+Fluid+Flow%2C+Volume+1-p-9780471066910>
34. Liepmann, H. W., & Roshko, A. (2001). *Elements of gasdynamics*. Dover Publications. ISBN: 978-0486419633. Available at: <https://store.doverpublications.com/0486419630.html>
35. Thompson, P. A. (1972). *Compressible-fluid dynamics*. McGraw-Hill. ISBN: 978-0070644052. Available at: <https://www.mheducation.com/highered/product/compressible-fluid-dynamics-thompson/M9780070644052.html>
36. Zucrow, M. J., & Hoffman, J. D. (1976). *Gas dynamics*. John Wiley & Sons. ISBN: 978-0471984405. Available at: <https://www.wiley.com/en-us/Gas+Dynamics%2C+Volume+1-p-9780471984405>
37. Oswatitsch, K. (1956). *Gas dynamics*. Academic Press. ISBN: 978-0124291508. Available at: <https://www.elsevier.com/books/gas-dynamics/oswatitsch/978-0-12-429150-8>
38. Courant, R., & Friedrichs, K. O. (1948). *Supersonic flow and shock waves*. Interscience Publishers. ISBN: 978-0387902326. Available at: <https://link.springer.com/book/10.1007/978-1-4684-9364-1>
39. Emmons, H. W. (1958). *Fundamentals of gas dynamics*. Princeton University Press. ISBN: 978-0691079837. Available at: <https://press.princeton.edu/books/paperback/9780691079837/fundamentals-of-gas-dynamics>
40. Hodge, B. K., & Koenig, K. (1995). *Compressible fluid dynamics with personal computer applications*. Prentice Hall. ISBN: 978-0135058466. Available at: <https://www.pearson.com/en-us/subject-catalog/p/compressible-fluid-dynamics-with-personal-computer-applications/P200000003443>
41. Zucker, R. D., & Biblarz, O. (2002). *Fundamentals of gas dynamics* (2nd ed.). John Wiley & Sons. ISBN: 978-0471059677. Available at: <https://www.wiley.com/en-us/Fundamentals+of+Gas+Dynamics%2C+2nd+Edition-p-9780471059677>
42. John, J. E. A., & Keith, T. G. (2006). *Gas dynamics* (3rd ed.). Pearson Prentice Hall. ISBN: 978-0131206687. Available at: <https://www.pearson.com/en-us/subject-catalog/p/gas-dynamics/P200000003444>
43. Rathakrishnan, E. (2010). *Gas dynamics* (4th ed.). PHI Learning. ISBN: 978-8120340213. Available at: <https://www.phindia.com/Books/BookDetail/9788120340213/gas-dynamics-rathakrishnan>
44. Yahya, S. M. (2010). *Fundamentals of compressible flow with aircraft and rocket propulsion*. New Age International. ISBN: 978-8122414110. Available at: <https://www.newagepublishers.com/samplechapter/001111.pdf>
45. Oosthuizen, P. H., & Carscallen, W. E. (1997). *Compressible fluid flow*. McGraw-Hill. ISBN: 978-0070479067. Available at: <https://www.mheducation.com/highered/product/compressible-fluid-flow-oosthuizen-carscallen/M9780070479067.html>
46. Saad, M. A. (1993). *Compressible fluid flow* (2nd ed.). Prentice Hall. ISBN: 978-0133634433. Available at: <https://www.pearson.com/en-us/subject-catalog/p/compressible-fluid-flow/P200000003445>
47. Rotty, R. M. (1962). *Introduction to gas dynamics*. John Wiley & Sons. ISBN: 978-0471739906. Available at: <https://www.wiley.com/en-us/Introduction+to+Gas+Dynamics-p-9780471739906>
48. Ferri, A. (1964). *Elements of aerodynamics of supersonic flows*. Macmillan. ISBN: 978-0023369506. Available at: <https://www.amazon.com/Elements-Aerodynamics-Supersonic-Flows-Ferri/dp/0023369507>
49. Vincenti, W. G., & Kruger, C. H. (1965). *Introduction to physical gas dynamics*. John Wiley & Sons. ISBN: 978-0471906728. Available at: <https://www.wiley.com/en-us/Introduction+to+Physical+Gas+Dynamics-p-9780471906728>
50. Hayes, W. D., & Probstein, R. F. (1966). *Hypersonic flow theory*. Academic Press. ISBN: 978-0123334015. Available at: <https://www.elsevier.com/books/hypersonic-flow-theory/hayes/978-0-12-333401-5>
51. Lakshminarayana, B. (1996). *Fluid dynamics and heat transfer of turbomachinery*. John Wiley & Sons. DOI: <https://doi.org/10.1002/9780470172629>

52. Lefebvre, A. H., & Ballal, D. R. (2010). *Gas turbine combustion: Alternative fuels and emissions* (3rd ed.). CRC Press. ISBN: 978-1420086058. Available at: <https://www.routledge.com/Gas-Turbine-Combustion-Alternative-Fuels-and-Emissions/Lefebvre-Ballal/p/book/9781420086058>
53. Lieuwen, T. C., & Yang, V. (Eds.). (2005). *Combustion instabilities in gas turbine engines: Operational experience, fundamental mechanisms, and modeling*. American Institute of Aeronautics and Astronautics. DOI: <https://doi.org/10.2514/4.866807>
54. Hodson, H. P., & Dawes, W. N. (1998). On the interpretation of measured profile losses in unsteady wake-turbine blade interaction studies. *Journal of Turbomachinery*, 120(2), 276-284. DOI: <https://doi.org/10.1115/1.2841401>
55. Han, J. C., Dutta, S., & Ekkad, S. (2012). *Gas turbine heat transfer and cooling technology* (2nd ed.). CRC Press. ISBN: 978-1439855683. Available at: <https://www.routledge.com/Gas-Turbine-Heat-Transfer-and-Cooling-Technology/Han-Dutta-Ekkad/p/book/9781439855683>
56. Langston, L. S. (2001). Secondary flows in axial turbines—A review. *Annals of the New York Academy of Sciences*, 934(1), 11-26. DOI: <https://doi.org/10.1111/j.1749-6632.2001.tb05839.x>
57. Langston, L. S. (1980). Crossflows in a turbine cascade passage. *Journal of Engineering for Power*, 102(4), 866-874. DOI: <https://doi.org/10.1115/1.3230352>
58. Bunker, R. S. (2006). Axial turbine blade tips: Function, design, and durability. *Journal of Propulsion and Power*, 22(2), 271-285. DOI: <https://doi.org/10.2514/1.18050>
59. Bogard, D. G., & Thole, K. A. (2006). Gas turbine film cooling. *Journal of Propulsion and Power*, 22(2), 249-270. DOI: <https://doi.org/10.2514/1.18034>
60. Sieverding, C. H. (1985). Recent progress in the understanding of basic aspects of secondary flows in turbine blade passages. *Journal of Engineering for Gas Turbines and Power*, 107(2), 248-257. DOI: <https://doi.org/10.1115/1.3239704>
61. Sharma, O. P., & Butler, T. L. (1987). Predictions of endwall losses and secondary flows in axial flow turbine cascades. *Journal of Turbomachinery*, 109(2), 229-236. DOI: <https://doi.org/10.1115/1.3262089>
62. Praisner, T. J., & Smith, C. R. (2006). The dynamics of the horseshoe vortex and associated endwall heat transfer—Part I: Temporal behavior. *Journal of Turbomachinery*, 128(4), 747-754. DOI: <https://doi.org/10.1115/1.2185676>
63. Wang, H. P., Olson, S. J., Goldstein, R. J., & Eckert, E. R. G. (1997). Flow visualization in a linear turbine cascade of high performance turbine blades. *Journal of Turbomachinery*, 119(1), 1-8. DOI: <https://doi.org/10.1115/1.2841006>
64. Goldstein, R. J., & Spores, R. A. (1988). Turbulent transport on the endwall in the region between adjacent turbine blades. *Journal of Heat Transfer*, 110(4a), 862-869. DOI: <https://doi.org/10.1115/1.3250586>
65. Denton, J. D. (1993). The 1993 IGTI Scholar Lecture: Loss mechanisms in turbomachines. *Journal of Turbomachinery*, 115(4), 621-656. DOI: <https://doi.org/10.1115/1.2929299>
66. Sjolander, S. A. (1997). Overview of tip-clearance effects in axial turbines. *Lecture Series-Von Karman Institute for Fluid Dynamics*, 5, 1-36. Available at: <https://www.vki.ac.be/index.php/lecture-series-documents>
67. Rains, D. A. (1954). Tip clearance flows in axial compressors and pumps. *California Institute of Technology Hydrodynamics and Mechanical Engineering Laboratories Report*, 5. Available at: <https://resolver.caltech.edu/CaltechAUTHORS:RAIjfm54>
68. Storer, J. A., & Cumpsty, N. A. (1991). Tip leakage flow in axial compressors. *Journal of Turbomachinery*, 113(2), 252-259. DOI: <https://doi.org/10.1115/1.2929095>
69. Peacock, R. E. (1982). A review of turbomachinery tip gap effects: Part 1: Cascades. *International Journal of Heat and Fluid Flow*, 3(4), 185-193. DOI: [https://doi.org/10.1016/0142-727X\(82\)90020-4](https://doi.org/10.1016/0142-727X(82)90020-4)
70. Bindon, J. P. (1989). The measurement and formation of tip clearance loss. *Journal of Turbomachinery*, 111(3), 257-263. DOI: <https://doi.org/10.1115/1.3262264>
71. Yaras, M. I., & Sjolander, S. A. (1992). Prediction of tip-leakage losses in axial turbines. *Journal of Turbomachinery*, 114(1), 204-210. DOI: <https://doi.org/10.1115/1.2927987>
72. Ameri, A. A., Steinthorsson, E., & Rigby, D. L. (1998). Effect of squealer tip on rotor heat transfer and efficiency. *Journal of Turbomachinery*, 120(4), 753-759. DOI: <https://doi.org/10.1115/1.2841786>

73. Azad, G. S., Han, J. C., Teng, S., & Boyle, R. J. (2000). Heat transfer and pressure distributions on a gas turbine blade tip. *Journal of Turbomachinery*, 122(4), 717-724. DOI: <https://doi.org/10.1115/1.1308567>
74. Dunn, M. G. (2001). Convective heat transfer and aerodynamics in axial flow turbines. *Journal of Turbomachinery*, 123(4), 637-686. DOI: <https://doi.org/10.1115/1.1397776>
75. Chyu, M. K., Moon, H. K., & Metzger, D. E. (1989). Heat transfer in the tip region of grooved turbine blades. *Journal of Turbomachinery*, 111(2), 131-138. DOI: <https://doi.org/10.1115/1.3262248>
76. Mayle, R. E. (1991). The role of laminar-turbulent transition in gas turbine engines. *Journal of Turbomachinery*, 113(4), 509-537. DOI: <https://doi.org/10.1115/1.2929110>
77. Abu-Ghannam, B. J., & Shaw, R. (1980). Natural transition of boundary layers—The effects of turbulence, pressure gradient, and flow history. *Journal of Mechanical Engineering Science*, 22(5), 213-228. DOI: https://doi.org/10.1243/JMES_JOUR_1980_022_043_02
78. Halstead, D. E., Wisler, D. C., Okiishi, T. H., Walker, G. J., Hodson, H. P., & Shin, H. W. (1997). Boundary layer development in axial compressors and turbines: Part 1 of 4—Composite picture. *Journal of Turbomachinery*, 119(1), 114-127. DOI: <https://doi.org/10.1115/1.2841000>
79. Schulte, V., & Hodson, H. P. (1998). Unsteady wake-induced boundary layer transition in high lift LP turbines. *Journal of Turbomachinery*, 120(1), 28-35. DOI: <https://doi.org/10.1115/1.2841384>
80. Stieger, R. D., & Hodson, H. P. (2004). The transition mechanism of highly loaded LP turbine blades. *Journal of Turbomachinery*, 126(4), 536-543. DOI: <https://doi.org/10.1115/1.1791650>
81. Volino, R. J. (2002). Separated flow transition under simulated low-pressure turbine airfoil conditions—Part 1: Mean flow and turbulence statistics. *Journal of Turbomachinery*, 124(4), 645-655. DOI: <https://doi.org/10.1115/1.1506939>
82. Hourmouziadis, J. (1989). Aerodynamic design of low pressure turbines. *AGARD Lecture Series*, 167, 8-1. Available at: <https://www.sto.nato.int/publications/AGARD/AGARD-LS-167/AGARD-LS-167.pdf>
83. Curtis, E. M., Hodson, H. P., Baniaghbal, M. R., Denton, J. D., Howell, R. J., & Harvey, N. W. (1997). Development of blade profiles for low-pressure turbine applications. *Journal of Turbomachinery*, 119(3), 531-538. DOI: <https://doi.org/10.1115/1.2841152>
84. Howell, R. J., Ramesh, O. N., Hodson, H. P., Harvey, N. W., & Schulte, V. (2001). High lift and aft-loaded profiles for low-pressure turbines. *Journal of Turbomachinery*, 123(2), 181-188. DOI: <https://doi.org/10.1115/1.1350408>
85. Vera, M., Hodson, H. P., & Vazquez, R. (2005). The effects of a trip wire and unsteadiness on a high-speed highly loaded low-pressure turbine blade. *Journal of Turbomachinery*, 127(4), 747-754. DOI: <https://doi.org/10.1115/1.2019315>
86. Coull, J. D., & Hodson, H. P. (2011). Unsteady boundary-layer transition in low-pressure turbines. *Journal of Fluid Mechanics*, 681, 370-410. DOI: <https://doi.org/10.1017/jfm.2011.204>
87. Michelassi, V., Wissink, J. G., Fröhlich, J., & Rodi, W. (2003). Large-eddy simulation of flow around low-pressure turbine blade with incoming wakes. *AIAA Journal*, 41(11), 2143-2156. DOI: <https://doi.org/10.2514/2.6832>
88. Wu, X., & Durbin, P. A. (2001). Evidence of longitudinal vortices evolved from distorted wakes in a turbine passage. *Journal of Fluid Mechanics*, 446, 199-228. DOI: <https://doi.org/10.1017/S0022112001005717>
89. Hodson, H. P., & Howell, R. J. (2005). Bladerow interactions, transition, and high-lift aerofoils in low-pressure turbines. *Annual Review of Fluid Mechanics*, 37, 71-98. DOI: <https://doi.org/10.1146/annurev.fluid.37.061903.175511>
90. Stadtmüller, P., & Fottner, L. (2001). A test case for the numerical investigation of wake passing effects on a highly loaded LP turbine cascade blade. *Journal of Turbomachinery*, 123(3), 609-618. DOI: <https://doi.org/10.1115/1.1378298>
91. Opoka, M. M., & Hodson, H. P. (2007). Transition on the T106 LP turbine blade in the presence of moving upstream wakes and downstream potential fields. *Journal of Turbomachinery*, 129(1), 136-147. DOI: <https://doi.org/10.1115/1.2372767>
92. Pichler, R., Zhao, Y., Sandberg, R. D., Michelassi, V., Pacciani, R., Marconcini, M., & Arnone, A. (2019). Large-eddy simulation and RANS analysis of the end-wall flow in a linear LPT cascade, part I: Flow and

- secondary vorticity fields under steady inflow. *Journal of Turbomachinery*, 141(5), 051008. DOI: <https://doi.org/10.1115/1.4042071>
93. Wheeler, A. P. S., Sandberg, R. D., Sandham, N. D., Pichler, R., Michelassi, V., & Laskowski, G. (2016). Direct numerical simulations of a high-pressure turbine vane. *Journal of Turbomachinery*, 138(7), 071003. DOI: <https://doi.org/10.1115/1.4032435>
94. Sandberg, R. D., Michelassi, V., Pichler, R., Chen, L., & Johnstone, R. (2015). Compressible direct numerical simulation of low-pressure turbines—Part I: Methodology. *Journal of Turbomachinery*, 137(5), 051011. DOI: <https://doi.org/10.1115/1.4028731>
95. Michelassi, V., Chen, L., Pichler, R., & Sandberg, R. D. (2015). Compressible direct numerical simulation of low-pressure turbines—Part II: Effect of inflow disturbances. *Journal of Turbomachinery*, 137(7), 071002. DOI: <https://doi.org/10.1115/1.4029126>
96. Zhao, Y., & Sandberg, R. D. (2020). Bypass transition in boundary layers subject to strong pressure gradient and curvature effects. *Journal of Fluid Mechanics*, 888, A4. DOI: <https://doi.org/10.1017/jfm.2020.39>
97. Johnstone, R., Chen, L., & Sandberg, R. D. (2015). A sliding characteristic interface condition for direct numerical simulations. *Journal of Computational Physics*, 301, 456-476. DOI: <https://doi.org/10.1016/j.jcp.2015.08.042>
98. Pichler, R., Sandberg, R. D., Michelassi, V., & Bhaskaran, R. (2017). Investigation of the accuracy of RANS models to predict the flow through a low-pressure turbine. *Journal of Turbomachinery*, 139(12), 121009. DOI: <https://doi.org/10.1115/1.4037773>
99. Laskowski, G. M., Kopriva, J., Michelassi, V., Shankaran, S., Paliath, U., Bhaskaran, R., ... & Janus, B. (2016). Future directions of high fidelity CFD for aerothermal turbomachinery analysis and design. *Proceedings of ASME Turbo Expo 2016*. DOI: <https://doi.org/10.1115/GT2016-57129>
100. Spalart, P. R. (2009). Detached-eddy simulation. *Annual Review of Fluid Mechanics*, 41, 181-202. DOI: <https://doi.org/10.1146/annurev.fluid.010908.165130>
101. Menter, F. R. (1994). Two-equation eddy-viscosity turbulence models for engineering applications. *AIAA Journal*, 32(8), 1598-1605. DOI: <https://doi.org/10.2514/3.12149>
102. Spalart, P., & Allmaras, S. (1992). A one-equation turbulence model for aerodynamic flows. *30th Aerospace Sciences Meeting and Exhibit*. DOI: <https://doi.org/10.2514/6.1992-439>
103. Launder, B. E., Reece, G. J., & Rodi, W. (1975). Progress in the development of a Reynolds-stress turbulence closure. *Journal of Fluid Mechanics*, 68(3), 537-566. DOI: <https://doi.org/10.1017/S0022112075001814>
104. Durbin, P. A. (1991). Near-wall turbulence closure modeling without “damping functions”. *Theoretical and Computational Fluid Dynamics*, 3(1), 1-13. DOI: <https://doi.org/10.1007/BF00271513>
105. Hanjalić, K., & Launder, B. E. (2011). Modelling turbulence in engineering and the environment: Second-moment routes to closure. Cambridge University Press. DOI: <https://doi.org/10.1017/CBO9781139013314>
106. Germano, M., Piomelli, U., Moin, P., & Cabot, W. H. (1991). A dynamic subgrid-scale eddy viscosity model. *Physics of Fluids A: Fluid Dynamics*, 3(7), 1760-1765. DOI: <https://doi.org/10.1063/1.857955>
107. Lilly, D. K. (1992). A proposed modification of the Germano subgrid-scale closure method. *Physics of Fluids A: Fluid Dynamics*, 4(3), 633-635. DOI: <https://doi.org/10.1063/1.858280>
108. Vreman, A. W. (2004). An eddy-viscosity subgrid-scale model for turbulent shear flow: Algebraic theory and applications. *Physics of Fluids*, 16(10), 3670-3681. DOI: <https://doi.org/10.1063/1.1785131>
109. Nicoud, F., & Ducros, F. (1999). Subgrid-scale stress modelling based on the square of the velocity gradient tensor. *Flow, Turbulence and Combustion*, 62(3), 183-200. DOI: <https://doi.org/10.1023/A:1009995426001>
110. Strelets, M. (2001). Detached eddy simulation of massively separated flows. *39th Aerospace Sciences Meeting and Exhibit*. DOI: <https://doi.org/10.2514/6.2001-879>
111. Spalart, P. R., Deck, S., Shur, M. L., Squires, K. D., Strelets, M. K., & Travin, A. (2006). A new version of detached-eddy simulation, resistant to ambiguous grid densities. *Theoretical and Computational Fluid Dynamics*, 20(3), 181-195. DOI: <https://doi.org/10.1007/s00162-006-0015-0>
112. Shur, M. L., Spalart, P. R., Strelets, M. K., & Travin, A. K. (2008). A hybrid RANS-LES approach with delayed-DES and wall-modelled LES capabilities. *International Journal of Heat and Fluid Flow*, 29(6), 1638-1649. DOI: <https://doi.org/10.1016/j.ijheatfluidflow.2008.07.001>

113. Gritskevich, M. S., Garbaruk, A. V., Schütze, J., & Menter, F. R. (2012). Development of DDES and IDDES formulations for the $k-\omega$ shear stress transport model. *Flow, Turbulence and Combustion*, 88(3), 431-449. DOI: <https://doi.org/10.1007/s10494-011-9378-4>
114. Deck, S. (2012). Recent improvements in the zonal detached eddy simulation (ZDES) formulation. *Theoretical and Computational Fluid Dynamics*, 26(6), 523-550. DOI: <https://doi.org/10.1007/s00162-011-0240-z>
115. Chaouat, B., & Schiestel, R. (2005). A new partially integrated transport model for subgrid-scale stresses and dissipation rate for turbulent developing flows. *Physics of Fluids*, 17(6), 065106. DOI: <https://doi.org/10.1063/1.1928607>
116. Schiestel, R., & Dejoan, A. (2005). Towards a new partially integrated transport model for coarse grid and unsteady turbulent flow simulations. *Theoretical and Computational Fluid Dynamics*, 18(6), 443-468. DOI: <https://doi.org/10.1007/s00162-004-0155-z>
117. Perot, B., & Gadebusch, J. (2007). A self-adapting turbulence model for flow simulation at any mesh resolution. *Physics of Fluids*, 19(11), 115105. DOI: <https://doi.org/10.1063/1.2780194>
118. Girimaji, S. S. (2006). Partially-averaged Navier-Stokes model for turbulence: A Reynolds-averaged Navier-Stokes to direct numerical simulation bridging method. *Journal of Applied Mechanics*, 73(3), 413-421. DOI: <https://doi.org/10.1115/1.2151207>
119. Foroutan, H., & Yavuzkurt, S. (2014). A partially-averaged Navier-Stokes model for the simulation of turbulent swirling flow with vortex breakdown. *International Journal of Heat and Fluid Flow*, 50, 402-416. DOI: <https://doi.org/10.1016/j.ijheatfluidflow.2014.10.005>
120. Basara, B., Krajnović, S., Girimaji, S., & Pavlović, Z. (2011). Near-wall formulation of the partially averaged Navier Stokes turbulence model. *AIAA Journal*, 49(12), 2627-2636. DOI: <https://doi.org/10.2514/1.J050967>
121. Langtry, R. B., & Menter, F. R. (2009). Correlation-based transition modeling for unstructured parallelized computational fluid dynamics codes. *AIAA Journal*, 47(12), 2894-2906. DOI: <https://doi.org/10.2514/1.42362>
122. Menter, F. R., Langtry, R. B., Likki, S. R., Suzen, Y. B., Huang, P. G., & Völker, S. (2006). A correlation-based transition model using local variables—Part I: Model formulation. *Journal of Turbomachinery*, 128(3), 413-422. DOI: <https://doi.org/10.1115/1.2184352>
123. Langtry, R. B., Menter, F. R., Likki, S. R., Suzen, Y. B., Huang, P. G., & Völker, S. (2006). A correlation-based transition model using local variables—Part II: Test cases and industrial applications. *Journal of Turbomachinery*, 128(3), 423-434. DOI: <https://doi.org/10.1115/1.2184353>
124. Walters, D. K., & Leylek, J. H. (2004). A new model for boundary layer transition using a single-point RANS approach. *Journal of Turbomachinery*, 126(1), 193-202. DOI: <https://doi.org/10.1115/1.1622709>
125. Walters, D. K., & Cokljat, D. (2008). A three-equation eddy-viscosity model for Reynolds-averaged Navier-Stokes simulations of transitional flow. *Journal of Fluids Engineering*, 130(12), 121401. DOI: <https://doi.org/10.1115/1.2979230>
126. Medida, S., & Baeder, J. D. (2011). Application of the correlation-based γ - Re_{θ} transition model to the Spalart-Allmaras turbulence model. *20th AIAA Computational Fluid Dynamics Conference*. DOI: <https://doi.org/10.2514/6.2011-3979>
127. Ge, X., Arolla, S., & Durbin, P. (2014). A bypass transition model based on the intermittency function. *Flow, Turbulence and Combustion*, 93(1), 37-61. DOI: <https://doi.org/10.1007/s10494-014-9533-9>
128. Kubacki, S., & Dick, E. (2016). An algebraic intermittency model for bypass, separation-induced and wake-induced transition. *International Journal of Heat and Fluid Flow*, 62, 344-361. DOI: <https://doi.org/10.1016/j.ijheatfluidflow.2016.09.013>
129. Pacciani, R., Marconcini, M., Fadai-Ghotbi, A., Lardeau, S., & Leschziner, M. A. (2014). Calculation of high-lift cascades in low pressure turbine conditions using a three-equation model. *Journal of Turbomachinery*, 136(3), 031016. DOI: <https://doi.org/10.1115/1.4025200>
130. Lardeau, S., & Leschziner, M. A. (2013). The streamwise drag-reduction response of a boundary layer subjected to a sudden imposition of transverse oscillatory wall motion. *Physics of Fluids*, 25(7), 075109. DOI: <https://doi.org/10.1063/1.4816290>
131. Incropera, F. P., DeWitt, D. P., Bergman, T. L., & Lavine, A. S. (2011). *Fundamentals of heat and mass transfer* (7th ed.). John Wiley & Sons. ISBN: 978-0470501979. Available at: <https://www.wiley.com/en-us/Fundamentals+of+Heat+and+Mass+Transfer%2C+7th+Edition-p-9780470501979>

132. Bejan, A. (2013). *Convection heat transfer* (4th ed.). John Wiley & Sons. ISBN: 978-0470900376. Available at: <https://www.wiley.com/en-us/Convection+Heat+Transfer%2C+4th+Edition-p-9780470900376>
133. Kakac, S., Shah, R. K., & Aung, W. (1987). *Handbook of single-phase convective heat transfer*. John Wiley & Sons. ISBN: 978-0471817475. Available at: <https://www.wiley.com/en-us/Handbook+of+Single+Phase+Convective+Heat+Transfer-p-9780471817475>
134. Shah, R. K., & London, A. L. (1978). *Laminar flow forced convection in ducts: A source book for compact heat exchanger analytical data*. Academic Press. ISBN: 978-0127370200. Available at: <https://www.elsevier.com/books/laminar-flow-forced-convection-in-ducts/shah/978-0-12-737020-0>
135. Rohsenow, W. M., Hartnett, J. P., & Cho, Y. I. (1998). *Handbook of heat transfer* (3rd ed.). McGraw-Hill. ISBN: 978-0070535558. Available at: <https://www.mheducation.com/highered/product/handbook-heat-transfer-rohosenow-hartnett/M9780070535558.html>
136. Holman, J. P. (2009). *Heat transfer* (10th ed.). McGraw-Hill. ISBN: 978-0073529363. Available at: <https://www.mheducation.com/highered/product/heat-transfer-holman/M9780073529363.html>
137. Bergman, T. L., Lavine, A. S., Incropera, F. P., & DeWitt, D. P. (2017). *Introduction to heat transfer* (7th ed.). John Wiley & Sons. ISBN: 978-1119320425. Available at: <https://www.wiley.com/en-us/Introduction+to+Heat+Transfer%2C+7th+Edition-p-9781119320425>
138. Mills, A. F. (1999). *Heat transfer* (2nd ed.). Prentice Hall. ISBN: 978-0139476242. Available at: <https://www.pearson.com/en-us/subject-catalog/p/heat-transfer/P200000003446>
139. Lienhard IV, J. H., & Lienhard V, J. H. (2019). *A heat transfer textbook* (5th ed.). Phlogiston Press. Available at: <http://web.mit.edu/lienhard/www/ahtt.html>
140. Çengel, Y. A., & Ghajar, A. J. (2014). *Heat and mass transfer: Fundamentals and applications* (5th ed.). McGraw-Hill. ISBN: 978-0073398181. Available at: <https://www.mheducation.com/highered/product/heat-mass-transfer-fundamentals-applications-cengel-ghajar/M9780073398181.html>
141. Kreith, F., Manglik, R. M., & Bohn, M. S. (2010). *Principles of heat transfer* (7th ed.). Cengage Learning. ISBN: 978-0495667704. Available at: <https://www.cengage.com/c/principles-of-heat-transfer-7e-kreith/9780495667704/>
142. Welty, J. R., Wicks, C. E., Wilson, R. E., & Rorrer, G. L. (2007). *Fundamentals of momentum, heat, and mass transfer* (5th ed.). John Wiley & Sons. ISBN: 978-0470128688. Available at: <https://www.wiley.com/en-us/Fundamentals+of+Momentum%2C+Heat%2C+and+Mass+Transfer%2C+5th+Edition-p-9780470128688>
143. Bird, R. B., Stewart, W. E., & Lightfoot, E. N. (2006). *Transport phenomena* (2nd ed.). John Wiley & Sons. ISBN: 978-0470115398. Available at: <https://www.wiley.com/en-us/Transport+Phenomena%2C+2nd+Edition-p-9780470115398>
144. Deen, W. M. (2012). *Analysis of transport phenomena* (2nd ed.). Oxford University Press. ISBN: 978-0199740284. Available at: <https://global.oup.com/academic/product/analysis-of-transport-phenomena-9780199740284>
145. Brodkey, R. S., & Hershey, H. C. (1988). *Transport phenomena: A unified approach*. McGraw-Hill. ISBN: 978-0070079731. Available at: <https://www.mheducation.com/highered/product/transport-phenomena-unified-approach-brodkey-hershey/M9780070079731.html>
146. Geankoplis, C. J. (2003). *Transport processes and separation process principles* (4th ed.). Prentice Hall. ISBN: 978-0131013674. Available at: <https://www.pearson.com/en-us/subject-catalog/p/transport-processes-and-separation-process-principles/P200000003447>
147. Middleman, S. (1998). *An introduction to mass and heat transfer: Principles of analysis and design*. John Wiley & Sons. ISBN: 978-0471111764. Available at: <https://www.wiley.com/en-us/An+Introduction+to+Mass+and+Heat+Transfer%3A+Principles+of+Analysis+and+Design-p-9780471111764>
148. Bennett, C. O., & Myers, J. E. (1982). *Momentum, heat, and mass transfer* (3rd ed.). McGraw-Hill. ISBN: 978-0070045675. Available at: <https://www.mheducation.com/highered/product/momentum-heat-mass-transfer-bennett-myers/M9780070045675.html>
149. Skelland, A. H. P. (1974). *Diffusional mass transfer*. John Wiley & Sons. ISBN: 978-0471792086. Available at: <https://www.wiley.com/en-us/Diffusional+Mass+Transfer-p-9780471792086>

150. Sherwood, T. K., Pigford, R. L., & Wilke, C. R. (1975). *Mass transfer*. McGraw-Hill. ISBN: 978-0070566859. Available at: <https://www.mheducation.com/highered/product/mass-transfer-sherwood-pigford/M9780070566859.html>
151. Treybal, R. E. (1980). *Mass-transfer operations* (3rd ed.). McGraw-Hill. ISBN: 978-0070651760. Available at: <https://www.mheducation.com/highered/product/mass-transfer-operations-treybal/M9780070651760.html>
152. Cussler, E. L. (2008). *Diffusion: Mass transfer in fluid systems* (3rd ed.). Cambridge University Press. DOI: <https://doi.org/10.1017/CBO9780511805134>
153. Taylor, R., & Krishna, R. (1993). *Multicomponent mass transfer*. John Wiley & Sons. ISBN: 978-0471574170. Available at: <https://www.wiley.com/en-us/Multicomponent+Mass+Transfer-p-9780471574170>
154. Wesselingh, J. A., & Krishna, R. (2000). *Mass transfer in multicomponent mixtures*. VSSD. ISBN: 978-9071301629. Available at: <https://www.vssd.nl/hlf/m006.htm>
155. Poling, B. E., Prausnitz, J. M., & O'Connell, J. P. (2000). *The properties of gases and liquids* (5th ed.). McGraw-Hill. ISBN: 978-0070116825. Available at: <https://www.mheducation.com/highered/product/properties-gases-liquids-poling-prausnitz/M9780070116825.html>
156. Emmons, H. W. (1951). The laminar-turbulent transition in a boundary layer-Part I. *Journal of the Aeronautical Sciences*, 18(7), 490-498. DOI: <https://doi.org/10.2514/8.2010>
157. Schlichting, H., & Gersten, K. (2016). *Boundary-layer theory* (9th ed.). Springer. DOI: <https://doi.org/10.1007/978-3-662-52919-5>
158. Cebeci, T., & Bradshaw, P. (1984). *Physical and computational aspects of convective heat transfer*. Springer. DOI: <https://doi.org/10.1007/978-1-4612-5284-3>
159. Kays, W. M., Crawford, M. E., & Weigand, B. (2004). *Convective heat and mass transfer* (4th ed.). McGraw-Hill. ISBN: 978-0072990737. Available at: <https://www.mheducation.com/highered/product/convective-heat-mass-transfer-kays-crawford/M9780072990737.html>
160. Eckert, E. R. G., & Drake, R. M. (1987). *Analysis of heat and mass transfer*. Hemisphere Publishing. ISBN: 978-0891165279. Available at: <https://www.routledge.com/Analysis-of-Heat-and-Mass-Transfer/Eckert-Drake/p/book/9780891165279>
161. Burmeister, L. C. (1993). *Convective heat transfer* (2nd ed.). John Wiley & Sons. ISBN: 978-0471575399. Available at: <https://www.wiley.com/en-us/Convective+Heat+Transfer%2C+2nd+Edition-p-9780471575399>
162. Jaluria, Y. (2007). *Design and optimization of thermal systems* (2nd ed.). CRC Press. ISBN: 978-0849337536. Available at: <https://www.routledge.com/Design-and-Optimization-of-Thermal-Systems/Jaluria/p/book/9780849337536>
163. Oosthuizen, P. H., & Naylor, D. (1999). *Introduction to convective heat transfer analysis*. McGraw-Hill. ISBN: 978-0070482128. Available at: <https://www.mheducation.com/highered/product/introduction-convective-heat-transfer-analysis-oosthuizen-naylor/M9780070482128.html>
164. Kaviany, M. (2001). *Principles of heat transfer*. John Wiley & Sons. ISBN: 978-0471305538. Available at: <https://www.wiley.com/en-us/Principles+of+Heat+Transfer-p-9780471305538>
165. Nellis, G., & Klein, S. (2008). *Heat transfer*. Cambridge University Press. DOI: <https://doi.org/10.1017/CBO9780511841606>
166. Tien, C. L., & Lienhard, J. H. (1979). *Statistical thermodynamics*. Hemisphere Publishing. ISBN: 978-0891162292. Available at: <https://www.routledge.com/Statistical-Thermodynamics/Tien-Lienhard/p/book/9780891162292>
167. Modest, M. F. (2013). *Radiative heat transfer* (3rd ed.). Academic Press. ISBN: 978-0123869449. Available at: <https://www.elsevier.com/books/radiative-heat-transfer/modest/978-0-12-386944-9>
168. Siegel, R., & Howell, J. R. (2002). *Thermal radiation heat transfer* (4th ed.). Taylor & Francis. ISBN: 978-1560328391. Available at: <https://www.routledge.com/Thermal-Radiation-Heat-Transfer/Siegel-Howell/p/book/9781560328391>
169. Sparrow, E. M., & Cess, R. D. (1978). *Radiation heat transfer*. Hemisphere Publishing. ISBN: 978-0891162391. Available at: <https://www.routledge.com/Radiation-Heat-Transfer/Sparrow-Cess/p/book/9780891162391>

170. Hottel, H. C., & Sarofim, A. F. (1967). *Radiative transfer*. McGraw-Hill. ISBN: 978-0070304178. Available at: <https://www.mheducation.com/highered/product/radiative-transfer-hottel-sarofim/M9780070304178.html>
171. Özişik, M. N. (1973). *Radiative transfer and interactions with conduction and convection*. John Wiley & Sons. ISBN: 978-0471652717. Available at: <https://www.wiley.com/en-us/Radiative+Transfer+and+Interactions+with+Conduction+and+Convection-p-9780471652717>
172. Love, T. J. (1968). *Radiative heat transfer*. Charles E. Merrill Publishing. ISBN: 978-0675095037. Available at: <https://www.amazon.com/Radiative-Heat-Transfer-T-Love/dp/0675095034>
173. Edwards, D. K. (1981). *Radiation heat transfer notes*. Hemisphere Publishing. ISBN: 978-0891162568. Available at: <https://www.routledge.com/Radiation-Heat-Transfer-Notes/Edwards/p/book/9780891162568>
174. Planck, M. (1914). *The theory of heat radiation*. P. Blakiston's Son & Co. Available at: <https://archive.org/details/theoryofheatradi00planrich>
175. Wien, W. (1896). Über die Energieverteilung im Emissionsspektrum eines schwarzen Körpers. *Annalen der Physik*, 58(8), 662-669. DOI: <https://doi.org/10.1002/andp.18962940803>
176. Stefan, J. (1879). Über die Beziehung zwischen der Wärmestrahlung und der Temperatur. *Sitzungsberichte der mathematisch-naturwissenschaftlichen Classe der kaiserlichen Akademie der Wissenschaften*, 79, 391-428. Available at: <https://www.biodiversitylibrary.org/item/110297>
177. Boltzmann, L. (1884). Ableitung des Stefan'schen Gesetzes, betreffend die Abhängigkeit der Wärmestrahlung von der Temperatur aus der elektromagnetischen Lichttheorie. *Annalen der Physik*, 22(2), 291-294. DOI: <https://doi.org/10.1002/andp.18842580616>
178. Kirchhoff, G. (1860). Über das Verhältnis zwischen dem Emissionsvermögen und dem Absorptionsvermögen der Körper für Wärme und Licht. *Annalen der Physik*, 109(2), 275-301. DOI: <https://doi.org/10.1002/andp.18601850205>
179. Lambert, J. H. (1760). *Photometria sive de mensura et gradibus luminis, colorum et umbrae*. Augsburg: Eberhard Klett. Available at: https://archive.org/details/bub_gb_ykcVAAAAQAAJ
250. Blazek, J. (2015). *Computational fluid dynamics: Principles and applications* (3rd ed.). Butterworth-Heinemann. ISBN: 978-0080999951. Available at: <https://www.elsevier.com/books/computational-fluid-dynamics/blazek/978-0-08-099995-1>
251. Versteeg, H. K., & Malalasekera, W. (2007). *An introduction to computational fluid dynamics: The finite volume method* (2nd ed.). Pearson Education. ISBN: 978-0131274983. Available at: <https://www.pearson.com/en-us/subject-catalog/p/introduction-to-computational-fluid-dynamics-the-finite-volume-method/P200000003448>
252. Ferziger, J. H., Perić, M., & Street, R. L. (2019). *Computational methods for fluid dynamics* (4th ed.). Springer. DOI: <https://doi.org/10.1007/978-3-319-99693-6>
253. Chung, T. J. (2010). *Computational fluid dynamics* (2nd ed.). Cambridge University Press. DOI: <https://doi.org/10.1017/CBO9780511780066>
254. Tannehill, J. C., Anderson, D. A., & Pletcher, R. H. (1997). *Computational fluid mechanics and heat transfer* (2nd ed.). Taylor & Francis. ISBN: 978-1560320463. Available at: <https://www.routledge.com/Computational-Fluid-Mechanics-and-Heat-Transfer/Tannehill-Anderson-Pletcher/p/book/9781560320463>
255. Patankar, S. V. (1980). *Numerical heat transfer and fluid flow*. Hemisphere Publishing. ISBN: 978-0891165224. Available at: <https://www.routledge.com/Numerical-Heat-Transfer-and-Fluid-Flow/Patankar/p/book/9780891165224>
256. Fletcher, C. A. J. (1991). *Computational techniques for fluid dynamics* (2nd ed.). Springer. DOI: <https://doi.org/10.1007/978-3-642-58239-4>
257. Roache, P. J. (1998). *Fundamentals of computational fluid dynamics*. Hermosa Publishers. ISBN: 978-0913478097. Available at: <https://www.hermosapublishers.com/fundamentals-of-computational-fluid-dynamics>
258. Wendt, J. F. (2008). *Computational fluid dynamics: An introduction* (3rd ed.). Springer. DOI: <https://doi.org/10.1007/978-3-540-85056-4>
259. Tu, J., Yeoh, G. H., & Liu, C. (2018). *Computational fluid dynamics: A practical approach* (3rd ed.). Butterworth-Heinemann. ISBN: 978-0081011270. Available at: <https://www.elsevier.com/books/computational-fluid-dynamics/tu/978-0-08-101127-0>

260. Lomax, H., Pulliam, T. H., & Zingg, D. W. (2001). *Fundamentals of computational fluid dynamics*. Springer. DOI: <https://doi.org/10.1007/978-3-662-04654-8>
261. Peyret, R., & Taylor, T. D. (1983). *Computational methods for fluid flow*. Springer. DOI: <https://doi.org/10.1007/978-3-642-85952-6>
262. Hoffmann, K. A., & Chiang, S. T. (2000). *Computational fluid dynamics* (4th ed.). Engineering Education System. ISBN: 978-0962373121. Available at: <https://www.eesbooks.com/computational-fluid-dynamics-volume-i>
263. Cebeci, T., Shao, J. P., Kafyeke, F., & Laurendeau, E. (2005). *Computational fluid dynamics for engineers*. Springer. DOI: <https://doi.org/10.1007/b138137>
264. Date, A. W. (2005). *Introduction to computational fluid dynamics*. Cambridge University Press. DOI: <https://doi.org/10.1017/CBO9780511808975>
265. Moukalled, F., Mangani, L., & Darwish, M. (2015). *The finite volume method in computational fluid dynamics: An advanced introduction with OpenFOAM and Matlab*. Springer. DOI: <https://doi.org/10.1007/978-3-319-16874-6>
266. Wesseling, P. (2001). *Principles of computational fluid dynamics*. Springer. DOI: <https://doi.org/10.1007/978-3-642-05146-3>
267. Quarteroni, A., Sacco, R., & Saleri, F. (2007). *Numerical mathematics*. Springer. DOI: <https://doi.org/10.1007/b98885>
268. LeVeque, R. J. (2002). *Finite volume methods for hyperbolic problems*. Cambridge University Press. DOI: <https://doi.org/10.1017/CBO9780511791253>
269. Toro, E. F. (2009). *Riemann solvers and numerical methods for fluid dynamics: A practical introduction* (3rd ed.). Springer. DOI: <https://doi.org/10.1007/b79761>
270. Godunov, S. K. (1959). A difference method for numerical calculation of discontinuous solutions of the equations of hydrodynamics. *Matematicheskii Sbornik*, 47(3), 271-306. Available at: <http://mi.mathnet.ru/eng/msb4873>
271. Van Leer, B. (1979). Towards the ultimate conservative difference scheme. V. A second-order sequel to Godunov's method. *Journal of Computational Physics*, 32(1), 101-136. DOI: [https://doi.org/10.1016/0021-9991\(79\)90145-1](https://doi.org/10.1016/0021-9991(79)90145-1)
272. Roe, P. L. (1981). Approximate Riemann solvers, parameter vectors, and difference schemes. *Journal of Computational Physics*, 43(2), 357-372. DOI: [https://doi.org/10.1016/0021-9991\(81\)90128-5](https://doi.org/10.1016/0021-9991(81)90128-5)
273. Harten, A. (1983). High resolution schemes for hyperbolic conservation laws. *Journal of Computational Physics*, 49(3), 357-393. DOI: [https://doi.org/10.1016/0021-9991\(83\)90136-5](https://doi.org/10.1016/0021-9991(83)90136-5)
274. Osher, S., & Sethian, J. A. (1988). Fronts propagating with curvature-dependent speed: Algorithms based on Hamilton-Jacobi formulations. *Journal of Computational Physics*, 79(1), 12-49. DOI: [https://doi.org/10.1016/0021-9991\(88\)90002-2](https://doi.org/10.1016/0021-9991(88)90002-2)
275. Sweby, P. K. (1984). High resolution schemes using flux limiters for hyperbolic conservation laws. *SIAM Journal on Numerical Analysis*, 21(5), 995-1011. DOI: <https://doi.org/10.1137/0721062>
276. Chakravarthy, S. R., & Osher, S. (1983). High resolution applications of the Osher upwind scheme for the Euler equations. *6th Computational Fluid Dynamics Conference*. DOI: <https://doi.org/10.2514/6.1983-1943>
277. Yee, H. C. (1989). A class of high resolution explicit and implicit shock-capturing methods. *NASA Technical Memorandum*, 101088. Available at: <https://ntrs.nasa.gov/citations/19890016302>
278. Liou, M. S., & Steffen Jr, C. J. (1993). A new flux splitting scheme. *Journal of Computational Physics*, 107(1), 23-39. DOI: <https://doi.org/10.1006/jcph.1993.1122>
279. Edwards, J. R., & Liou, M. S. (1998). Low-diffusion flux-splitting methods for flows at all speeds. *AIAA Journal*, 36(9), 1610-1617. DOI: <https://doi.org/10.2514/2.587>
280. Steger, J. L., & Warming, R. F. (1981). Flux vector splitting of the inviscid gasdynamic equations with application to finite-difference methods. *Journal of Computational Physics*, 40(2), 263-293. DOI: [https://doi.org/10.1016/0021-9991\(81\)90210-2](https://doi.org/10.1016/0021-9991(81)90210-2)
281. Van Leer, B. (1982). Flux-vector splitting for the Euler equations. *Lecture Notes in Physics*, 170, 507-512. DOI: https://doi.org/10.1007/3-540-11948-5_66

282. Harten, A., Lax, P. D., & van Leer, B. (1983). On upstream differencing and Godunov-type schemes for hyperbolic conservation laws. *SIAM Review*, 25(1), 35-61. DOI: <https://doi.org/10.1137/1025002>
283. Einfeldt, B. (1988). On Godunov-type methods for gas dynamics. *SIAM Journal on Numerical Analysis*, 25(2), 294-318. DOI: <https://doi.org/10.1137/0725021>
284. Toro, E. F., Spruce, M., & Speares, W. (1994). Restoration of the contact surface in the HLL-Riemann solver. *Shock Waves*, 4(1), 25-34. DOI: <https://doi.org/10.1007/BF01414629>
285. Batten, P., Clarke, N., Lambert, C., & Causon, D. M. (1997). On the choice of wavespeeds for the HLLC Riemann solver. *SIAM Journal on Scientific Computing*, 18(6), 1553-1570. DOI: <https://doi.org/10.1137/S1064827593260140>
286. Kurganov, A., & Tadmor, E. (2000). New high-resolution central schemes for nonlinear conservation laws and convection-diffusion equations. *Journal of Computational Physics*, 160(1), 241-282. DOI: <https://doi.org/10.1006/jcph.2000.6459>
287. Liu, X. D., Osher, S., & Chan, T. (1994). Weighted essentially non-oscillatory schemes. *Journal of Computational Physics*, 115(1), 200-212. DOI: <https://doi.org/10.1006/jcph.1994.1187>
288. Jiang, G. S., & Shu, C. W. (1996). Efficient implementation of weighted ENO schemes. *Journal of Computational Physics*, 126(1), 202-228. DOI: <https://doi.org/10.1006/jcph.1996.0130>
289. Shu, C. W. (1998). Essentially non-oscillatory and weighted essentially non-oscillatory schemes for hyperbolic conservation laws. *Advanced Numerical Approximation of Nonlinear Hyperbolic Equations*, 1697, 325-432. DOI: <https://doi.org/10.1007/BFb0096355>
290. Cockburn, B., & Shu, C. W. (1998). The Runge-Kutta discontinuous Galerkin method for conservation laws V: Multidimensional systems. *Journal of Computational Physics*, 141(2), 199-224. DOI: <https://doi.org/10.1006/jcph.1998.5892>
291. Reed, W. H., & Hill, T. R. (1973). Triangular mesh methods for the neutron transport equation. *Los Alamos Scientific Laboratory Report, LA-UR-73-479*. Available at: <https://www.osti.gov/biblio/4491151>
292. Bassi, F., & Rebay, S. (1997). A high-order accurate discontinuous finite element method for the numerical solution of the compressible Navier-Stokes equations. *Journal of Computational Physics*, 131(2), 267-279. DOI: <https://doi.org/10.1006/jcph.1996.5572>
293. Cockburn, B., Karniadakis, G. E., & Shu, C. W. (2000). *Discontinuous Galerkin methods: Theory, computation and applications*. Springer. DOI: <https://doi.org/10.1007/978-3-642-59721-3>
294. Hesthaven, J. S., & Warburton, T. (2007). *Nodal discontinuous Galerkin methods: Algorithms, analysis, and applications*. Springer. DOI: <https://doi.org/10.1007/978-0-387-72067-8>
295. Kopriva, D. A. (2009). *Implementing spectral methods for partial differential equations: Algorithms for scientists and engineers*. Springer. DOI: <https://doi.org/10.1007/978-90-481-2261-5>
296. Canuto, C., Hussaini, M. Y., Quarteroni, A., & Zang, T. A. (2006). *Spectral methods: Fundamentals in single domains*. Springer. DOI: <https://doi.org/10.1007/978-3-540-30726-6>
297. Boyd, J. P. (2001). *Chebyshev and Fourier spectral methods* (2nd ed.). Dover Publications. ISBN: 978-0486411835. Available at: <https://store.doverpublications.com/0486411834.html>
298. Gottlieb, D., & Orszag, S. A. (1977). *Numerical analysis of spectral methods: Theory and applications*. SIAM. DOI: <https://doi.org/10.1137/1.9781611970425>
299. Trefethen, L. N. (2000). *Spectral methods in MATLAB*. SIAM. DOI: <https://doi.org/10.1137/1.9780898719598>
300. Fornberg, B. (1996). *A practical guide to pseudospectral methods*. Cambridge University Press. DOI: <https://doi.org/10.1017/CBO9780511626357>
301. Karniadakis, G., & Sherwin, S. (2013). *Spectral/hp element methods for computational fluid dynamics* (2nd ed.). Oxford University Press. ISBN: 978-0199678549. Available at: <https://global.oup.com/academic/product/spectralhp-element-methods-for-computational-fluid-dynamics-9780199678549>
302. Deville, M. O., Fischer, P. F., & Mund, E. H. (2002). *High-order methods for incompressible fluid flow*. Cambridge University Press. DOI: <https://doi.org/10.1017/CBO9780511546792>
303. Sherwin, S. J., & Karniadakis, G. E. (1995). A triangular spectral element method; applications to the incompressible Navier-Stokes equations. *Computer Methods in Applied Mechanics and Engineering*, 123(1-4), 189-229. DOI: [https://doi.org/10.1016/0045-7825\(94\)00745-9](https://doi.org/10.1016/0045-7825(94)00745-9)

304. Patera, A. T. (1984). A spectral element method for fluid dynamics: Laminar flow in a channel expansion. *Journal of Computational Physics*, 54(3), 468-488. DOI: [https://doi.org/10.1016/0021-9991\(84\)90128-1](https://doi.org/10.1016/0021-9991(84)90128-1)
305. Maday, Y., & Patera, A. T. (1989). Spectral element methods for the incompressible Navier-Stokes equations. *State-of-the-art surveys on computational mechanics*, 71-143. Available at: <https://www.osti.gov/biblio/6845707>
306. Fischer, P. F., Lottes, J. W., & Kerkemeier, S. G. (2008). *Nek5000 web page*. Available at: <http://nek5000.mcs.anl.gov>
307. Blackburn, H. M., & Sherwin, S. J. (2004). Formulation of a Galerkin spectral element–Fourier method for three-dimensional incompressible flows in cylindrical geometries. *Journal of Computational Physics*, 197(2), 759-778. DOI: <https://doi.org/10.1016/j.jcp.2004.02.013>
308. Cantwell, C. D., Moxey, D., Comerford, A., Bolis, A., Rocco, G., Mengaldo, G., ... & Kirby, R. M. (2015). Nektar++: An open-source spectral/hp element framework. *Computer Physics Communications*, 192, 205-219. DOI: <https://doi.org/10.1016/j.cpc.2015.02.008>
309. Xu, H., Cantwell, C. D., Monteserin, C., Eskilsson, C., Engsig-Karup, A. P., & Sherwin, S. J. (2018). Spectral/hp element methods: Recent developments, applications, and perspectives. *Journal of Hydrodynamics*, 30(1), 1-22. DOI: <https://doi.org/10.1007/s42241-018-0001-1>
310. Mengaldo, G., De Grazia, D., Moxey, D., Vincent, P. E., & Sherwin, S. J. (2015). Dealiasing techniques for high-order spectral element methods on regular and irregular grids. *Journal of Computational Physics*, 299, 56-81. DOI: <https://doi.org/10.1016/j.jcp.2015.06.032>
311. Kirby, R. M., & Sherwin, S. J. (2006). Stabilisation of spectral/hp element methods through spectral vanishing viscosity: Application to fluid mechanics modelling. *Computer Methods in Applied Mechanics and Engineering*, 195(23-24), 3128-3144. DOI: <https://doi.org/10.1016/j.cma.2004.09.019>
312. Karamanos, G. S., & Karniadakis, G. E. (2000). A spectral vanishing viscosity method for large-eddy simulations. *Journal of Computational Physics*, 163(1), 22-50. DOI: <https://doi.org/10.1006/jcph.2000.6552>
313. Tadmor, E. (1989). Convergence of spectral methods for nonlinear conservation laws. *SIAM Journal on Numerical Analysis*, 26(1), 30-44. DOI: <https://doi.org/10.1137/0726003>
314. Maday, Y., Tadmor, E., et al. (1993). Analysis of the spectral vanishing viscosity method for periodic conservation laws. *SIAM Journal on Numerical Analysis*, 26(4), 854-870. DOI: <https://doi.org/10.1137/0726047>
315. Lomtev, I., Quillen, C. B., & Karniadakis, G. E. (1998). Spectral/hp methods for viscous compressible flows on unstructured 2D meshes. *Journal of Computational Physics*, 144(2), 325-357. DOI: <https://doi.org/10.1006/jcph.1998.5999>
316. Warburton, T., & Karniadakis, G. E. (1999). A discontinuous Galerkin method for the viscous MHD equations. *Journal of Computational Physics*, 152(2), 608-641. DOI: <https://doi.org/10.1006/jcph.1999.6248>
317. Karniadakis, G. E., Israeli, M., & Orszag, S. A. (1991). High-order splitting methods for the incompressible Navier-Stokes equations. *Journal of Computational Physics*, 97(2), 414-443. DOI: [https://doi.org/10.1016/0021-9991\(91\)90007-8](https://doi.org/10.1016/0021-9991(91)90007-8)
318. Guermond, J. L., Mineev, P., & Shen, J. (2006). An overview of projection methods for incompressible flows. *Computer Methods in Applied Mechanics and Engineering*, 195(44-47), 6011-6045. DOI: <https://doi.org/10.1016/j.cma.2005.10.010>
319. Brown, D. L., Cortez, R., & Minion, M. L. (2001). Accurate projection methods for the incompressible Navier–Stokes equations. *Journal of Computational Physics*, 168(2), 464-499. DOI: <https://doi.org/10.1006/jcph.2001.6715>
320. Chorin, A. J. (1968). Numerical solution of the Navier-Stokes equations. *Mathematics of Computation*, 22(104), 745-762. DOI: <https://doi.org/10.1090/S0025-5718-1968-0242392-2>
321. Temam, R. (1969). Sur l'approximation de la solution des équations de Navier-Stokes par la méthode des pas fractionnaires (II). *Archive for Rational Mechanics and Analysis*, 33(5), 377-385. DOI: <https://doi.org/10.1007/BF00247696>
322. Kim, J., & Moin, P. (1985). Application of a fractional-step method to incompressible Navier-Stokes equations. *Journal of Computational Physics*, 59(2), 308-323. DOI: [https://doi.org/10.1016/0021-9991\(85\)90148-2](https://doi.org/10.1016/0021-9991(85)90148-2)

323. Bell, J. B., Colella, P., & Glaz, H. M. (1989). A second-order projection method for the incompressible Navier-Stokes equations. *Journal of Computational Physics*, 85(2), 257-283. DOI: [https://doi.org/10.1016/0021-9991\(89\)90151-4](https://doi.org/10.1016/0021-9991(89)90151-4)
324. Van Kan, J. (1986). A second-order accurate pressure-correction scheme for viscous incompressible flow. *SIAM Journal on Scientific and Statistical Computing*, 7(3), 870-891. DOI: <https://doi.org/10.1137/0907059>
325. Gresho, P. M., & Sani, R. L. (1987). On pressure boundary conditions for the incompressible Navier-Stokes equations. *International Journal for Numerical Methods in Fluids*, 7(10), 1111-1145. DOI: <https://doi.org/10.1002/flid.1650071010>
326. Orszag, S. A., Israeli, M., & Deville, M. O. (1986). Boundary conditions for incompressible flows. *Journal of Scientific Computing*, 1(1), 75-111. DOI: <https://doi.org/10.1007/BF01061454>
327. Shen, J. (1992). On error estimates of projection methods for Navier-Stokes equations: First-order schemes. *SIAM Journal on Numerical Analysis*, 29(1), 57-77. DOI: <https://doi.org/10.1137/0729004>
328. Guermond, J. L., & Shen, J. (2003). Velocity-correction projection methods for incompressible flows. *SIAM Journal on Numerical Analysis*, 41(1), 112-134. DOI: <https://doi.org/10.1137/S0036142901395400>
329. Timmermans, L. J. P., Mineev, P. D., & Van De Vosse, F. N. (1996). An approximate projection scheme for incompressible flow using spectral elements. *International Journal for Numerical Methods in Fluids*, 22(7), 673-688. DOI: [https://doi.org/10.1002/\(SICI\)1097-0363\(19960415\)22:7<673::AID-FLD373>3.0.CO;2-O](https://doi.org/10.1002/(SICI)1097-0363(19960415)22:7<673::AID-FLD373>3.0.CO;2-O)
330. Karniadakis, G. E., & Sherwin, S. J. (2005). *Spectral/hp element methods for computational fluid dynamics* (2nd ed.). Oxford University Press. ISBN: 978-0195152401. Available at: <https://global.oup.com/academic/product/spectralhp-element-methods-for-computational-fluid-dynamics-9780195152401>
331. Deville, M. O., Fischer, P. F., & Mund, E. H. (2002). *High-order methods for incompressible fluid flow*. Cambridge University Press. DOI: <https://doi.org/10.1017/CBO9780511546792>
332. Bernardi, C., & Maday, Y. (1997). Spectral methods. *Handbook of Numerical Analysis*, 5, 209-485. DOI: [https://doi.org/10.1016/S1570-8659\(97\)80003-8](https://doi.org/10.1016/S1570-8659(97)80003-8)
333. Quarteroni, A., & Valli, A. (1994). *Numerical approximation of partial differential equations*. Springer. DOI: <https://doi.org/10.1007/978-3-540-85268-1>
334. Brenner, S., & Scott, R. (2007). *The mathematical theory of finite element methods* (3rd ed.). Springer. DOI: <https://doi.org/10.1007/978-0-387-75934-0>
335. Ciarlet, P. G. (2002). *The finite element method for elliptic problems*. SIAM. DOI: <https://doi.org/10.1137/1.9780898719208>
336. Hughes, T. J. R. (2012). *The finite element method: Linear static and dynamic finite element analysis*. Dover Publications. ISBN: 978-0486411811. Available at: <https://store.doverpublications.com/0486411811.html>
337. Zienkiewicz, O. C., Taylor, R. L., & Zhu, J. Z. (2013). *The finite element method: Its basis and fundamentals* (7th ed.). Butterworth-Heinemann. ISBN: 978-1856176330. Available at: <https://www.elsevier.com/books/the-finite-element-method-its-basis-and-fundamentals/zienkiewicz/978-1-85617-633-0>
338. Reddy, J. N. (2019). *Introduction to the finite element method* (4th ed.). McGraw-Hill. ISBN: 978-0073398143. Available at: <https://www.mheducation.com/highered/product/introduction-finite-element-method-reddy/M9780073398143.html>
339. Bathe, K. J. (2014). *Finite element procedures* (2nd ed.). Klaus-Jürgen Bathe. ISBN: 978-0979004957. Available at: https://web.mit.edu/kjb/www/Books/FEP_2nd_Edition_4th_Printing.pdf
340. Cook, R. D., Malkus, D. S., Plesha, M. E., & Witt, R. J. (2001). *Concepts and applications of finite element analysis* (4th ed.). John Wiley & Sons. ISBN: 978-0471356059. Available at: <https://www.wiley.com/en-us/Concepts+and+Applications+of+Finite+Element+Analysis%2C+4th+Edition-p-9780471356059>
341. Fish, J., & Belytschko, T. (2007). *A first course in finite elements*. John Wiley & Sons. ISBN: 978-0470035801. Available at: <https://www.wiley.com/en-us/A+First+Course+in+Finite+Elements-p-9780470035801>
342. Logan, D. L. (2016). *A first course in the finite element method* (6th ed.). Cengage Learning. ISBN: 978-1305635111. Available at: <https://www.cengage.com/c/a-first-course-in-the-finite-element-method-6e-logan/9781305635111/>

343. Chandrupatla, T. R., & Belegundu, A. D. (2011). *Introduction to finite elements in engineering* (4th ed.). Pearson. ISBN: 978-0132162746. Available at: <https://www.pearson.com/en-us/subject-catalog/p/introduction-to-finite-elements-in-engineering/P200000003449>
344. Segerlind, L. J. (1984). *Applied finite element analysis* (2nd ed.). John Wiley & Sons. ISBN: 978-0471806622. Available at: <https://www.wiley.com/en-us/Applied+Finite+Element+Analysis%2C+2nd+Edition-p-9780471806622>
345. Hutton, D. V. (2003). *Fundamentals of finite element analysis*. McGraw-Hill. ISBN: 978-0072922363. Available at: <https://www.mheducation.com/highered/product/fundamentals-finite-element-analysis-hutton/M9780072922363.html>
346. Bhatti, M. A. (2005). *Fundamental finite element analysis and applications: With Mathematica and MATLAB computations*. John Wiley & Sons. ISBN: 978-0471648086. Available at: <https://www.wiley.com/en-us/Fundamental+Finite+Element+Analysis+and+Applications%3A+with+Mathematica+and+Matlab+Computations-p-9780471648086>
347. Kwon, Y. W., & Bang, H. (2018). *The finite element method using MATLAB* (2nd ed.). CRC Press. ISBN: 978-0849300967. Available at: <https://www.routledge.com/The-Finite-Element-Method-Using-MATLAB/Kwon-Bang/p/book/9780849300967>
348. Ferreira, A. J. M. (2008). *MATLAB codes for finite element analysis: Solids and structures*. Springer. DOI: <https://doi.org/10.1007/978-1-4020-9200-8>
349. Liu, G. R., & Quek, S. S. (2013). *The finite element method: A practical course* (2nd ed.). Butterworth-Heinemann. ISBN: 978-0080983561. Available at: <https://www.elsevier.com/books/the-finite-element-method/liu/978-0-08-098356-1>
350. Rao, S. S. (2017). *The finite element method in engineering* (6th ed.). Butterworth-Heinemann. ISBN: 978-0128007921. Available at: <https://www.elsevier.com/books/the-finite-element-method-in-engineering/rao/978-0-12-800792-1>. (References 351-450 (Turbomachinery CFD Applications and Unsteady Flow Methods))
351. Denton, J. D. (2002). The effects of lean and sweep on transonic fan performance: A computational study. *Proceedings of ASME Turbo Expo 2002*. DOI: <https://doi.org/10.1115/GT2002-30327>
352. Giles, M. B. (1990). Stator/rotor interaction in a transonic turbine. *Journal of Propulsion and Power*, 6(5), 621-627. DOI: <https://doi.org/10.2514/3.23263>
353. He, L. (1992). Method of simulating unsteady turbomachinery flows with multiple perturbations. *AIAA Journal*, 30(11), 2730-2735. DOI: <https://doi.org/10.2514/3.11291>
354. Hall, K. C., Thomas, J. P., & Clark, W. S. (2002). Computation of unsteady nonlinear flows in cascades using a harmonic balance technique. *AIAA Journal*, 40(5), 879-886. DOI: <https://doi.org/10.2514/2.1754>
355. McMullen, M., Jameson, A., & Alonso, J. J. (2006). Demonstration of nonlinear frequency domain methods. *AIAA Journal*, 44(7), 1428-1435. DOI: <https://doi.org/10.2514/1.15127>
356. Ekici, K., & Hall, K. C. (2007). Nonlinear analysis of unsteady flows in multistage turbomachines using harmonic balance. *AIAA Journal*, 45(5), 1047-1057. DOI: <https://doi.org/10.2514/1.22888>
357. Gopinath, A. K., & Jameson, A. (2005). Time spectral method for periodic unsteady computations over two- and three-dimensional bodies. *43rd AIAA Aerospace Sciences Meeting and Exhibit*. DOI: <https://doi.org/10.2514/6.2005-1220>
358. van der Weide, E., Gopinath, A. K., & Jameson, A. (2005). Turbomachinery applications with the time spectral method. *35th AIAA Fluid Dynamics Conference and Exhibit*. DOI: <https://doi.org/10.2514/6.2005-4905>
359. Ning, W., & He, L. (1998). Computation of unsteady flows around oscillating blades using linear and nonlinear harmonic Euler methods. *Journal of Turbomachinery*, 120(3), 508-514. DOI: <https://doi.org/10.1115/1.2841747>
360. Chen, T., Vasanthakumar, P., & He, L. (2001). Analysis of unsteady blade row interaction using nonlinear harmonic approach. *Journal of Propulsion and Power*, 17(3), 651-658. DOI: <https://doi.org/10.2514/2.5792>
361. Vilmin, S., Lorrain, E., Hirsch, C., & Swoboda, M. (2006). Unsteady flow modeling across the rotor/stator interface using the nonlinear harmonic method. *Proceedings of ASME Turbo Expo 2006*. DOI: <https://doi.org/10.1115/GT2006-90210>

362. Sicot, F., Puigt, G., & Montagnac, M. (2008). Block-Jacobi implicit algorithms for the time spectral method. *AIAA Journal*, 46(12), 3080-3089. DOI: <https://doi.org/10.2514/1.36792>
363. Nadarajah, S., & Jameson, A. (2007). Optimum shape design for unsteady flows with time-accurate continuous and discrete adjoint methods. *AIAA Journal*, 45(7), 1478-1491. DOI: <https://doi.org/10.2514/1.24332>
364. Thomas, J. P., Dowell, E. H., & Hall, K. C. (2002). Nonlinear inviscid aerodynamic effects on transonic divergence, flutter, and limit-cycle oscillations. *AIAA Journal*, 40(4), 638-646. DOI: <https://doi.org/10.2514/2.1720>
365. Woodgate, M. A., & Badcock, K. J. (2007). Fast prediction of transonic aeroelastic stability and limit cycles. *AIAA Journal*, 45(6), 1370-1381. DOI: <https://doi.org/10.2514/1.25604>
366. Campobasso, M. S., & Giles, M. B. (2003). Effects of flow instabilities on the linear analysis of turbomachinery aeroelasticity. *Journal of Propulsion and Power*, 19(2), 250-259. DOI: <https://doi.org/10.2514/2.6111>
367. Sayma, A. I., Vahdati, M., Sbardella, L., & Imregun, M. (2000). Modeling of three-dimensional viscous compressible turbomachinery flows using unstructured hybrid grids. *AIAA Journal*, 38(6), 945-954. DOI: <https://doi.org/10.2514/2.1062>
368. Vahdati, M., Sayma, A. I., Freeman, C., & Imregun, M. (2005). On the use of atmospheric boundary conditions for axial-flow compressor stall simulations. *Journal of Turbomachinery*, 127(2), 349-351. DOI: <https://doi.org/10.1115/1.1861912>
369. Chima, R. V. (1998). Calculation of multistage turbomachinery using steady characteristic boundary conditions. *36th AIAA Aerospace Sciences Meeting and Exhibit*. DOI: <https://doi.org/10.2514/6.1998-968>
370. Giles, M. B. (1988). UNSFLO: A numerical method for unsteady inviscid flow in turbomachinery. *MIT Gas Turbine Laboratory Report*, 195. Available at: <https://dspace.mit.edu/handle/1721.1/2879>
371. Rai, M. M. (1987). Navier-Stokes simulations of rotor/stator interaction using patched and overlaid grids. *Journal of Propulsion and Power*, 3(5), 387-396. DOI: <https://doi.org/10.2514/3.23003>
372. Rai, M. M. (1989). Three-dimensional Navier-Stokes simulations of turbine rotor-stator interaction; Part I—Methodology. *Journal of Propulsion and Power*, 5(3), 305-311. DOI: <https://doi.org/10.2514/3.23154>
373. Rai, M. M. (1989). Three-dimensional Navier-Stokes simulations of turbine rotor-stator interaction; Part II—Results. *Journal of Propulsion and Power*, 5(3), 312-319. DOI: <https://doi.org/10.2514/3.23155>
374. Dawes, W. N. (1992). The simulation of three-dimensional viscous flow in turbomachinery geometries using a solution-adaptive unstructured mesh methodology. *Journal of Turbomachinery*, 114(3), 528-537. DOI: <https://doi.org/10.1115/1.2929177>
375. Dawes, W. N. (1993). A numerical study of the interaction of a transonic compressor rotor overtight vortex with the following stator. *Journal of Turbomachinery*, 115(4), 946-955. DOI: <https://doi.org/10.1115/1.2929320>
376. Denton, J. D., & Singh, U. K. (1979). Time marching methods for turbomachinery flow calculation. *Lecture Series-Von Karman Institute for Fluid Dynamics*, 7, 1-48. Available at: <https://www.vki.ac.be/index.php/lecture-series-documents>
377. Denton, J. D. (1992). The calculation of three-dimensional viscous flow through multistage turbomachines. *Journal of Turbomachinery*, 114(1), 18-26. DOI: <https://doi.org/10.1115/1.2927983>
378. Arnone, A., Liou, M. S., & Povinelli, L. A. (1992). Navier-Stokes solution of transonic cascade flows using non-periodic C-type grids. *Journal of Propulsion and Power*, 8(2), 410-417. DOI: <https://doi.org/10.2514/3.23494>
379. Arnone, A., & Pacciani, R. (1996). Rotor-stator interaction analysis using the Navier-Stokes equations and a multigrid method. *Journal of Turbomachinery*, 118(4), 679-689. DOI: <https://doi.org/10.1115/1.2840923>
380. Dorney, D. J., & Verdon, J. M. (1994). Numerical simulations of unsteady cascade flow. *Journal of Turbomachinery*, 116(4), 665-675. DOI: <https://doi.org/10.1115/1.2929460>
381. Dorney, D. J., & Sharma, O. P. (1996). A study of turbine performance increases through airfoil clocking. *34th Aerospace Sciences Meeting and Exhibit*. DOI: <https://doi.org/10.2514/6.1996-2816>

382. Gundy-Burlet, K. L., & Dorney, D. J. (1997). Three-dimensional simulations of hot streak clocking in a 1-1/2 stage turbine. *International Journal of Turbo and Jet Engines*, 14(3), 123-132. DOI: <https://doi.org/10.1515/TJJ.1997.14.3.123>
383. Sharma, O. P., Pickett, G. F., & Ni, R. H. (1992). Assessment of unsteady flows in turbines. *Journal of Turbomachinery*, 114(1), 79-90. DOI: <https://doi.org/10.1115/1.2927991>
384. Ni, R. H. (1982). A multiple-grid scheme for solving the Euler equations. *AIAA Journal*, 20(11), 1565-1571. DOI: <https://doi.org/10.2514/3.51220>
385. Ni, R. H., & Bogoian, J. C. (1989). Prediction of 3-D multi-stage turbine flow field using a multiple-grid Euler solver. *27th Aerospace Sciences Meeting*. DOI: <https://doi.org/10.2514/6.1989-203>
386. Chima, R. V. (1987). Explicit multigrid algorithm for quasi-three-dimensional viscous flows in turbomachinery. *Journal of Propulsion and Power*, 3(5), 397-405. DOI: <https://doi.org/10.2514/3.23004>
387. Chima, R. V., & Yokota, J. W. (1990). Numerical analysis of three-dimensional viscous internal flows. *AIAA Journal*, 28(5), 798-806. DOI: <https://doi.org/10.2514/3.25118>
388. Steinthorsson, E., Liou, M. S., & Povinelli, L. A. (1993). Development of an explicit multiblock/multigrid flow solver for viscous flows in complex geometries. *31st Aerospace Sciences Meeting*. DOI: <https://doi.org/10.2514/6.1993-668>
389. Ameri, A. A., & Arnone, A. (1994). Prediction of turbine blade passage heat transfer using a zero and a two-equation turbulence model. *Proceedings of ASME Turbo Expo 1994*. DOI: <https://doi.org/10.1115/94-GT-122>
390. Ameri, A. A., & Steinthorsson, E. (1995). Prediction of unshrouded rotor blade tip heat transfer using an unstructured grid. *Proceedings of ASME Turbo Expo 1995*. DOI: <https://doi.org/10.1115/95-GT-142>
391. Boyle, R. J., & Giel, P. W. (1992). Three-dimensional Navier-Stokes heat transfer predictions for turbine blade rows. *Proceedings of ASME Turbo Expo 1992*. DOI: <https://doi.org/10.1115/92-GT-018>
392. Boyle, R. J. (1991). Navier-Stokes analysis of turbine blade heat transfer. *Journal of Turbomachinery*, 113(3), 392-403. DOI: <https://doi.org/10.1115/1.2927894>
393. Hylton, L. D., Mihelc, M. S., Turner, E. R., Nealy, D. A., & York, R. E. (1983). Analytical and experimental evaluation of the heat transfer distribution over the surfaces of turbine vanes. *NASA Contractor Report, 168015*. Available at: <https://ntrs.nasa.gov/citations/19830018880>
394. Arts, T., Lambert de Rouvroit, M., & Rutherford, A. W. (1990). Aero-thermal investigation of a highly loaded transonic linear turbine guide vane cascade. *Technical Note 174, Von Karman Institute for Fluid Dynamics*. Available at: <https://www.vki.ac.be/index.php/technical-notes>
395. Kiock, R., Lehthaus, F., Baines, N. C., & Sieverding, C. H. (1986). The transonic flow through a plane turbine cascade as measured in four European wind tunnels. *Journal of Turbomachinery*, 108(2), 277-284. DOI: <https://doi.org/10.1115/1.3262045>
396. Sieverding, C. H., & Arts, T. (1992). The VKI compression tube annular cascade facility CT3. *Proceedings of ASME Turbo Expo 1992*. DOI: <https://doi.org/10.1115/92-GT-336>
397. Graziani, R. A., Blair, M. F., Taylor, J. R., & Mayle, R. E. (1980). An experimental study of endwall and airfoil surface heat transfer in a large scale turbine blade cascade. *Journal of Engineering for Power*, 102(2), 257-267. DOI: <https://doi.org/10.1115/1.3230256>
398. Blair, M. F. (1974). An experimental study of heat transfer and film cooling on large-scale turbine endwalls. *Journal of Heat Transfer*, 96(4), 524-529. DOI: <https://doi.org/10.1115/1.3450239>
399. Goldstein, R. J., & Spores, R. A. (1988). Turbulent transport on the endwall in the region between adjacent turbine blades. *Journal of Heat Transfer*, 110(4a), 862-869. DOI: <https://doi.org/10.1115/1.3250586>
400. Langston, L. S., Nice, M. L., & Hooper, R. M. (1977). Three-dimensional flow within a turbine cascade passage. *Journal of Engineering for Power*, 99(1), 21-28. DOI: <https://doi.org/10.1115/1.3446247>
401. Marchal, P., & Sieverding, C. H. (1977). Secondary flows within turbomachinery bladings. *Secondary Flows in Turbomachines*, 2, 1-28. Available at: <https://www.vki.ac.be/index.php/lecture-series-documents>
402. Hawthorne, W. R. (1955). Rotational flow through cascades: Part I—The components of vorticity. *Quarterly Journal of Mechanics and Applied Mathematics*, 8(3), 266-279. DOI: <https://doi.org/10.1093/qjmam/8.3.266>
403. Squire, H. B., & Winter, K. G. (1951). The secondary flow in a cascade of aerofoils in a non-uniform stream. *Journal of the Aeronautical Sciences*, 18(4), 271-277. DOI: <https://doi.org/10.2514/8.1936>

404. Herzig, H. Z., Hansen, A. G., & Costello, G. R. (1954). A visualization study of secondary flows in cascades. *NACA Report, 1163*. Available at: <https://ntrs.nasa.gov/citations/19930092246>
405. Klein, A. (1966). Investigation of the entry boundary layer on the secondary flows in the blading of axial turbines. *BHRA Translation, TN 1004*. Available at: <https://www.bhra.co.uk/publications>
406. Came, P. M., & Marsh, H. (1974). Secondary flow in cascades: Two simple derivations for the components of vorticity. *Journal of Mechanical Engineering Science, 16*(6), 391-401. DOI: https://doi.org/10.1243/JMES_JOUR_1974_016_068_02
407. Horlock, J. H., & Lakshminarayana, B. (1973). Secondary flows: Theory, experiment, and application in turbomachinery aerodynamics. *Annual Review of Fluid Mechanics, 5*(1), 247-280. DOI: <https://doi.org/10.1146/annurev.fl.05.010173.001335>
408. Lakshminarayana, B. (1991). An assessment of computational fluid dynamic techniques in the analysis and design of turbomachinery—The 1990 Freeman Scholar Lecture. *Journal of Fluids Engineering, 113*(3), 315-352. DOI: <https://doi.org/10.1115/1.2909503>
409. Lakshminarayana, B., & Horlock, J. H. (1967). Generalized expressions for secondary vorticity using intrinsic co-ordinates. *Journal of Fluid Mechanics, 27*(2), 279-284. DOI: <https://doi.org/10.1017/S0022112067000308>
410. Moore, J., & Gregory-Smith, D. G. (1996). Transition effects on secondary flows in a turbine cascade. *Proceedings of ASME Turbo Expo 1996*. DOI: <https://doi.org/10.1115/96-GT-100>
411. Gregory-Smith, D. G., & Cleak, J. G. E. (1992). Secondary flow measurements in a turbine cascade with high inlet turbulence. *Journal of Turbomachinery, 114*(1), 173-183. DOI: <https://doi.org/10.1115/1.2927985>
412. Perdichizzi, A. (1990). Mach number effects on secondary flow development downstream of a turbine cascade. *Journal of Turbomachinery, 112*(4), 643-651. DOI: <https://doi.org/10.1115/1.2927714>
413. Harrison, S. (1990). The influence of blade lean on turbine losses. *Journal of Turbomachinery, 112*(2), 165-172. DOI: <https://doi.org/10.1115/1.2927631>
414. Denton, J. D., & Xu, L. (1999). The exploitation of three-dimensional flow in turbomachinery design. *Proceedings of the Institution of Mechanical Engineers, Part C: Journal of Mechanical Engineering Science, 213*(2), 125-137. DOI: <https://doi.org/10.1243/0954406991522220>
415. Harvey, N. W., Rose, M. G., Taylor, M. D., Shahpar, S., Hartland, J., & Gregory-Smith, D. G. (2000). Nonaxisymmetric turbine end wall design: Part I—Three-dimensional linear design system. *Journal of Turbomachinery, 122*(2), 278-285. DOI: <https://doi.org/10.1115/1.555445>
416. Rose, M. G., Harvey, N. W., Seaman, P., Newman, D. A., & McManus, D. (2001). Improving the efficiency of the Trent 500 HP turbine using nonaxisymmetric end walls: Part II—Experimental validation. *Proceedings of ASME Turbo Expo 2001*. DOI: <https://doi.org/10.1115/2001-GT-0505>
417. Hartland, J. C., Gregory-Smith, D. G., Harvey, N. W., & Rose, M. G. (1999). Nonaxisymmetric turbine end wall design: Part II—Experimental validation. *Journal of Turbomachinery, 122*(2), 286-293. DOI: <https://doi.org/10.1115/1.555446>
418. Ingram, G., Gregory-Smith, D., Rose, M., Harvey, N., & Brennan, G. (2002). The effect of end-wall profiling on secondary flow and loss development in a turbine cascade. *Proceedings of ASME Turbo Expo 2002*. DOI: <https://doi.org/10.1115/GT2002-30339>
419. Brennan, G., Harvey, N. W., Rose, M. G., Fomison, N., & Taylor, M. D. (2003). Improving the efficiency of the Trent 500-HP turbine using nonaxisymmetric end walls—Part I: Turbine design. *Journal of Turbomachinery, 125*(3), 497-504. DOI: <https://doi.org/10.1115/1.1540118>
420. Harvey, N. W., Brennan, G., Newman, D. A., & Rose, M. G. (2002). Improving turbine efficiency using non-axisymmetric end walls: Validation in the multi-row environment and with low aspect ratio blading. *Proceedings of ASME Turbo Expo 2002*. DOI: <https://doi.org/10.1115/GT2002-30337>
421. Praisner, T. J., Allen-Bradley, E., Grover, E. A., Knezevici, D. C., & Sjolander, S. A. (2013). Application of nonaxisymmetric endwall contouring to conventional and high-lift turbine airfoils. *Journal of Turbomachinery, 135*(6), 061006. DOI: <https://doi.org/10.1115/1.4023911>
422. Knezevici, D. C., Sjolander, S. A., Praisner, T. J., Allen-Bradley, E., & Grover, E. A. (2010). Measurements of secondary losses in a turbine cascade with the implementation of nonaxisymmetric endwall contouring. *Journal of Turbomachinery, 132*(1), 011013. DOI: <https://doi.org/10.1115/1.3072520>

423. Sauer, H., Müller, R., & Vogeler, K. (2001). Reduction of secondary flow losses in turbine cascades by leading edge modifications at the endwall. *Proceedings of ASME Turbo Expo 2001*. DOI: <https://doi.org/10.1115/2001-GT-0473>
424. Zess, G. A., & Thole, K. A. (2002). Computational design and experimental evaluation of using a leading edge fillet on a gas turbine vane. *Journal of Turbomachinery*, 124(2), 167-175. DOI: <https://doi.org/10.1115/1.1460914>
425. Becz, S., Majewski, M. S., & Langston, L. S. (2004). An experimental investigation of contoured leading edges for secondary flow loss reduction. *Proceedings of ASME Turbo Expo 2004*. DOI: <https://doi.org/10.1115/GT2004-53964>
426. Mahmood, G. I., Hill, M. L., Nelson, D. L., Turner, P. M., & Ligrani, P. M. (2001). Local heat transfer and flow structure on and above a dimpled surface in a channel. *Journal of Turbomachinery*, 123(1), 115-123. DOI: <https://doi.org/10.1115/1.1333694>
427. Ligrani, P. M., Harrison, J. L., Mahmood, G. I., & Hill, M. L. (2001). Flow structure due to dimple depressions on a channel surface. *Physics of Fluids*, 13(11), 3442-3451. DOI: <https://doi.org/10.1063/1.1404139>
428. Chyu, M. K., Yu, Y., Ding, H., Downs, J. P., & Soechting, F. O. (1997). Concavity enhanced heat transfer in an internal cooling passage. *Proceedings of ASME Turbo Expo 1997*. DOI: <https://doi.org/10.1115/97-GT-437>
429. Moon, H. K., O'Connell, T., & Glezer, B. (2000). Channel height effect on heat transfer and friction in a dimpled passage. *Journal of Engineering for Gas Turbines and Power*, 122(2), 307-313. DOI: <https://doi.org/10.1115/1.483208>
430. Isaev, S. A., Leontiev, A. I., Kornev, N. V., Hassel, E., & Chudnovsky, Y. P. (2010). Influence of the Reynolds number and the spherical dimple depth on turbulent heat transfer and hydraulic loss in a narrow channel. *International Journal of Heat and Mass Transfer*, 53(1-3), 178-197. DOI: <https://doi.org/10.1016/j.ijheatmasstransfer.2009.09.042>
431. Turnow, J., Kornev, N., Isaev, S., & Hassel, E. (2012). Vortex mechanism of heat transfer enhancement in a channel with spherical and oval dimples. *Heat and Mass Transfer*, 48(2), 301-313. DOI: <https://doi.org/10.1007/s00231-011-0881-y>
432. Elyyan, M. A., Rozati, A., & Tafti, D. K. (2008). Investigation of dimpled fins for heat transfer enhancement in compact heat exchangers. *International Journal of Heat and Mass Transfer*, 51(11-12), 2950-2966. DOI: <https://doi.org/10.1016/j.ijheatmasstransfer.2007.09.013>
433. Rao, Y., Wan, C., & Xu, Y. (2012). An experimental study of pressure loss and heat transfer in the pin fin-dimple channels with various dimple depths. *International Journal of Heat and Mass Transfer*, 55(23-24), 6723-6733. DOI: <https://doi.org/10.1016/j.ijheatmasstransfer.2012.06.081>
434. Silva, C., Marotta, E., & Fletcher, L. S. (2007). Flow structure and enhanced heat transfer in channel flow with dimpled surfaces: Application to heat sinks in microelectronic cooling. *Journal of Electronic Packaging*, 129(2), 157-166. DOI: <https://doi.org/10.1115/1.2721087>
435. Bunker, R. S., & Donnellan, K. F. (2003). Heat transfer and friction factors for flows inside circular tubes with concavity surfaces. *Journal of Turbomachinery*, 125(4), 665-672. DOI: <https://doi.org/10.1115/1.1622712>
436. Park, J., Desam, P. R., & Ligrani, P. M. (2004). Numerical predictions of flow structure above a dimpled surface in a channel. *Numerical Heat Transfer, Part A: Applications*, 45(1), 1-20. DOI: <https://doi.org/10.1080/10407780490250409>
437. Lan, J., Xie, Y., & Zhang, D. (2012). Flow and heat transfer in microchannels with dimples and protrusions. *Journal of Heat Transfer*, 134(2), 021901. DOI: <https://doi.org/10.1115/1.4005096>
438. Kanokjaruvijit, K., & Martinez-Botas, R. F. (2005). Jet impingement on a dimpled surface with different crossflow schemes. *International Journal of Heat and Mass Transfer*, 48(1), 161-170. DOI: <https://doi.org/10.1016/j.ijheatmasstransfer.2004.08.005>
439. Griffith, T. S., Al-Hadhrami, L., & Han, J. C. (2002). Heat transfer in rotating rectangular cooling channels (AR=4) with dimples. *Journal of Turbomachinery*, 124(4), 488-498. DOI: <https://doi.org/10.1115/1.1505851>
440. Zhou, F., & Acharya, S. (2008). Heat transfer at high rotation numbers in a two-pass 4:1 aspect ratio rectangular channel with 45° skewed ribs. *Journal of Turbomachinery*, 130(2), 021019. DOI: <https://doi.org/10.1115/1.2752188>

441. Huh, M., Liu, Y. H., & Han, J. C. (2009). Effect of rib height on heat transfer in a two pass rectangular channel (AR= 1: 4) with a sharp entrance at high rotation numbers. *International Journal of Heat and Mass Transfer*, 52(19-20), 4635-4649. DOI: <https://doi.org/10.1016/j.ijheatmasstransfer.2009.03.022>
442. Wright, L. M., Fu, W. L., & Han, J. C. (2004). Thermal performance of angled, V-shaped, and W-shaped rib turbulators in rotating rectangular cooling channels (AR= 4: 1). *Journal of Turbomachinery*, 126(4), 604-614. DOI: <https://doi.org/10.1115/1.1791286>
443. Dutta, S., & Han, J. C. (1996). Local heat transfer in rotating smooth and ribbed two-pass square channels with three channel orientations. *Journal of Heat Transfer*, 118(3), 578-584. DOI: <https://doi.org/10.1115/1.2822670>
444. Johnson, B. V., Wagner, J. H., Steuber, G. D., & Yeh, F. C. (1994). Heat transfer in rotating serpentine passages with trips skewed to the flow. *Journal of Turbomachinery*, 116(1), 113-123. DOI: <https://doi.org/10.1115/1.2928265>
445. Zhang, Y. M., Gu, W. Z., & Han, J. C. (1994). Heat transfer and friction in rectangular channels with ribbed or ribbed-grooved walls. *Journal of Heat Transfer*, 116(1), 58-65. DOI: <https://doi.org/10.1115/1.2910884>
446. Han, J. C., Glicksman, L. R., & Rohsenow, W. M. (1978). An investigation of heat transfer and friction for rib-roughened surfaces. *International Journal of Heat and Mass Transfer*, 21(8), 1143-1156. DOI: [https://doi.org/10.1016/0017-9310\(78\)90113-8](https://doi.org/10.1016/0017-9310(78)90113-8)
447. Webb, R. L., Eckert, E. R. G., & Goldstein, R. J. (1971). Heat transfer and friction in tubes with repeated-rib roughness. *International Journal of Heat and Mass Transfer*, 14(4), 601-617. DOI: [https://doi.org/10.1016/0017-9310\(71\)90009-3](https://doi.org/10.1016/0017-9310(71)90009-3)
448. Taslim, M. E., Li, T., & Kercher, D. M. (1996). Experimental heat transfer and friction in channels roughened with angled, V-shaped, and discrete ribs on two opposite walls. *Journal of Turbomachinery*, 118(1), 20-28. DOI: <https://doi.org/10.1115/1.2836602>
449. Lau, S. C., Kukreja, R. T., & McMillin, R. D. (1991). Effects of V-shaped rib arrays on turbulent heat transfer and friction of fully developed flow in a square channel. *International Journal of Heat and Mass Transfer*, 34(7), 1605-1616. DOI: [https://doi.org/10.1016/0017-9310\(91\)90140-A](https://doi.org/10.1016/0017-9310(91)90140-A)
450. Ekkad, S. V., & Han, J. C. (1997). Detailed heat transfer distributions in two-pass square channels with rib turbulators. *International Journal of Heat and Mass Transfer*, 40(11), 2525-2537. DOI: [https://doi.org/10.1016/S0017-9310\(96\)00318-3](https://doi.org/10.1016/S0017-9310(96)00318-3). (References 451-550 (Advanced Cooling Technologies and Experimental Methods))
451. Kercher, D. M., & Tabakoff, W. (1970). Heat transfer by a square array of round air jets impinging perpendicular to a flat surface including the effect of spent air. *Journal of Engineering for Power*, 92(1), 73-82. DOI: <https://doi.org/10.1115/1.3445306>
452. Florschuetz, L. W., Truman, C. R., & Metzger, D. E. (1981). Streamwise flow and heat transfer distributions for jet array impingement with crossflow. *Journal of Heat Transfer*, 103(2), 337-342. DOI: <https://doi.org/10.1115/1.3244463>
453. Metzger, D. E., Florschuetz, L. W., Takeuchi, D. I., Behee, R. D., & Berry, R. A. (1979). Heat transfer characteristics for inline and staggered arrays of circular jets with crossflow of spent air. *Journal of Heat Transfer*, 101(3), 526-531. DOI: <https://doi.org/10.1115/1.3451022>
454. Obot, N. T., & Trabold, T. A. (1987). Impingement heat transfer within arrays of circular jets: Part 1—Effects of minimum, intermediate, and complete crossflow for small and large spacings. *Journal of Heat Transfer*, 109(4), 872-879. DOI: <https://doi.org/10.1115/1.3248197>
455. Huber, A. M., & Viskanta, R. (1994). Effect of jet-jet spacing on convective heat transfer to confined, impinging arrays of axisymmetric air jets. *International Journal of Heat and Mass Transfer*, 37(18), 2859-2869. DOI: [https://doi.org/10.1016/0017-9310\(94\)90340-9](https://doi.org/10.1016/0017-9310(94)90340-9)
456. Womac, D. J., Ramadhyani, S., & Incropera, F. P. (1993). Correlating equations for impingement cooling of small heat sources with single circular liquid jets. *Journal of Heat Transfer*, 115(1), 106-115. DOI: <https://doi.org/10.1115/1.2910635>
457. Gardon, R., & Akfirat, J. C. (1965). The role of turbulence in determining the heat-transfer characteristics of impinging jets. *International Journal of Heat and Mass Transfer*, 8(10), 1261-1272. DOI: [https://doi.org/10.1016/0017-9310\(65\)90054-2](https://doi.org/10.1016/0017-9310(65)90054-2)

458. Goldstein, R. J., & Behbahani, A. I. (1982). Impingement of a circular jet with and without cross flow. *International Journal of Heat and Mass Transfer*, 25(9), 1377-1382. DOI: [https://doi.org/10.1016/0017-9310\(82\)90131-4](https://doi.org/10.1016/0017-9310(82)90131-4)
459. Lytle, D., & Webb, B. W. (1994). Air jet impingement heat transfer at low nozzle-plate spacings. *International Journal of Heat and Mass Transfer*, 37(12), 1687-1697. DOI: [https://doi.org/10.1016/0017-9310\(94\)90059-0](https://doi.org/10.1016/0017-9310(94)90059-0)
460. Lee, J., & Lee, S. J. (2000). The effect of nozzle configuration on stagnation region heat transfer enhancement of axisymmetric jet impingement. *International Journal of Heat and Mass Transfer*, 43(18), 3497-3509. DOI: [https://doi.org/10.1016/S0017-9310\(99\)00349-X](https://doi.org/10.1016/S0017-9310(99)00349-X)
461. Chupp, R. E., Helms, H. E., McFadden, P. W., & Brown, T. R. (1969). Evaluation of internal heat-transfer coefficients for impingement-cooled turbine airfoils. *Journal of Aircraft*, 6(3), 203-208. DOI: <https://doi.org/10.2514/3.44036>
462. Bunker, R. S., & Metzger, D. E. (1990). Local heat transfer in internally cooled turbine airfoil leading edge regions: Part I—Impingement cooling without film coolant extraction. *Journal of Turbomachinery*, 112(3), 451-458. DOI: <https://doi.org/10.1115/1.2927684>
463. Bunker, R. S., & Metzger, D. E. (1990). Local heat transfer in internally cooled turbine airfoil leading edge regions: Part II—Impingement cooling with film coolant extraction. *Journal of Turbomachinery*, 112(3), 459-466. DOI: <https://doi.org/10.1115/1.2927685>
464. Hrycak, P. (1981). Heat transfer from a row of impinging jets to concave cylindrical surfaces. *International Journal of Heat and Mass Transfer*, 24(3), 407-419. DOI: [https://doi.org/10.1016/0017-9310\(81\)90048-0](https://doi.org/10.1016/0017-9310(81)90048-0)
465. Tabakoff, W., & Clewenger, W. (1972). Gas turbine blade heat transfer augmentation by impingement of air jets having various configurations. *Journal of Engineering for Power*, 94(1), 51-60. DOI: <https://doi.org/10.1115/1.3445612>
466. Chance, J. L. (1974). Experimental investigation of air impingement heat transfer under an array of round jets. *TAPPI Journal*, 57(6), 108-112. Available at: <https://www.tappi.org/publications/tappi-journal/>
467. Hollworth, B. R., & Berry, R. D. (1978). Heat transfer from arrays of impinging jets with large jet-to-jet spacing. *Journal of Heat Transfer*, 100(2), 352-357. DOI: <https://doi.org/10.1115/1.3450809>
468. Goldstein, R. J., & Timmers, J. F. (1982). Visualization of heat transfer from arrays of impinging jets. *International Journal of Heat and Mass Transfer*, 25(12), 1857-1868. DOI: [https://doi.org/10.1016/0017-9310\(82\)90108-9](https://doi.org/10.1016/0017-9310(82)90108-9)
469. Hrycak, P. (1983). Heat transfer from impinging jets to a flat plate with conical and ring protuberances. *International Journal of Heat and Mass Transfer*, 26(2), 269-278. DOI: [https://doi.org/10.1016/0017-9310\(83\)90052-X](https://doi.org/10.1016/0017-9310(83)90052-X)
470. Downs, S. J., & James, E. H. (1987). Jet impingement heat transfer—A literature survey. *Proceedings of the National Heat Transfer Conference, HTC-107*, 35-42. Available at: <https://www.asme.org/publications-submissions/proceedings>
471. Martin, H. (1977). Heat and mass transfer between impinging gas jets and solid surfaces. *Advances in Heat Transfer*, 13, 1-60. DOI: [https://doi.org/10.1016/S0065-2717\(08\)70221-1](https://doi.org/10.1016/S0065-2717(08)70221-1)
472. Jambunathan, K., Lai, E., Moss, M. A., & Button, B. L. (1992). A review of heat transfer data for single circular jet impingement. *International Journal of Heat and Fluid Flow*, 13(2), 106-115. DOI: [https://doi.org/10.1016/0142-727X\(92\)90017-4](https://doi.org/10.1016/0142-727X(92)90017-4)
473. Viskanta, R. (1993). Heat transfer to impinging isothermal gas and flame jets. *Experimental Thermal and Fluid Science*, 6(2), 111-134. DOI: [https://doi.org/10.1016/0894-1777\(93\)90022-B](https://doi.org/10.1016/0894-1777(93)90022-B)
474. Polat, S., Huang, B., Mujumdar, A. S., & Douglas, W. J. M. (1989). Numerical flow and heat transfer under impinging jets: A review. *Annual Review of Numerical Fluid Mechanics and Heat Transfer*, 2, 157-197. Available at: <https://www.begellhouse.com/journals/annual-review-of-heat-transfer.html>
475. Webb, B. W., & Ma, C. F. (1995). Single-phase liquid jet impingement heat transfer. *Advances in Heat Transfer*, 26, 105-217. DOI: [https://doi.org/10.1016/S0065-2717\(08\)70296-X](https://doi.org/10.1016/S0065-2717(08)70296-X)
476. Zuckerman, N., & Lior, N. (2006). Jet impingement heat transfer: Physics, correlations, and numerical modeling. *Advances in Heat Transfer*, 39, 565-631. DOI: [https://doi.org/10.1016/S0065-2717\(06\)39006-5](https://doi.org/10.1016/S0065-2717(06)39006-5)
477. Weigand, B., & Spring, S. (2011). Multiple jet impingement—A review. *Heat Transfer Research*, 42(2), 101-142. DOI: <https://doi.org/10.1615/HeatTransRes.v42.i2.30>

478. Carlomagno, G. M., & Ianiro, A. (2014). Thermo-fluid-dynamics of submerged jets impinging at short nozzle-to-plate distance: A review. *Experimental Thermal and Fluid Science*, 58, 15-35. DOI: <https://doi.org/10.1016/j.expthermflusci.2014.06.010>
479. Dewan, A., Dutta, R., & Srinivasan, B. (2012). Recent trends in computation of turbulent jet impingement heat transfer. *Heat Transfer Engineering*, 33(4-5), 447-460. DOI: <https://doi.org/10.1080/01457632.2012.614154>
480. Behnia, M., Parneix, S., Shabany, Y., & Durbin, P. A. (1999). Numerical study of turbulent heat transfer in confined and unconfined impinging jets. *International Journal of Heat and Fluid Flow*, 20(1), 1-9. DOI: [https://doi.org/10.1016/S0142-727X\(98\)10040-1](https://doi.org/10.1016/S0142-727X(98)10040-1)
481. Craft, T. J., Graham, L. J. W., & Launder, B. E. (1993). Impinging jet studies for turbulence model assessment—II. An examination of the performance of four turbulence models. *International Journal of Heat and Mass Transfer*, 36(10), 2685-2697. DOI: [https://doi.org/10.1016/S0017-9310\(05\)80205-4](https://doi.org/10.1016/S0017-9310(05)80205-4)
482. Hattori, H., & Nagano, Y. (2004). Direct numerical simulation of turbulent heat transfer in plane impinging jet. *International Journal of Heat and Fluid Flow*, 25(5), 749-758. DOI: <https://doi.org/10.1016/j.ijheatfluidflow.2004.05.004>
483. Uddin, N., Neumann, S. O., & Weigand, B. (2013). LES simulations of an impinging jet: On the origin of the second peak in the Nusselt number distribution. *International Journal of Heat and Mass Transfer*, 57(1), 356-368. DOI: <https://doi.org/10.1016/j.ijheatmasstransfer.2012.10.052>
484. Hadžiabdić, M., & Hanjalić, K. (2008). Vortical structures and heat transfer in a round impinging jet. *Journal of Fluid Mechanics*, 596, 221-260. DOI: <https://doi.org/10.1017/S002211200700955X>
485. Dairay, T., Fortuné, V., Lamballais, E., & Brizzi, L. E. (2015). Direct numerical simulation of a turbulent jet impinging on a heated wall. *Journal of Fluid Mechanics*, 764, 362-394. DOI: <https://doi.org/10.1017/jfm.2014.715>
486. Wilke, R., & Sesterhenn, J. (2017). Statistics of fully turbulent impinging jets. *Journal of Fluid Mechanics*, 825, 795-824. DOI: <https://doi.org/10.1017/jfm.2017.414>
487. Vinze, R., Chandel, S., Limaye, M. D., & Prabhu, S. V. (2017). Influence of jet temperature and nozzle shape on the heat transfer distribution between a smooth plate and impinging air jets. *International Journal of Thermal Sciences*, 99, 136-151. DOI: <https://doi.org/10.1016/j.ijthermalsci.2015.08.009>
488. Royne, A., & Dey, C. J. (2006). Experimental study of heat transfer from a disk in an impinging air jet. *International Journal of Heat and Mass Transfer*, 49(23-24), 4567-4570. DOI: <https://doi.org/10.1016/j.ijheatmasstransfer.2006.04.012>
489. Teamah, M. A., Khairat, M. M., & Massoud, M. Z. (2015). Numerical and experimental investigation of flow structure and behavior of nanofluids flow impingement on horizontal flat plate. *Experimental Thermal and Fluid Science*, 74, 235-246. DOI: <https://doi.org/10.1016/j.expthermflusci.2015.12.012>
490. Lienhard, J. H. (1995). Liquid jet impingement. *Annual Review of Heat Transfer*, 6(6), 199-270. DOI: <https://doi.org/10.1615/AnnualRevHeatTransfer.v6.60>
491. Stevens, J., & Webb, B. W. (1991). Local heat transfer coefficients under an axisymmetric, single-phase liquid jet. *Journal of Heat Transfer*, 113(1), 71-78. DOI: <https://doi.org/10.1115/1.2910554>
492. Liu, X., Lienhard, J. H., & Lombara, J. S. (1991). Convective heat transfer by impingement of circular liquid jets. *Journal of Heat Transfer*, 113(3), 571-582. DOI: <https://doi.org/10.1115/1.2910604>
493. Pan, Y., & Webb, B. W. (1995). Heat transfer characteristics of arrays of free-surface liquid jets. *Journal of Heat Transfer*, 117(4), 878-883. DOI: <https://doi.org/10.1115/1.2836307>
494. Vader, D. T., Incropera, F. P., & Viskanta, R. (1991). Local convective heat transfer from a heated surface to an impinging, planar jet of water. *International Journal of Heat and Mass Transfer*, 34(3), 611-623. DOI: [https://doi.org/10.1016/0017-9310\(91\)90111-Q](https://doi.org/10.1016/0017-9310(91)90111-Q)
495. Ma, C. F., Zheng, Q., Lee, S. C., & Gomi, T. (1997). Impingement heat transfer and recovery effect with submerged jets of large Prandtl number liquid—I. Unconfined circular jets. *International Journal of Heat and Mass Transfer*, 40(6), 1481-1490. DOI: [https://doi.org/10.1016/S0017-9310\(96\)00170-6](https://doi.org/10.1016/S0017-9310(96)00170-6)
496. Womac, D. J., Incropera, F. P., & Ramadhyani, S. (1994). Correlating equations for impingement cooling of small heat sources with multiple circular liquid jets. *Journal of Heat Transfer*, 116(2), 482-486. DOI: <https://doi.org/10.1115/1.2911422>

497. Oliphant, K., Webb, B. W., & McQuay, M. Q. (1998). An experimental comparison of liquid jet array and spray impingement cooling in the non-boiling regime. *Experimental Thermal and Fluid Science*, 18(1), 1-10. DOI: [https://doi.org/10.1016/S0894-1777\(98\)10013-4](https://doi.org/10.1016/S0894-1777(98)10013-4)
498. Rybicki, J. R., & Mudawar, I. (2006). Single-phase and two-phase cooling characteristics of upward-facing and downward-facing sprays. *International Journal of Heat and Mass Transfer*, 49(1-2), 5-16. DOI: <https://doi.org/10.1016/j.ijheatmasstransfer.2005.07.040>
499. Mudawar, I., & Estes, K. A. (1996). Optimizing and predicting CHF in spray cooling of a square surface. *Journal of Heat Transfer*, 118(3), 672-679. DOI: <https://doi.org/10.1115/1.2822685>
500. Pautsch, A. G., & Shedd, T. A. (2005). Spray impingement cooling with single-and multiple-nozzle arrays. Part I: Heat transfer data using FC-72. *International Journal of Heat and Mass Transfer*, 48(15), 3167-3175. DOI: <https://doi.org/10.1016/j.ijheatmasstransfer.2005.02.012>
501. Silk, E. A., Kim, J., & Kiger, K. (2006). Spray cooling of enhanced surfaces: Impact of structured surface geometry and spray axis inclination. *International Journal of Heat and Mass Transfer*, 49(25-26), 4910-4920. DOI: <https://doi.org/10.1016/j.ijheatmasstransfer.2006.05.031>
502. Horacek, B., Kiger, K. T., & Kim, J. (2005). Single nozzle spray cooling heat transfer mechanisms. *International Journal of Heat and Mass Transfer*, 48(8), 1425-1438. DOI: <https://doi.org/10.1016/j.ijheatmasstransfer.2004.10.026>
503. Chow, L. C., Sehmbey, M. S., & Pais, M. R. (1997). High heat flux spray cooling. *Annual Review of Heat Transfer*, 8(8), 291-318. DOI: <https://doi.org/10.1615/AnnualRevHeatTransfer.v8.80>
504. Kim, J. (2007). Spray cooling heat transfer: The state of the art. *International Journal of Heat and Fluid Flow*, 28(4), 753-767. DOI: <https://doi.org/10.1016/j.ijheatfluidflow.2006.09.003>
505. Liang, G., & Mudawar, I. (2017). Review of spray cooling—Part 1: Single-phase and nucleate boiling regimes, and critical heat flux. *International Journal of Heat and Mass Transfer*, 115, 1174-1205. DOI: <https://doi.org/10.1016/j.ijheatmasstransfer.2017.06.029>
506. Liang, G., & Mudawar, I. (2017). Review of spray cooling—Part 2: High temperature boiling regimes and quenching applications. *International Journal of Heat and Mass Transfer*, 115, 1206-1222. DOI: <https://doi.org/10.1016/j.ijheatmasstransfer.2017.06.022>
507. Breitenbach, J., Roisman, I. V., & Tropea, C. (2018). From drop impact physics to spray cooling models: A critical review. *Experiments in Fluids*, 59(3), 1-21. DOI: <https://doi.org/10.1007/s00348-018-2514-3>
508. Yarin, A. L. (2006). Drop impact dynamics: Splashing, spreading, receding, bouncing. *Annual Review of Fluid Mechanics*, 38, 159-192. DOI: <https://doi.org/10.1146/annurev.fluid.38.050304.092144>
509. Josserand, C., & Thoroddsen, S. T. (2016). Drop impact on a solid surface. *Annual Review of Fluid Mechanics*, 48, 365-391. DOI: <https://doi.org/10.1146/annurev-fluid-122414-034401>
510. Marengo, M., Antonini, C., Roisman, I. V., & Tropea, C. (2011). Drop collisions with simple and complex surfaces. *Current Opinion in Colloid & Interface Science*, 16(4), 292-302. DOI: <https://doi.org/10.1016/j.cocis.2011.06.009>
511. Roisman, I. V. (2009). Inertia dominated drop collisions. I. On the universal flow in the lamella. *Physics of Fluids*, 21(5), 052103. DOI: <https://doi.org/10.1063/1.3129282>
512. Roisman, I. V. (2010). Inertia dominated drop collisions. II. An analytical solution of the Navier–Stokes equations for a spreading viscous film. *Physics of Fluids*, 21(5), 052104. DOI: <https://doi.org/10.1063/1.3129283>
513. Eggers, J., Fontelos, M. A., Josserand, C., & Zaleski, S. (2010). Drop dynamics after impact on a solid wall: Theory and simulations. *Physics of Fluids*, 22(6), 062101. DOI: <https://doi.org/10.1063/1.3432498>
514. Wildeman, S., Visser, C. W., Sun, C., & Lohse, D. (2016). On the spreading of impacting drops. *Journal of Fluid Mechanics*, 805, 636-655. DOI: <https://doi.org/10.1017/jfm.2016.584>
515. Clanet, C., Béguin, C., Richard, D., & Quéré, D. (2004). Maximal deformation of an impacting drop. *Journal of Fluid Mechanics*, 517, 199-208. DOI: <https://doi.org/10.1017/S0022112004000904>
516. Pasandideh-Fard, M., Qiao, Y. M., Chandra, S., & Mostaghimi, J. (1996). Capillary effects during droplet impact on a solid surface. *Physics of Fluids*, 8(3), 650-659. DOI: <https://doi.org/10.1063/1.868850>
517. Ukiwe, C., & Kwok, D. Y. (2005). On the maximum spreading diameter of impacting droplets on well-prepared solid surfaces. *Langmuir*, 21(2), 666-673. DOI: <https://doi.org/10.1021/la0481288>

518. Scheller, B. L., & Bousfield, D. W. (1995). Newtonian drop impact with a solid surface. *AIChE Journal*, 41(6), 1357-1367. DOI: <https://doi.org/10.1002/aic.690410602>
519. Mao, T., Kuhn, D. C. S., & Tran, H. (1997). Spread and rebound of liquid droplets upon impact on flat surfaces. *AIChE Journal*, 43(9), 2169-2179. DOI: <https://doi.org/10.1002/aic.690430903>
520. Rioboo, R., Marengo, M., & Tropea, C. (2002). Time evolution of liquid drop impact onto solid, dry surfaces. *Experiments in Fluids*, 33(1), 112-124. DOI: <https://doi.org/10.1007/s00348-002-0431-x>
521. Chandra, S., & Avedisian, C. T. (1991). On the collision of a droplet with a solid surface. *Proceedings of the Royal Society of London. Series A: Mathematical and Physical Sciences*, 432(1884), 13-41. DOI: <https://doi.org/10.1098/rspa.1991.0002>
522. Bussmann, M., Chandra, S., & Mostaghimi, J. (2000). Modeling the splash of a droplet impacting a solid surface. *Physics of Fluids*, 12(12), 3121-3132. DOI: <https://doi.org/10.1063/1.1321258>
523. Fukai, J., Shiiba, Y., Yamamoto, T., Miyatake, O., Poulikakos, D., Megaridis, C. M., & Zhao, Z. (1995). Wetting effects on the spreading of a liquid droplet colliding with a flat surface: Experiment and modeling. *Physics of Fluids*, 7(2), 236-247. DOI: <https://doi.org/10.1063/1.868622>
524. Mundo, C., Sommerfeld, M., & Tropea, C. (1995). Droplet-wall collisions: Experimental studies of the deformation and breakup process. *International Journal of Multiphase Flow*, 21(2), 151-173. DOI: [https://doi.org/10.1016/0301-9322\(94\)00069-V](https://doi.org/10.1016/0301-9322(94)00069-V)
525. Cossali, G. E., Coghe, A., & Marengo, M. (1997). The impact of a single drop on a wetted solid surface. *Experiments in Fluids*, 22(6), 463-472. DOI: <https://doi.org/10.1007/s003480050073>
526. Yarin, A. L., & Weiss, D. A. (1995). Impact of drops on solid surfaces: Self-similar capillary waves, and splashing as a new type of kinematic discontinuity. *Journal of Fluid Mechanics*, 283, 141-173. DOI: <https://doi.org/10.1017/S0022112095002266>
527. Thoroddsen, S. T., Etoh, T. G., & Takehara, K. (2008). High-speed imaging of drops and bubbles. *Annual Review of Fluid Mechanics*, 40, 257-285. DOI: <https://doi.org/10.1146/annurev.fluid.40.111406.102215>
528. Villermaux, E., & Bossa, B. (2011). Single-drop fragmentation determines size distribution of raindrops. *Nature Physics*, 7(12), 1006-1009. DOI: <https://doi.org/10.1038/nphys2107>
529. Thoroddsen, S. T., Takehara, K., & Etoh, T. G. (2012). Micro-splashing by drop impacts. *Journal of Fluid Mechanics*, 706, 560-570. DOI: <https://doi.org/10.1017/jfm.2012.281>
530. Riboux, G., & Gordillo, J. M. (2014). Experiments of drops impacting a smooth solid surface: A model of the critical impact speed for drop splashing. *Physical Review Letters*, 113(2), 024507. DOI: <https://doi.org/10.1103/PhysRevLett.113.024507>
531. Xu, L., Zhang, W. W., & Nagel, S. R. (2005). Drop splashing on a dry smooth surface. *Physical Review Letters*, 94(18), 184505. DOI: <https://doi.org/10.1103/PhysRevLett.94.184505>
532. Stevens, C. S., Latka, A., & Nagel, S. R. (2014). Comparison of splashing in high-and low-viscosity liquids. *Physical Review E*, 89(6), 063006. DOI: <https://doi.org/10.1103/PhysRevE.89.063006>
533. Latka, A., Strandburg-Peshkin, A., Driscoll, M. M., Stevens, C. S., & Nagel, S. R. (2012). Creation of prompt and thin-sheet splashing by varying surface roughness or increasing air pressure. *Physical Review Letters*, 109(5), 054501. DOI: <https://doi.org/10.1103/PhysRevLett.109.054501>
534. Mandre, S., Mani, M., & Brenner, M. P. (2009). Precursors to splashing of liquid droplets on a solid surface. *Physical Review Letters*, 102(13), 134502. DOI: <https://doi.org/10.1103/PhysRevLett.102.134502>
535. Hicks, P. D., & Purvis, R. (2010). Air cushioning and bubble entrapment in three-dimensional droplet impacts. *Journal of Fluid Mechanics*, 649, 135-163. DOI: <https://doi.org/10.1017/S0022112009994009>
536. Kolinski, J. M., Rubinstein, S. M., Mandre, S., Brenner, M. P., Weitz, D. A., & Mahadevan, L. (2012). Skating on a film of air: Drops impacting on a surface. *Physical Review Letters*, 108(7), 074503. DOI: <https://doi.org/10.1103/PhysRevLett.108.074503>
537. de Ruitter, J., Lagraauw, R., van den Ende, D., & Mugele, F. (2015). Wettability-independent bouncing on flat surfaces mediated by thin air films. *Nature Physics*, 11(1), 48-53. DOI: <https://doi.org/10.1038/nphys3145>
538. Liu, Y., Tan, P., & Xu, L. (2015). Kelvin-Helmholtz instability in an ultrathin air film causes drop splashing on smooth surfaces. *Proceedings of the National Academy of Sciences*, 112(11), 3280-3284. DOI: <https://doi.org/10.1073/pnas.1417718112>

539. Li, E. Q., & Thoroddsen, S. T. (2015). Time-resolved imaging of a compressible air disc under a drop impacting on a solid surface. *Journal of Fluid Mechanics*, 780, 636-648. DOI: <https://doi.org/10.1017/jfm.2015.466>
540. Bouwhuis, W., van der Veen, R. C., Tran, T., Keij, D. L., Winkels, K. G., Peters, I. R., ... & Snoeijer, J. H. (2012). Maximal air bubble entrainment at liquid-drop impact. *Physical Review Letters*, 109(26), 264501. DOI: <https://doi.org/10.1103/PhysRevLett.109.264501>
541. van der Veen, R. C., Tran, T., Lohse, D., & Sun, C. (2012). Direct measurements of air layer profiles under impacting droplets using high-speed color interferometry. *Physical Review E*, 85(2), 026315. DOI: <https://doi.org/10.1103/PhysRevE.85.026315>
542. Tran, T., Staat, H. J., Prosperetti, A., Sun, C., & Lohse, D. (2012). Drop impact on superheated surfaces. *Physical Review Letters*, 108(3), 036101. DOI: <https://doi.org/10.1103/PhysRevLett.108.036101>
543. Staat, H. J., Tran, T., Geerdink, B., Riboux, G., Sun, C., Gordillo, J. M., & Lohse, D. (2015). Phase diagram for droplet impact on superheated surfaces. *Journal of Fluid Mechanics*, 779, R3. DOI: <https://doi.org/10.1017/jfm.2015.465>
544. Shirota, M., van Limbeek, M. A., Sun, C., Prosperetti, A., & Lohse, D. (2016). Dynamic Leidenfrost effect: Relevant time and length scales. *Physical Review Letters*, 116(6), 064501. DOI: <https://doi.org/10.1103/PhysRevLett.116.064501>
545. Bernardin, J. D., & Mudawar, I. (1999). The Leidenfrost point: Experimental study and assessment of existing models. *Journal of Heat Transfer*, 121(4), 894-903. DOI: <https://doi.org/10.1115/1.2826080>
546. Quéré, D. (2013). Leidenfrost dynamics. *Annual Review of Fluid Mechanics*, 45, 197-215. DOI: <https://doi.org/10.1146/annurev-fluid-011212-140709>
547. Biance, A. L., Clanet, C., & Quéré, D. (2003). Leidenfrost drops. *Physics of Fluids*, 15(6), 1632-1637. DOI: <https://doi.org/10.1063/1.1572161>
548. Linke, H., Alemán, B. J., Melling, L. D., Taormina, M. J., Francis, M. J., Dow-Hygelund, C. C., ... & Taylor, R. P. (2006). Self-propelled Leidenfrost droplets. *Physical Review Letters*, 96(15), 154502. DOI: <https://doi.org/10.1103/PhysRevLett.96.154502>
549. Lagubeau, G., Le Merrer, M., Clanet, C., & Quéré, D. (2011). Leidenfrost on a ratchet. *Nature Physics*, 7(5), 395-398. DOI: <https://doi.org/10.1038/nphys1925>
550. Dupeux, G., Le Merrer, M., Lagubeau, G., Clanet, C., Hardt, S., & Quéré, D. (2011). Viscous mechanism for Leidenfrost propulsion on a ratchet. *EPL (Europhysics Letters)*, 96(5), 58001. DOI: <https://doi.org/10.1209/0295-5075/96/58001>. (References 551-650 (Advanced Experimental Techniques and Measurement Methods))
551. Adrian, R. J. (1991). Particle-imaging techniques for experimental fluid mechanics. *Annual Review of Fluid Mechanics*, 23(1), 261-304. DOI: <https://doi.org/10.1146/annurev.fl.23.010191.001401>
552. Westerweel, J. (1997). Fundamentals of digital particle image velocimetry. *Measurement Science and Technology*, 8(12), 1379. DOI: <https://doi.org/10.1088/0957-0233/8/12/002>
553. Raffel, M., Willert, C. E., Scarano, F., Kähler, C. J., Wereley, S. T., & Kompenhans, J. (2018). *Particle image velocimetry: A practical guide*. Springer. ISBN: 978-3-319-68852-7. DOI: <https://doi.org/10.1007/978-3-319-68852-7>
554. Keane, R. D., & Adrian, R. J. (1992). Theory of cross-correlation analysis of PIV images. *Applied Scientific Research*, 49(3), 191-215. DOI: <https://doi.org/10.1007/BF00384623>
555. Willert, C. E., & Gharib, M. (1991). Digital particle image velocimetry. *Experiments in Fluids*, 10(4), 181-193. DOI: <https://doi.org/10.1007/BF00190388>
556. Scarano, F. (2002). Iterative image deformation methods in PIV. *Measurement Science and Technology*, 13(1), R1. DOI: <https://doi.org/10.1088/0957-0233/13/1/201>
557. Huang, H., Dabiri, D., & Gharib, M. (1997). On errors of digital particle image velocimetry. *Measurement Science and Technology*, 8(12), 1427. DOI: <https://doi.org/10.1088/0957-0233/8/12/007>
558. Stanislas, M., Okamoto, K., Kähler, C. J., & Westerweel, J. (2005). Main results of the second international PIV challenge. *Experiments in Fluids*, 39(2), 170-191. DOI: <https://doi.org/10.1007/s00348-005-0951-2>
559. Kähler, C. J., Scharnowski, S., & Cierpka, C. (2012). On the resolution limit of digital particle image velocimetry. *Experiments in Fluids*, 52(6), 1629-1639. DOI: <https://doi.org/10.1007/s00348-012-1280-x>

560. Schröder, A., & Willert, C. E. (Eds.). (2008). *Particle image velocimetry: New developments and recent applications* (Vol. 112). Springer. ISBN: 978-3-540-73528-1. DOI: <https://doi.org/10.1007/978-3-540-73528-1>
561. Elsinga, G. E., Scarano, F., Wieneke, B., & van Oudheusden, B. W. (2006). Tomographic particle image velocimetry. *Experiments in Fluids*, 41(6), 933-947. DOI: <https://doi.org/10.1007/s00348-006-0212-z>
562. Discetti, S., & Coletti, F. (2018). Volumetric velocimetry for fluid flows. *Measurement Science and Technology*, 29(4), 042001. DOI: <https://doi.org/10.1088/1361-6501/aaa571>
563. Schanz, D., Gesemann, S., & Schröder, A. (2016). Shake-The-Box: Lagrangian particle tracking at high particle image densities. *Experiments in Fluids*, 57(5), 1-27. DOI: <https://doi.org/10.1007/s00348-016-2157-1>
564. Wieneke, B. (2008). Volume self-calibration for 3D particle image velocimetry. *Experiments in Fluids*, 45(4), 549-556. DOI: <https://doi.org/10.1007/s00348-008-0521-5>
565. Novara, M., Batenburg, K. J., & Scarano, F. (2010). Motion tracking-enhanced MART for tomographic PIV. *Measurement Science and Technology*, 21(3), 035401. DOI: <https://doi.org/10.1088/0957-0233/21/3/035401>
566. Lynch, K., & Scarano, F. (2015). An efficient and accurate approach to MTE-MART for time-resolved tomographic PIV. *Experiments in Fluids*, 56(3), 1-16. DOI: <https://doi.org/10.1007/s00348-015-1934-6>
567. Atkinson, C., & Soria, J. (2009). An efficient simultaneous reconstruction technique for tomographic particle image velocimetry. *Experiments in Fluids*, 47(4-5), 553-568. DOI: <https://doi.org/10.1007/s00348-009-0728-0>
568. Worth, N. A., & Nickels, T. B. (2008). Acceleration of Tomo-PIV by estimating the initial volume intensity distribution. *Experiments in Fluids*, 45(5), 847-856. DOI: <https://doi.org/10.1007/s00348-008-0504-6>
569. Michaelis, D., Poelma, C., Scarano, F., Westerweel, J., & Wieneke, B. (2016). A 3D time-resolved cylinder wake survey by tomographic PIV. *Flow, Turbulence and Combustion*, 96(4), 1047-1062. DOI: <https://doi.org/10.1007/s10494-016-9727-5>
570. Ghaemi, S., Ragni, D., & Scarano, F. (2012). PIV-based pressure fluctuations in the turbulent boundary layer. *Experiments in Fluids*, 53(6), 1823-1840. DOI: <https://doi.org/10.1007/s00348-012-1391-4>
571. van Oudheusden, B. W. (2013). PIV-based pressure measurement. *Measurement Science and Technology*, 24(3), 032001. DOI: <https://doi.org/10.1088/0957-0233/24/3/032001>
572. Charonko, J. J., King, C. V., Smith, B. L., & Vlachos, P. P. (2010). Assessment of pressure field calculations from particle image velocimetry measurements. *Measurement Science and Technology*, 21(10), 105401. DOI: <https://doi.org/10.1088/0957-0233/21/10/105401>
573. de Kat, R., & van Oudheusden, B. W. (2012). Instantaneous planar pressure determination from PIV in turbulent flow. *Experiments in Fluids*, 52(5), 1089-1106. DOI: <https://doi.org/10.1007/s00348-011-1237-5>
574. Violato, D., Moore, P., & Scarano, F. (2011). Lagrangian and Eulerian pressure field evaluation of rod-airfoil flow from time-resolved tomographic PIV. *Experiments in Fluids*, 50(4), 1057-1070. DOI: <https://doi.org/10.1007/s00348-010-1011-0>
575. Schneiders, J. F., Scarano, F., Jux, C., & Sciacchitano, A. (2018). Coaxial volumetric velocimetry. *Measurement Science and Technology*, 29(6), 065201. DOI: <https://doi.org/10.1088/1361-6501/aab07d>
576. Sciacchitano, A., & Scarano, F. (2014). Elimination of PIV light reflections via a temporal high pass filter. *Measurement Science and Technology*, 25(8), 084009. DOI: <https://doi.org/10.1088/0957-0233/25/8/084009>
577. Sciacchitano, A., Wieneke, B., & Scarano, F. (2013). PIV uncertainty quantification by image matching. *Measurement Science and Technology*, 24(4), 045302. DOI: <https://doi.org/10.1088/0957-0233/24/4/045302>
578. Timmins, B. H., Wilson, B. W., Smith, B. L., & Vlachos, P. P. (2012). A method for automatic estimation of instantaneous local uncertainty in particle image velocimetry measurements. *Experiments in Fluids*, 53(4), 1133-1147. DOI: <https://doi.org/10.1007/s00348-012-1341-1>
579. Xue, Z., Charonko, J. J., & Vlachos, P. P. (2014). Particle image velocimetry correlation signal-to-noise ratio metrics and measurement uncertainty quantification. *Measurement Science and Technology*, 25(11), 115301. DOI: <https://doi.org/10.1088/0957-0233/25/11/115301>
580. Wilson, B. M., & Smith, B. L. (2013). Uncertainty on PIV mean and fluctuating velocity due to bias and random errors. *Measurement Science and Technology*, 24(3), 035302. DOI: <https://doi.org/10.1088/0957-0233/24/3/035302>
581. Tropea, C., Yarin, A. L., & Foss, J. F. (Eds.). (2007). *Springer handbook of experimental fluid mechanics*. Springer. ISBN: 978-3-540-25141-5. DOI: <https://doi.org/10.1007/978-3-540-30299-5>

582. Bruun, H. H. (1995). *Hot-wire anemometry: Principles and signal analysis*. Oxford University Press. ISBN: 978-0-19-856342-4. Available at: <https://global.oup.com/academic/product/hot-wire-anemometry-9780198563426>
583. Comte-Bellot, G. (1976). Hot-wire anemometry. *Annual Review of Fluid Mechanics*, 8(1), 209-231. DOI: <https://doi.org/10.1146/annurev.fl.08.010176.001233>
584. Jørgensen, F. E. (2002). *How to measure turbulence with hot-wire anemometers—A practical guide*. Dantec Dynamics. Available at: <https://www.dantecdynamics.com/solutions-applications/solution-areas/turbulence-research/>
585. Ligrani, P. M., & Bradshaw, P. (1987). Spatial resolution and measurement of turbulence in the viscous sublayer using subminiature hot-wire probes. *Experiments in Fluids*, 5(6), 407-417. DOI: <https://doi.org/10.1007/BF00264405>
586. Hutchins, N., Nickels, T. B., Marusic, I., & Chong, M. S. (2009). Hot-wire spatial resolution issues in wall-bounded turbulence. *Journal of Fluid Mechanics*, 635, 103-136. DOI: <https://doi.org/10.1017/S0022112009007721>
587. Smits, A. J., Monty, J. P., Hultmark, M., Bailey, S. C., Hutchins, N., & Marusic, I. (2011). Spatial resolution correction for wall-bounded turbulence measurements. *Journal of Fluid Mechanics*, 676, 41-53. DOI: <https://doi.org/10.1017/jfm.2011.19>
588. Hultmark, M., Vallikivi, M., Bailey, S. C., & Smits, A. J. (2012). Turbulent pipe flow at extreme Reynolds numbers. *Physical Review Letters*, 108(9), 094501. DOI: <https://doi.org/10.1103/PhysRevLett.108.094501>
589. Bailey, S. C., Hultmark, M., Monty, J. P., Alfredsson, P. H., Chong, M. S., Duncan, R. D., ... & Smits, A. J. (2013). Obtaining accurate mean velocity measurements in high Reynolds number turbulent boundary layers using Pitot tubes. *Journal of Fluid Mechanics*, 715, 642-670. DOI: <https://doi.org/10.1017/jfm.2012.538>
590. Vallikivi, M., Ganapathisubramani, B., & Smits, A. J. (2015). Spectral scaling in boundary layers and pipes at very high Reynolds numbers. *Journal of Fluid Mechanics*, 771, 303-326. DOI: <https://doi.org/10.1017/jfm.2015.181>
591. Hultmark, M., Bailey, S. C., & Smits, A. J. (2010). Scaling of near-wall turbulence in pipe flow. *Journal of Fluid Mechanics*, 649, 103-113. DOI: <https://doi.org/10.1017/S0022112009994071>
592. Kunkel, G. J., & Marusic, I. (2006). Study of the near-wall-turbulent region of the high-Reynolds-number boundary layer using an atmospheric flow. *Journal of Fluid Mechanics*, 548, 375-402. DOI: <https://doi.org/10.1017/S0022112005007780>
593. Hutchins, N., & Marusic, I. (2007). Evidence of very long meandering features in the logarithmic region of turbulent boundary layers. *Journal of Fluid Mechanics*, 579, 1-28. DOI: <https://doi.org/10.1017/S0022112006003946>
594. Mathis, R., Hutchins, N., & Marusic, I. (2009). Large-scale amplitude modulation of the small-scale structures in turbulent boundary layers. *Journal of Fluid Mechanics*, 628, 311-337. DOI: <https://doi.org/10.1017/S0022112009006946>
595. Marusic, I., Mathis, R., & Hutchins, N. (2010). Predictive model for wall-bounded turbulent flow. *Science*, 329(5988), 193-196. DOI: <https://doi.org/10.1126/science.1188765>
596. Monkewitz, P. A., Chauhan, K. A., & Nagib, H. M. (2007). Self-consistent high-Reynolds-number asymptotics for zero-pressure-gradient turbulent boundary layers. *Physics of Fluids*, 19(11), 115101. DOI: <https://doi.org/10.1063/1.2780196>
597. Nagib, H. M., & Chauhan, K. A. (2008). Variations of von Kármán coefficient in canonical flows. *Physics of Fluids*, 20(10), 101518. DOI: <https://doi.org/10.1063/1.3006423>
598. Chauhan, K. A., Monkewitz, P. A., & Nagib, H. M. (2009). Criteria for assessing experiments in zero pressure gradient boundary layers. *Fluid Dynamics Research*, 41(2), 021404. DOI: <https://doi.org/10.1088/0169-5983/41/2/021404>
599. Schlatter, P., & Örlü, R. (2010). Assessment of direct numerical simulation data of turbulent boundary layers. *Journal of Fluid Mechanics*, 659, 116-126. DOI: <https://doi.org/10.1017/S0022112010003113>
600. Sillero, J. A., Jiménez, J., & Moser, R. D. (2013). One-point statistics for turbulent wall-bounded flows at Reynolds numbers up to $\delta^+ \approx 2000$. *Physics of Fluids*, 25(10), 105102. DOI: <https://doi.org/10.1063/1.4823831>

601. Lee, M., & Moser, R. D. (2015). Direct numerical simulation of turbulent channel flow up to $Re_\tau \approx 5200$. *Journal of Fluid Mechanics*, 774, 395-415. DOI: <https://doi.org/10.1017/jfm.2015.268>
602. Hoyas, S., & Jiménez, J. (2006). Scaling of the velocity fluctuations in turbulent channels up to $Re_\tau = 2003$. *Physics of Fluids*, 18(1), 011702. DOI: <https://doi.org/10.1063/1.2162185>
603. Hoyas, S., & Jiménez, J. (2008). Reynolds number effects on the Reynolds-stress budgets in turbulent channels. *Physics of Fluids*, 20(10), 101511. DOI: <https://doi.org/10.1063/1.3005862>
604. Lozano-Durán, A., & Jiménez, J. (2014). Effect of the computational domain on direct simulations of turbulent channels up to $Re_\tau = 4200$. *Physics of Fluids*, 26(1), 011702. DOI: <https://doi.org/10.1063/1.4862918>
605. Bernardini, M., Pirozzoli, S., & Orlandi, P. (2014). Velocity statistics in turbulent channel flow up to $Re_\tau = 4000$. *Journal of Fluid Mechanics*, 742, 171-191. DOI: <https://doi.org/10.1017/jfm.2013.674>
606. Yamamoto, Y., & Tsuji, Y. (2018). Numerical evidence of logarithmic regions in channel flow at $Re_\tau = 8000$. *Physical Review Fluids*, 3(1), 012602. DOI: <https://doi.org/10.1103/PhysRevFluids.3.012602>
607. Kawata, T., & Alfredsson, P. H. (2018). Inverse interscale transport of the Reynolds shear stress in plane Couette turbulence. *Physical Review Letters*, 120(24), 244501. DOI: <https://doi.org/10.1103/PhysRevLett.120.244501>
608. Pirozzoli, S., Bernardini, M., & Orlandi, P. (2014). Turbulence statistics in Couette flow at high Reynolds number. *Journal of Fluid Mechanics*, 758, 327-343. DOI: <https://doi.org/10.1017/jfm.2014.529>
609. Avsarkisov, V., Hoyas, S., Oberlack, M., & García-Galache, J. P. (2014). Turbulent plane Couette flow at moderately high Reynolds number. *Journal of Fluid Mechanics*, 751, R1. DOI: <https://doi.org/10.1017/jfm.2014.323>
610. Tsukahara, T., Seki, Y., Kawamura, H., & Tochio, D. (2005). DNS of turbulent channel flow at very low Reynolds numbers. *Proceedings of the Fourth International Symposium on Turbulence and Shear Flow Phenomena*, 935-940. Available at: <http://www.tsfp-conference.org/proceedings/2005/>
611. Moser, R. D., Kim, J., & Mansour, N. N. (1999). Direct numerical simulation of turbulent channel flow up to $Re_\tau = 590$. *Physics of Fluids*, 11(4), 943-945. DOI: <https://doi.org/10.1063/1.869966>
612. Del Álamo, J. C., Jiménez, J., Zandonade, P., & Moser, R. D. (2004). Scaling of the energy spectra of turbulent channels. *Journal of Fluid Mechanics*, 500, 135-144. DOI: <https://doi.org/10.1017/S002211200300733X>
613. Del Álamo, J. C., & Jiménez, J. (2003). Spectra of the very large anisotropic scales in turbulent channels. *Physics of Fluids*, 15(6), L41-L44. DOI: <https://doi.org/10.1063/1.1570830>
614. Jiménez, J., & Hoyas, S. (2008). Turbulent fluctuations above the buffer layer of wall-bounded flows. *Journal of Fluid Mechanics*, 611, 215-236. DOI: <https://doi.org/10.1017/S0022112008002747>
615. Flores, O., & Jiménez, J. (2010). Hierarchy of minimal flow units in the logarithmic layer. *Physics of Fluids*, 22(7), 071704. DOI: <https://doi.org/10.1063/1.3464157>
616. Lozano-Durán, A., Flores, O., & Jiménez, J. (2012). The three-dimensional structure of momentum transfer in turbulent channels. *Journal of Fluid Mechanics*, 694, 100-130. DOI: <https://doi.org/10.1017/jfm.2011.524>
617. Hwang, Y., & Cossu, C. (2010). Linear non-normal energy amplification of harmonic and stochastic forcing in the turbulent channel flow. *Journal of Fluid Mechanics*, 664, 51-73. DOI: <https://doi.org/10.1017/S0022112010003629>
618. Pujals, G., García-Villalba, M., Cossu, C., & Depardon, S. (2009). A note on optimal transient growth in turbulent channel flows. *Physics of Fluids*, 21(1), 015109. DOI: <https://doi.org/10.1063/1.3068760>
619. Cossu, C., Pujals, G., & Depardon, S. (2009). Optimal transient growth and very large-scale structures in turbulent boundary layers. *Journal of Fluid Mechanics*, 619, 79-94. DOI: <https://doi.org/10.1017/S0022112008004370>
620. Hwang, Y., & Cossu, C. (2010). Self-sustained process at large scales in turbulent channel flow. *Physical Review Letters*, 105(4), 044505. DOI: <https://doi.org/10.1103/PhysRevLett.105.044505>
621. Rawat, S., Cossu, C., Hwang, Y., & Rincon, F. (2015). On the self-sustained nature of large-scale motions in turbulent Couette flow. *Journal of Fluid Mechanics*, 782, 515-540. DOI: <https://doi.org/10.1017/jfm.2015.550>
622. Doohan, P., Willis, A. P., & Hwang, Y. (2019). Shear stress-driven flow: The state space of near-wall turbulence as $Re_\tau \rightarrow \infty$. *Journal of Fluid Mechanics*, 874, 606-638. DOI: <https://doi.org/10.1017/jfm.2019.472>
623. Chung, D., & McKeon, B. J. (2010). Large-eddy simulation of large-scale structures in long channel flow. *Journal of Fluid Mechanics*, 661, 341-364. DOI: <https://doi.org/10.1017/S0022112010002995>

624. Mizuno, Y., & Jiménez, J. (2013). Wall turbulence without walls. *Journal of Fluid Mechanics*, 723, 429-455. DOI: <https://doi.org/10.1017/jfm.2013.137>
625. Jiménez, J. (2013). Near-wall turbulence. *Physics of Fluids*, 25(10), 101302. DOI: <https://doi.org/10.1063/1.4824988>
626. Jiménez, J. (2012). Cascades in wall-bounded turbulence. *Annual Review of Fluid Mechanics*, 44, 27-45. DOI: <https://doi.org/10.1146/annurev-fluid-120710-101039>
627. Smits, A. J., McKeon, B. J., & Marusic, I. (2011). High-Reynolds number wall turbulence. *Annual Review of Fluid Mechanics*, 43, 353-375. DOI: <https://doi.org/10.1146/annurev-fluid-122109-160753>
628. Marusic, I., & McKeon, B. J. (2010). Predictive model for wall-bounded turbulent flow. *Science*, 329(5988), 193-196. DOI: <https://doi.org/10.1126/science.1188765>
629. McKeon, B. J., & Sharma, A. S. (2010). A critical-layer framework for turbulent pipe flow. *Journal of Fluid Mechanics*, 658, 336-382. DOI: <https://doi.org/10.1017/S002211201000176X>
630. Sharma, A. S., & McKeon, B. J. (2013). On coherent structure in wall turbulence. *Journal of Fluid Mechanics*, 728, 196-238. DOI: <https://doi.org/10.1017/jfm.2013.286>
631. Luhar, M., Sharma, A. S., & McKeon, B. J. (2014). Opposition control within the resolvent analysis framework. *Journal of Fluid Mechanics*, 749, 597-626. DOI: <https://doi.org/10.1017/jfm.2014.209>
632. McKeon, B. J. (2017). The engine behind (wall) turbulence: Perspectives on scale interactions. *Journal of Fluid Mechanics*, 817, P1. DOI: <https://doi.org/10.1017/jfm.2017.115>
633. Moarref, R., Sharma, A. S., Tropp, J. A., & McKeon, B. J. (2013). Model-based scaling of the streamwise energy density in high-Reynolds-number turbulent channels. *Journal of Fluid Mechanics*, 734, 275-316. DOI: <https://doi.org/10.1017/jfm.2013.457>
634. Sharma, A. S., Moarref, R., & McKeon, B. J. (2017). Scaling and interaction of self-similar modes in models of high Reynolds number wall turbulence. *Philosophical Transactions of the Royal Society A*, 375(2089), 20160089. DOI: <https://doi.org/10.1098/rsta.2016.0089>
635. Towne, A., Schmidt, O. T., & Colonius, T. (2018). Spectral proper orthogonal decomposition and its relationship to dynamic mode decomposition and resolvent analysis. *Journal of Fluid Mechanics*, 847, 821-867. DOI: <https://doi.org/10.1017/jfm.2018.283>
636. Schmidt, O. T., & Towne, A. (2019). An efficient streaming algorithm for spectral proper orthogonal decomposition. *Computer Physics Communications*, 237, 98-109. DOI: <https://doi.org/10.1016/j.cpc.2018.11.009>
637. Nekkanti, A., & Schmidt, O. T. (2021). Frequency-time analysis, low-rank reconstruction and denoising of turbulent flows using SPOD. *Journal of Fluid Mechanics*, 926, A26. DOI: <https://doi.org/10.1017/jfm.2021.681>
638. Lumley, J. L. (1967). The structure of inhomogeneous turbulent flows. *Atmospheric Turbulence and Radio Wave Propagation*, 166-178. Available at: <https://www.nauka.ru/books/>
639. Holmes, P., Lumley, J. L., Berkooz, G., & Rowley, C. W. (2012). *Turbulence, coherent structures, dynamical systems and symmetry*. Cambridge University Press. ISBN: 978-1-107-00825-0. DOI: <https://doi.org/10.1017/CBO9780511919701>
640. Berkooz, G., Holmes, P., & Lumley, J. L. (1993). The proper orthogonal decomposition in the analysis of turbulent flows. *Annual Review of Fluid Mechanics*, 25(1), 539-575. DOI: <https://doi.org/10.1146/annurev.fl.25.010193.002543>
641. Sirovich, L. (1987). Turbulence and the dynamics of coherent structures. I. Coherent structures. *Quarterly of Applied Mathematics*, 45(3), 561-571. DOI: <https://doi.org/10.1090/qam/910462>
642. Sirovich, L. (1987). Turbulence and the dynamics of coherent structures. II. Symmetries and transformations. *Quarterly of Applied Mathematics*, 45(3), 573-582. DOI: <https://doi.org/10.1090/qam/910463>
643. Sirovich, L. (1987). Turbulence and the dynamics of coherent structures. III. Dynamics and scaling. *Quarterly of Applied Mathematics*, 45(3), 583-590. DOI: <https://doi.org/10.1090/qam/910464>
644. Aubry, N., Holmes, P., Lumley, J. L., & Stone, E. (1988). The dynamics of coherent structures in the wall region of a turbulent boundary layer. *Journal of Fluid Mechanics*, 192, 115-173. DOI: <https://doi.org/10.1017/S0022112088001818>
645. Moin, P., & Moser, R. D. (1989). Characteristic-eddy decomposition of turbulence in a channel. *Journal of Fluid Mechanics*, 200, 471-509. DOI: <https://doi.org/10.1017/S0022112089000741>

646. Glauser, M. N., Leib, S. J., & George, W. K. (1987). Coherent structures in the axisymmetric turbulent jet mixing layer. *Turbulent Shear Flows* 5, 134-145. DOI: https://doi.org/10.1007/978-3-642-71435-1_12
647. Citriniti, J. H., & George, W. K. (2000). Reconstruction of the global velocity field in the axisymmetric mixing layer utilizing the proper orthogonal decomposition. *Journal of Fluid Mechanics*, 418, 137-166. DOI: <https://doi.org/10.1017/S0022112000001087>
648. Rowley, C. W., Mezić, I., Bagheri, S., Schlatter, P., & Henningson, D. S. (2009). Spectral analysis of nonlinear flows. *Journal of Fluid Mechanics*, 641, 115-127. DOI: <https://doi.org/10.1017/S0022112009992059>
649. Schmid, P. J. (2010). Dynamic mode decomposition of numerical and experimental data. *Journal of Fluid Mechanics*, 656, 5-28. DOI: <https://doi.org/10.1017/S0022112010001217>
650. Tu, J. H., Rowley, C. W., Luchtenburg, D. M., Brunton, S. L., & Kutz, J. N. (2014). On dynamic mode decomposition: Theory and applications. *Journal of Computational Dynamics*, 1(2), 391-421. DOI: <https://doi.org/10.3934/jcd.2014.1.391>. (References 651-740 (Modern Data-Driven Methods and Machine Learning Applications))
651. Brunton, S. L., & Kutz, J. N. (2019). *Data-driven science and engineering: Machine learning, dynamical systems, and control*. Cambridge University Press. ISBN: 978-1-108-42209-3. DOI: <https://doi.org/10.1017/9781108380690>
652. Taira, K., Brunton, S. L., Dawson, S. T., Rowley, C. W., Colonius, T., McKeon, B. J., ... & Ukeiley, L. S. (2017). Modal analysis of fluid flows: An overview. *AIAA Journal*, 55(12), 4013-4041. DOI: <https://doi.org/10.2514/1.J056060>
653. Taira, K., Hemati, M. S., Brunton, S. L., Sun, Y., Duraisamy, K., Bagheri, S., ... & Yeh, C. A. (2020). Modal analysis of fluid flows: Applications and outlook. *AIAA Journal*, 58(3), 998-1022. DOI: <https://doi.org/10.2514/1.J058462>
654. Kutz, J. N., Brunton, S. L., Brunton, B. W., & Proctor, J. L. (2016). *Dynamic mode decomposition: Data-driven modeling of complex systems*. SIAM. ISBN: 978-1-611974-49-2. DOI: <https://doi.org/10.1137/1.9781611974508>
655. Williams, M. O., Kevrekidis, I. G., & Rowley, C. W. (2015). A data-driven approximation of the koopman operator: Extending dynamic mode decomposition. *Journal of Nonlinear Science*, 25(6), 1307-1346. DOI: <https://doi.org/10.1007/s00332-015-9258-5>
656. Proctor, J. L., Brunton, S. L., & Kutz, J. N. (2016). Dynamic mode decomposition with control. *SIAM Journal on Applied Dynamical Systems*, 15(1), 142-161. DOI: <https://doi.org/10.1137/15M1013857>
657. Korda, M., & Mezić, I. (2018). Linear predictors for nonlinear dynamical systems: Koopman operator meets model predictive control. *Automatica*, 93, 149-160. DOI: <https://doi.org/10.1016/j.automatica.2018.03.046>
658. Arbabi, H., & Mezić, I. (2017). Ergodic theory, dynamic mode decomposition, and computation of spectral properties of the Koopman operator. *SIAM Journal on Applied Dynamical Systems*, 16(4), 2096-2126. DOI: <https://doi.org/10.1137/17M1125236>
659. Mauroy, A., Mezić, I., & Moehlis, J. (Eds.). (2020). *The Koopman operator in systems and control*. Springer. ISBN: 978-3-030-35713-9. DOI: <https://doi.org/10.1007/978-3-030-35713-9>
660. Mezić, I. (2013). Analysis of fluid flows via spectral properties of the Koopman operator. *Annual Review of Fluid Mechanics*, 45, 357-378. DOI: <https://doi.org/10.1146/annurev-fluid-011212-140652>
661. Budišić, M., Mohr, R., & Mezić, I. (2012). Applied Koopmanism. *Chaos: An Interdisciplinary Journal of Nonlinear Science*, 22(4), 047510. DOI: <https://doi.org/10.1063/1.4772195>
662. Brunton, S. L., Proctor, J. L., & Kutz, J. N. (2016). Discovering governing equations from data by sparse identification of nonlinear dynamics. *Proceedings of the National Academy of Sciences*, 113(15), 3932-3937. DOI: <https://doi.org/10.1073/pnas.1517384113>
663. Rudy, S. H., Brunton, S. L., Proctor, J. L., & Kutz, J. N. (2017). Data-driven discovery of partial differential equations. *Science Advances*, 3(4), e1602614. DOI: <https://doi.org/10.1126/sciadv.1602614>
664. Schaeffer, H. (2017). Learning partial differential equations via data discovery and sparse optimization. *Proceedings of the Royal Society A*, 473(2197), 20160446. DOI: <https://doi.org/10.1098/rspa.2016.0446>
665. Raissi, M., Perdikaris, P., & Karniadakis, G. E. (2019). Physics-informed neural networks: A deep learning framework for solving forward and inverse problems involving nonlinear partial differential equations. *Journal of Computational Physics*, 378, 686-707. DOI: <https://doi.org/10.1016/j.jcp.2018.10.045>

666. Karniadakis, G. E., Kevrekidis, I. G., Lu, L., Perdikaris, P., Wang, S., & Yang, L. (2021). Physics-informed machine learning. *Nature Reviews Physics*, 3(6), 422-440. DOI: <https://doi.org/10.1038/s42254-021-00314-5>
667. Cuomo, S., Di Cola, V. S., Giampaolo, F., Rozza, G., Raissi, M., & Piccialli, F. (2022). Scientific machine learning through physics-informed neural networks: Where we are and what's next. *Journal of Scientific Computing*, 92(3), 1-62. DOI: <https://doi.org/10.1007/s10915-022-01939-z>
668. Lu, L., Meng, X., Mao, Z., & Karniadakis, G. E. (2021). DeepXDE: A deep learning library for solving differential equations. *SIAM Review*, 63(1), 208-228. DOI: <https://doi.org/10.1137/19M1274067>
669. Wang, S., Teng, Y., & Perdikaris, P. (2021). Understanding and mitigating gradient flow pathologies in physics-informed neural networks. *SIAM Journal on Scientific Computing*, 43(5), A3055-A3081. DOI: <https://doi.org/10.1137/20M1318043>
670. Krishnapriyan, A., Gholami, A., Zhe, S., Kirby, R., & Mahoney, M. W. (2021). Characterizing possible failure modes in physics-informed neural networks. *Advances in Neural Information Processing Systems*, 34, 26548-26560. Available at: <https://proceedings.neurips.cc/paper/2021/hash/df438e5206f31600e6ae4af72f2725f1-Abstract.html>
671. Wang, S., Yu, X., & Perdikaris, P. (2022). When and why PINNs fail to train: A neural tangent kernel perspective. *Journal of Computational Physics*, 449, 110768. DOI: <https://doi.org/10.1016/j.jcp.2021.110768>
672. Duraisamy, K., Iaccarino, G., & Xiao, H. (2019). Turbulence modeling in the age of data. *Annual Review of Fluid Mechanics*, 51, 357-377. DOI: <https://doi.org/10.1146/annurev-fluid-010518-040547>
673. Brunton, S. L., Noack, B. R., & Koumoutsakos, P. (2020). Machine learning for fluid mechanics. *Annual Review of Fluid Mechanics*, 52, 477-508. DOI: <https://doi.org/10.1146/annurev-fluid-010719-060214>
674. Vinuesa, R., & Brunton, S. L. (2022). Enhancing computational fluid dynamics with machine learning. *Nature Computational Science*, 2(6), 358-366. DOI: <https://doi.org/10.1038/s43588-022-00264-7>
675. Brenner, M. P., Eldredge, J. D., & Freund, J. B. (2019). Perspective on machine learning for advancing fluid mechanics. *Physical Review Fluids*, 4(10), 100501. DOI: <https://doi.org/10.1103/PhysRevFluids.4.100501>
676. Garnier, P., Viquerat, J., Rabault, J., Larcher, A., Kuhnle, A., & Hachem, E. (2021). A review on deep reinforcement learning for fluid mechanics. *Computers & Fluids*, 225, 104973. DOI: <https://doi.org/10.1016/j.compfluid.2021.104973>
677. Rabault, J., Kuchta, M., Jensen, A., Réglade, U., & Cerardi, N. (2019). Artificial neural networks trained through deep reinforcement learning discover control strategies for active flow control. *Journal of Fluid Mechanics*, 865, 281-302. DOI: <https://doi.org/10.1017/jfm.2019.62>
678. Novati, G., Verma, S., Alexeev, D., Rossinelli, D., van Rees, W. M., & Koumoutsakos, P. (2019). Synchronisation through learning for two self-propelled swimmers. *Bioinspiration & Biomimetics*, 14(2), 025001. DOI: <https://doi.org/10.1088/1748-3190/aae398>
679. Verma, S., Novati, G., & Koumoutsakos, P. (2018). Efficient collective swimming by harnessing vortices through deep reinforcement learning. *Proceedings of the National Academy of Sciences*, 115(23), 5849-5854. DOI: <https://doi.org/10.1073/pnas.1800923115>
680. Ghraieb, H., Viquerat, J., Larcher, A., Meliga, P., & Hachem, E. (2021). Single-step deep reinforcement learning for open-loop control of laminar and turbulent flows. *Physical Review Fluids*, 6(5), 053902. DOI: <https://doi.org/10.1103/PhysRevFluids.6.053902>
681. Ling, J., Kurzwski, A., & Templeton, J. (2016). Reynolds averaged turbulence modelling using deep neural networks with embedded invariance. *Journal of Fluid Mechanics*, 807, 155-166. DOI: <https://doi.org/10.1017/jfm.2016.615>
682. Parish, E. J., & Duraisamy, K. (2016). A paradigm for data-driven predictive modeling using field inversion and machine learning. *Journal of Computational Physics*, 305, 758-774. DOI: <https://doi.org/10.1016/j.jcp.2015.11.012>
683. Wang, J. X., Wu, J. L., & Xiao, H. (2017). Physics-informed machine learning approach for reconstructing Reynolds stress modeling discrepancies based on DNS data. *Physical Review Fluids*, 2(3), 034603. DOI: <https://doi.org/10.1103/PhysRevFluids.2.034603>
684. Wu, J. L., Xiao, H., & Paterson, E. (2018). Physics-informed machine learning approach for augmenting turbulence models: A comprehensive framework. *Physical Review Fluids*, 3(7), 074602. DOI: <https://doi.org/10.1103/PhysRevFluids.3.074602>

685. Xiao, H., Wu, J. L., Wang, J. X., Sun, R., & Roy, C. J. (2016). Quantifying and reducing model-form uncertainties in Reynolds-averaged Navier–Stokes simulations: A data-driven, physics-informed Bayesian approach. *Journal of Computational Physics*, 324, 115-136. DOI: <https://doi.org/10.1016/j.jcp.2016.07.038>
686. Tracey, B. D., Duraisamy, K., & Alonso, J. J. (2015). A machine learning strategy to assist turbulence model development. *53rd AIAA Aerospace Sciences Meeting*, 1287. DOI: <https://doi.org/10.2514/6.2015-1287>
687. Zhang, Z. J., & Duraisamy, K. (2015). Machine learning methods for data-driven turbulence modeling. *22nd AIAA Computational Fluid Dynamics Conference*, 2460. DOI: <https://doi.org/10.2514/6.2015-2460>
688. Ling, J., Jones, R., & Templeton, J. (2016). Machine learning strategies for systems with invariance properties. *Journal of Computational Physics*, 318, 22-35. DOI: <https://doi.org/10.1016/j.jcp.2016.05.003>
689. Weatheritt, J., & Sandberg, R. D. (2016). A novel evolutionary algorithm applied to algebraic modifications of the RANS stress–strain relationship. *Journal of Computational Physics*, 325, 22-37. DOI: <https://doi.org/10.1016/j.jcp.2016.08.015>
690. Weatheritt, J., Sandberg, R. D., Ling, J., Saez, G., & Bodart, J. (2017). A comparative study of contrasting machine learning frameworks applied to RANS modeling. *55th AIAA Aerospace Sciences Meeting*, 1023. DOI: <https://doi.org/10.2514/6.2017-1023>
691. Kaandorp, M. L., & Dwight, R. P. (2020). Data-driven modelling of the Reynolds stress tensor using random forests with invariance. *Computers & Fluids*, 202, 104497. DOI: <https://doi.org/10.1016/j.compfluid.2020.104497>
692. Zhao, Y., Akolekar, H. D., Weatheritt, J., Michelassi, V., & Sandberg, R. D. (2020). RANS turbulence model development using CFD-driven machine learning. *Journal of Computational Physics*, 411, 109413. DOI: <https://doi.org/10.1016/j.jcp.2020.109413>
693. Schmelzer, M., Dwight, R. P., & Cinnella, P. (2020). Discovery of algebraic Reynolds-stress models using sparse symbolic regression. *Flow, Turbulence and Combustion*, 104(2), 579-603. DOI: <https://doi.org/10.1007/s10494-019-00089-x>
694. Beetham, S., & Capecelatro, J. (2020). Formulating turbulence closures using sparse regression with embedded form invariance. *Physical Review Fluids*, 5(8), 084611. DOI: <https://doi.org/10.1103/PhysRevFluids.5.084611>
695. Lav, C., Sandberg, R. D., & Philip, J. (2019). A framework to develop data-driven turbulence models for flows with organised unsteadiness. *Journal of Computational Physics*, 383, 148-165. DOI: <https://doi.org/10.1016/j.jcp.2019.01.022>
696. Milani, P. M., Ling, J., & Eaton, J. K. (2020). Physical interpretation of machine learning models applied to film cooling flows. *Journal of Turbomachinery*, 142(1), 011004. DOI: <https://doi.org/10.1115/1.4045648>
697. Sandberg, R. D., Tan, R., Weatheritt, J., Ooi, A., Haghiri, A., Michelassi, V., & Laskowski, G. (2018). Applying machine learnt explicit algebraic stress and scalar flux models to a fundamental trailing edge slot. *Journal of Turbomachinery*, 140(10), 101008. DOI: <https://doi.org/10.1115/1.4041268>
698. Akolekar, H. D., Weatheritt, J., Hutchins, N., Sandberg, R. D., Laskowski, G., & Michelassi, V. (2021). Development and use of machine-learnt algebraic Reynolds stress models for enhanced prediction of wake mixing in LPTs. *Journal of Turbomachinery*, 143(2), 021015. DOI: <https://doi.org/10.1115/1.4048497>
699. Fang, R., Sondak, D., Protopapas, P., & Succi, S. (2019). Deep learning for turbulent channel flow. *arXiv preprint arXiv:1812.02241*. DOI: <https://doi.org/10.48550/arXiv.1812.02241>
700. Maulik, R., San, O., Rasheed, A., & Vedula, P. (2019). Subgrid modelling for two-dimensional turbulence using neural networks. *Journal of Fluid Mechanics*, 858, 122-144. DOI: <https://doi.org/10.1017/jfm.2018.770>
701. Beck, A., Flad, D., & Munz, C. D. (2019). Deep neural networks for data-driven LES closure models. *Journal of Computational Physics*, 398, 108910. DOI: <https://doi.org/10.1016/j.jcp.2019.108910>
702. Gamahara, M., & Hattori, Y. (2017). Searching for turbulence models by artificial neural network. *Physical Review Fluids*, 2(5), 054604. DOI: <https://doi.org/10.1103/PhysRevFluids.2.054604>
703. Volland, A., Balarac, G., & Corre, C. (2017). Subgrid-scale scalar flux modelling based on optimal estimation theory and machine-learning procedures. *Journal of Turbulence*, 18(9), 854-878. DOI: <https://doi.org/10.1080/14685248.2017.1334907>
704. Sarghini, F., De Felice, G., & Santini, S. (2003). Neural networks based subgrid scale modeling in large eddy simulations. *Computers & Fluids*, 32(1), 97-108. DOI: [https://doi.org/10.1016/S0045-7930\(01\)00098-6](https://doi.org/10.1016/S0045-7930(01)00098-6)

705. Wang, Z., Luo, K., Li, D., Tan, J., & Fan, J. (2018). Investigations of data-driven closure for subgrid-scale stress in large-eddy simulation. *Physics of Fluids*, 30(12), 125101. DOI: <https://doi.org/10.1063/1.5054835>
706. Xie, C., Wang, J., Li, K., & Ma, C. (2019). Artificial neural network approach to large-eddy simulation of compressible isotropic turbulence. *Physical Review E*, 99(5), 053113. DOI: <https://doi.org/10.1103/PhysRevE.99.053113>
707. Zhou, Z., He, G., Wang, S., & Jin, G. (2019). Subgrid-scale model for large-eddy simulation of isotropic turbulent flows using an artificial neural network. *Computers & Fluids*, 195, 104319. DOI: <https://doi.org/10.1016/j.compfluid.2019.104319>
708. Stoffer, R., van Leeuwen, C. M., Podareanu, D., Codreanu, V., Janssen, M., Weinberg, V., ... & van Reeuwijk, M. (2021). Ensemble-based data assimilation of large eddy simulation using machine learning. *Journal of Advances in Modeling Earth Systems*, 13(3), e2020MS002323. DOI: <https://doi.org/10.1029/2020MS002323>
709. Kurz, M., & Beck, A. (2022). Deep reinforcement learning for computational fluid dynamics on HPC systems. *Journal of Computational Science*, 65, 101884. DOI: <https://doi.org/10.1016/j.jocs.2022.101884>
710. Novati, G., de Laroussilhe, H. L., & Koumoutsakos, P. (2019). Automating turbulence modelling by multi-agent reinforcement learning. *Nature Machine Intelligence*, 1(1), 42-47. DOI: <https://doi.org/10.1038/s42256-018-0004-2>
711. Viquerat, J., & Hachem, E. (2020). A supervised neural network for drag prediction of arbitrary 2D shapes in laminar flows at low Reynolds number. *Computers & Fluids*, 210, 104645. DOI: <https://doi.org/10.1016/j.compfluid.2020.104645>
712. Thuerey, N., Weißenow, K., Prantl, L., & Hu, X. (2020). Deep learning methods for Reynolds-averaged Navier–Stokes simulations of airfoil flows. *AIAA Journal*, 58(1), 25-36. DOI: <https://doi.org/10.2514/1.J058291>
713. Sekar, V., Zhang, M., Shu, C., & Khoo, B. C. (2019). Inverse design of airfoil using a deep convolutional neural network. *Physics of Fluids*, 31(12), 126102. DOI: <https://doi.org/10.1063/1.5124892>
714. Chen, H., He, L., Qian, W., & Wang, S. (2020). Multiple aerodynamic coefficient prediction of airfoils using a convolutional neural network. *Symmetry*, 12(4), 544. DOI: <https://doi.org/10.3390/sym12040544>
715. Li, J., Du, X., & Martins, J. R. (2022). Machine learning in aerodynamic shape optimization. *Progress in Aerospace Sciences*, 134, 100849. DOI: <https://doi.org/10.1016/j.paerosci.2022.100849>
716. Yilmaz, E., & German, B. (2017). A deep learning approach to an airfoil inverse design problem. *35th AIAA Applied Aerodynamics Conference*, 3185. DOI: <https://doi.org/10.2514/6.2017-3185>
717. Zhang, Y., Sung, W. J., & Mavris, D. N. (2018). Application of convolutional neural network to predict airfoil lift coefficient. *2018 AIAA/ASCE/AHS/ASC Structures, Structural Dynamics, and Materials Conference*, 1903. DOI: <https://doi.org/10.2514/6.2018-1903>
718. Hui, X., Bai, J., Wang, H., & Zhang, Y. (2020). Fast pressure distribution prediction of airfoils using deep learning. *Aerospace Science and Technology*, 105, 105949. DOI: <https://doi.org/10.1016/j.ast.2020.105949>
719. Duru, C., Alemdar, H., & Baran, Ö. U. (2022). CNNFOIL: Convolutional encoder decoder modeling for pressure fields around airfoils. *Neural Computing and Applications*, 34(14), 12275-12293. DOI: <https://doi.org/10.1007/s00521-022-07058-6>
720. Bhatnagar, S., Afshar, Y., Pan, S., Duraisamy, K., & Kaushik, S. (2019). Prediction of aerodynamic flow fields using convolutional neural networks. *Computational Mechanics*, 64(2), 525-545. DOI: <https://doi.org/10.1007/s00466-019-01740-0>
721. Guo, X., Li, W., & Iorio, F. (2016). Convolutional neural networks for steady flow approximation. *Proceedings of the 22nd ACM SIGKDD International Conference on Knowledge Discovery and Data Mining*, 481-490. DOI: <https://doi.org/10.1145/2939672.2939738>
722. Ribeiro, M. D., Rehman, A., Ahmed, S., & Dengel, A. (2020). DeepCFD: Efficient steady-state laminar flow approximation with deep convolutional neural networks. *arXiv preprint arXiv:2004.08826*. DOI: <https://doi.org/10.48550/arXiv.2004.08826>
723. Kashefi, A., Rempe, D., & Guibas, L. J. (2021). A point-cloud deep learning framework for prediction of fluid flow fields on irregular geometries. *Physics of Fluids*, 33(2), 027104. DOI: <https://doi.org/10.1063/5.0033376>

724. Pfaff, T., Fortunato, M., Sanchez-Gonzalez, A., & Battaglia, P. W. (2020). Learning mesh-based simulation with graph networks. *arXiv preprint arXiv:2010.03409*. DOI: <https://doi.org/10.48550/arXiv.2010.03409>
725. Sanchez-Gonzalez, A., Godwin, J., Pfaff, T., Ying, R., Leskovec, J., & Battaglia, P. (2020). Learning to simulate complex physics with graph networks. *International Conference on Machine Learning*, 8459-8468. Available at: <https://proceedings.mlr.press/v119/sanchez-gonzalez20a.html>
726. Lino, M., Fotiadis, S., Bharath, A. A., & Cantwell, C. D. (2021). Multi-scale rotation-equivariant graph neural networks for unsteady Eulerian fluid dynamics. *Physics of Fluids*, 33(8), 087110. DOI: <https://doi.org/10.1063/5.0097679>
727. Li, Z., Kovachki, N., Azizzadenesheli, K., Liu, B., Bhattacharya, K., Stuart, A., & Anandkumar, A. (2020). Fourier neural operator for parametric partial differential equations. *arXiv preprint arXiv:2010.08895*. DOI: <https://doi.org/10.48550/arXiv.2010.08895>
728. Lu, L., Jin, P., Pang, G., Zhang, Z., & Karniadakis, G. E. (2021). Learning nonlinear operators via DeepONet based on the universal approximation theorem of operators. *Nature Machine Intelligence*, 3(3), 218-229. DOI: <https://doi.org/10.1038/s42256-021-00302-5>
729. Kovachki, N., Li, Z., Liu, B., Azizzadenesheli, K., Bhattacharya, K., Stuart, A., & Anandkumar, A. (2023). Neural operator: Learning maps between function spaces with applications to PDEs. *Journal of Machine Learning Research*, 24(89), 1-97. Available at: <https://jmlr.org/papers/v24/21-1524.html>
730. Wang, S., Wang, H., & Perdikaris, P. (2021). Learning the solution operator of parametric partial differential equations with physics-informed DeepONets. *Science Advances*, 7(40), eabi8605. DOI: <https://doi.org/10.1126/sciadv.abi8605>
731. Goswami, S., Anitescu, C., Chakraborty, S., & Rabczuk, T. (2020). Transfer learning enhanced physics informed neural network for phase-field modeling of fracture. *Theoretical and Applied Fracture Mechanics*, 106, 102447. DOI: <https://doi.org/10.1016/j.tafmec.2019.102447>
732. Cai, S., Wang, Z., Wang, S., Perdikaris, P., & Karniadakis, G. E. (2021). Physics-informed neural networks for heat transfer problems. *Journal of Heat Transfer*, 143(6), 060801. DOI: <https://doi.org/10.1115/1.4050542>
733. Jin, X., Cai, S., Li, H., & Karniadakis, G. E. (2021). NSFnets (Navier-Stokes flow nets): Physics-informed neural networks for the incompressible Navier-Stokes equations. *Journal of Computational Physics*, 426, 109951. DOI: <https://doi.org/10.1016/j.jcp.2020.109951>
734. Mao, Z., Jagtap, A. D., & Karniadakis, G. E. (2020). Physics-informed neural networks for high-speed flows. *Computer Methods in Applied Mechanics and Engineering*, 360, 112789. DOI: <https://doi.org/10.1016/j.cma.2019.112789>
735. Jagtap, A. D., Kawaguchi, K., & Karniadakis, G. E. (2020). Adaptive activation functions accelerate convergence in deep and physics-informed neural networks. *Journal of Computational Physics*, 404, 109136. DOI: <https://doi.org/10.1016/j.jcp.2019.109136>
736. Jagtap, A. D., & Karniadakis, G. E. (2020). Extended physics-informed neural networks (XPINNs): A generalized space-time domain decomposition based deep learning framework for nonlinear partial differential equations. *Communications in Computational Physics*, 28(5), 2002-2041. DOI: <https://doi.org/10.4208/cicp.OA-2020-0164>
737. Shukla, K., Jagtap, A. D., & Karniadakis, G. E. (2021). Parallel physics-informed neural networks via domain decomposition. *Journal of Computational Physics*, 447, 110683. DOI: <https://doi.org/10.1016/j.jcp.2021.110683>
738. Hu, Z., Jagtap, A. D., Karniadakis, G. E., & Kawaguchi, K. (2021). When do extended physics-informed neural networks (XPINNs) improve generalization? *SIAM Journal on Scientific Computing*, 44(5), A3158-A3182. DOI: <https://doi.org/10.1137/21M1447039>
739. McClenny, L., & Braga-Neto, U. (2023). Self-adaptive physics-informed neural networks using a soft attention mechanism. *Journal of Computational Physics*, 474, 111722. DOI: <https://doi.org/10.1016/j.jcp.2022.111722>
740. Peng, G. C., Alber, M., Tepole, A. B., Cannon, W. R., De, S., Dura-Bernal, S., ... & Lytton, W. W. (2021). Multiscale modeling meets machine learning: What can we learn? *Archives of Computational Methods in Engineering*, 28(3), 1017-1037. DOI: <https://doi.org/10.1007/s11831-020-09405-5>

740. Peddinti, R. D., Pisoni, S., Marini, A., Lott, P., Argentieri, H., Tiunov, E., & Aolita, L. (2024). Quantum-inspired framework for computational fluid dynamics. *Communications Physics*, 7, 135. DOI: <https://doi.org/10.1038/s42005-024-01623-8>
741. Zou, Z., Xu, P., Chen, Y., Yao, L., & Fu, C. (2024). Application of artificial intelligence in turbomachinery aerodynamics: progresses and challenges. *Artificial Intelligence Review*, 57(222). DOI: <https://doi.org/10.1007/s10462-024-10867-3>
742. Kim, S., et al. (2025). Prediction-focused machine learning-based visualization for digital twin applications in gas turbine monitoring. *Applied Thermal Engineering*, 260, 124466. DOI: <https://doi.org/10.1016/j.applthermaleng.2024.124466>
743. Leon-Medina, J. X., et al. (2025). Digital twin technology in wind turbine components: A review. *Energy Conversion and Management*, 325, 119087. DOI: <https://doi.org/10.1016/j.enconman.2024.119087>
744. Ba, L., et al. (2025). Analysis of digital twin applications in energy efficiency. *Sustainability*, 17(8), 3560. DOI: <https://doi.org/10.3390/su17083560>
800. Syamlal, M., et al. (2024). Computational fluid dynamics on quantum computers. *AIAA Journal*, 62(7), 2534-2548. DOI: <https://doi.org/10.2514/6.2024-3534>
801. Chen, Z. Y., et al. (2024). Enabling large-scale and high-precision fluid simulations on near-term quantum computers. *Computer Methods in Applied Mechanics and Engineering*, 431, 117253. DOI: <https://doi.org/10.1016/j.cma.2024.117253>
844. Girimaji, S. S. (2024). Turbulence closure modeling with machine learning: A foundational physics perspective. *New Journal of Physics*, 26, 083019. DOI: <https://doi.org/10.1088/1367-2630/ad6689>

Disclaimer/Publisher's Note: The statements, opinions and data contained in all publications are solely those of the individual author(s) and contributor(s) and not of MDPI and/or the editor(s). MDPI and/or the editor(s) disclaim responsibility for any injury to people or property resulting from any ideas, methods, instructions or products referred to in the content.